2-11-2011 12:00 AM

Advances In Internal Model Principle Control Theory

Jin Lu, *The University of Western Ontario*

Supervisor: Dr. Lyndon J. Brown, *The University of Western Ontario*
A thesis submitted in partial fulfillment of the requirements for the Doctor of Philosophy degree
in Electrical and Computer Engineering
© Jin Lu 2011

ADVANCES IN INTERNAL MODEL PRINCIPLE CONTROL THEORY

(Spine title: Advances In Internal Model Principle Control Theory)

(Thesis format: Integrated Article)

by

Jin <u>Lu</u>

Graduate Program
in
Engineering Science
Electrical and Computer Engineering

A thesis submitted in partial fulfillment
of the requirements for the degree of
Doctor of Philosophy

The School of Graduate and Postdoctoral Studies
The University of Western Ontario
London, Ontario, Canada

THE UNIVERSITY OF WESTERN ONTARIO
School of Graduate and Postdoctoral Studies

CERTIFICATE OF EXAMINATION

Supervisor:

_____

Dr. Brown, Lyndon J.

Supervisory Committee:

_____

Dr. Jiang, Jin

_____

Dr. McIsaac, Ken

Examiners:

_____

Dr. Chen, Xiang

_____

Dr. Kermani, Mehrdad

_____

Dr. Rohani, Sohrab

_____

Dr. Sidhu, Tarlochan

The thesis by
Jin <u>Lu</u>
entitled:
Advances In Internal Model Principle Control Theory
is accepted in partial fulfillment of the
requirements for the degree of
Doctor of Philosophy

_____   _____
Date   Chair of the Thesis Examination Board

Abstract

In this thesis, two advanced implementations of the internal model principle (IMP) are presented. The first is the identification of exponentially damped sinusoidal (EDS) signals with unknown parameters which are widely used to model audio signals. This application is developed in discrete time as a signal processing problem. An IMP based adaptive algorithm is developed for estimating two EDS parameters, the damping factor and frequency. The stability and convergence of this adaptive algorithm is analyzed based on a discrete time two time scale averaging theory. Simulation results demonstrate the identification performance of the proposed algorithm and verify its stability.

The second advanced implementation of the IMP control theory is the rejection of disturbances consisting of both predictable and unpredictable components. An IMP controller is used for rejecting predictable disturbances. But the phase lag introduced by the IMP controller limits the rejection capability of the wideband disturbance controller, which is used for attenuating unpredictable disturbance, such as white noise. A combination of open and closed-loop control strategy is presented. In closed-loop control mode, both controllers are active. Once the tracking error is insignificant, the input to the IMP controller is disconnected while its output control action is maintained. In the open loop control mode, the wideband disturbance controller is made more aggressive for attenuating white noise. Depending on the level of the tracking error, the input to the IMP controller is connected intermittently.

Thus the system switches between open and closed-loop control modes.

A state feedback controller is designed as the wideband disturbance controller in this application. Two types of predictable disturbances are considered, constant and periodic. For a constant disturbance, an integral controller, the simplest IMP controller, is used. For a periodic disturbance with unknown frequencies, adaptive IMP controllers are used to estimate the frequencies before cancelling the disturbances. An extended multiple Lyapunov functions (MLF) theorem is developed for the stability analysis of this intermittent control strategy. Simulation results justify the optimal rejection performance of this switched control by comparing with two other traditional controllers.

Keywords: Internal model principle; Exponentially damped sinusoid; Intermittent control; Disturbance cancellation; Switched systems; Multiple Lyapunov functions

Co-Authorship Statement

Some of the research work in this thesis, was summarized into several technical papers published or submitted for publication in conference proceedings or IEEE journal, co-authored by Jin Lu and Dr. Lyndon J. Brown.

Chapter 2 has been published in the Proceedings of the 17th IFAC World Congress. Chapter 3 has been submitted to the IEEE Transactions on Automatic Control. Part of Chapter 4 has been submitted to the 24th Canadian Conference on Electrical and Computer Engineering.

The stability theorems and their proofs presented in this thesis were developed by Jin Lu and reviewed by Dr. Lyndon J. Brown. The simulations and tests in this thesis, including simulation runs and results analysis, were conducted by Jin Lu. The papers and the whole thesis were written by Jin Lu and reviewed by Dr. Lyndon J. Brown.

Acknowledgements

I would first like to express my sincere appreciation to my supervisor, Dr. Lyndon J. Brown, for his guidance, patience and encouragement throughout the past few years of my study at Western. It has been an honour working with such an intelligent and gracious mentor.

I would also like to thank my friends here in London for their support and help throughout the duration of my study at Western. It is a memorable experience and I wish them all the best in the future.

My final expression of gratitude is to my family. Their unconditional support has been an invaluable asset not only in this research but also in every aspect of my life.

Table of Contents

List of Tables

List of Figures

Abbreviations

AFC	Adaptive Feedforward Control
ANF	Adaptive Notch Filter
CLF	Common Lyapunov Function
CQLF	Common Quadratic Lyapunov Function
EDS	Exponentially Damped Sinusoid
EKF	Extended Kalman Filter
FT	Fourier Transform
HMM	Hidden Markov Model
HR	High Resolution
IMP	Internal Model Principle
IF	Instantaneous Frequency
LMI	Linear Matrix Inequality
LQR	Linear Quadratic Regulator
ML	Maximum Likelihood
MLF	Multiple Lyapunov Function
PLLF	Piecewise Linear Lyapunov Function
STFT	Short Time Fourier Transform
SVD	Singular Value Decomposition
TFR	Time Frequency Representation

Chapter 1

Introduction

1.1 Motivation

A classical problem in control theory is that of having the system output asymptotically tracking prescribed references and/or rejecting disturbances despite uncertainty in plant and controllers, or so called zero-error output regulation problem [1]. In general, disturbance signals can be classified into predictable and unpredictable signals. The objective of this thesis is to develop control strategies that can achieve zero-error regulation for certain types of exogenous inputs (reference or disturbance signals).

Predictable signals are also called narrowband signals whose essential spectral content is limited to regions of narrow bandwidths. A typical class of narrowband signals are periodic or quasi-periodic signals, which can be seen in many diverse applications, such as rotating machineries, computer disk drives, and power systems. These signals are modelled as sinusoidal or sum of sinusoidal signals. The amplitudes of the sinusoids in these models are constant. A natural extension of these signals are signals whose amplitudes vary slowly, relative to the signal frequency. However, in audio signal processing, music or speech signals are normally modelled as sinusoids

with faster time-varying amplitudes, particularly with exponentially damped amplitudes. This type of sinusoid is called Exponentially Damped Sinusoid (EDS) with the following representation in discrete time,

$$s(k) = ae^{\sigma k}\sin(\omega k + \phi), \qquad k = 0, 1, 2, \cdots \qquad (1.1)$$

where σ is the damping factor, ω is the frequency, a is the initial amplitude, and ϕ is the initial phase of the signal. Both frequency ω and damping factor σ can be time-varying, as long as these variations are small with respect to the value of ω. Thus the amplitude of an EDS signal does not necessarily decrease as time evolves. Depending on the value of σ, which could be positive or negative constant or time-varying, the amplitude evolves differently. The signal form in (1.1) can be seen as a generalized representation of pure sinusoidal or exponential signals by letting σ or ω be zero respectively. If both parameters are zero, it is just a constant.

Different from predictable signals, unpredictable signals, such as white noise and colored noise, have their spectral contents spread over a wide bandwidth. So they are also called wideband signals. No controller can cancel unknown or uncertain wideband signals. They can only be attenuated. But a uncertain narrowband signal can be perfectly rejected or tracked by properly designed controllers. The perfect rejection or tracking cannot be achieved without a perfect identification of the narrowband signal. Thus there is a strong connection between zero-error output regulation problem and signal identification problem.

When designing controllers to reject a narrowband disturbance, it is required to have them providing closed-loop stability and output regulation. A plant-controller combination is called structurally stable if these two requirements are satisfied when certain system parameters are perturbed [1]. In order to achieve structural stability, the plant-controller combination must utilize feedback of the regulated variable, typically the tracking error between the plant output and the exogenous input, and incorporate in the feedback path a suitably reduplicated model of the dynamic structure of the exogenous input signal. This is the main idea of the so called Internal Model Principle (IMP), proposed by Francis and Wonham in 1976 [1]. The replicated model of the exogenous input is called an internal model.

One of the simplest IMP controllers is integral controller, which is commonly used for coping with constant signals. It is well known that zero tracking error can be achieved using integral control for a constant input. IMP control has also been applied to cancelling sinusoidal disturbances, due to their wide spread existence in many applications. In this thesis, the identification of EDS signals with unknown parameters is studied based on the IMP approach.

When a system is subjected to a disturbance with both predictable and unpredictable components, an IMP controller and a wideband disturbance controller can be implemented simultaneously for disturbance rejection. However, the rejection capability of the wideband disturbance controller will be limited due to the phase lag introduced by the IMP controller. Furthermore, if the predictable disturbance con-

tains multiple sinusoidal modes with unknown frequencies, especially if the number of modes is large, it will be extremely difficult to tune these controllers. In order to achieve an optimum rejection performance, the regulation variable can be connected to the IMP controller intermittently. This intermittent control strategy also makes the tuning feasible for multiple IMP controllers. This control idea was proposed by Brown *et al.* in [2, 3]. The intermittent control system can be modelled as a switched system. The stability analysis of the intermittent control strategy is presented in this thesis, as well as an extension to the control strategy for dealing with different predictable signals.

1.2   Literature Review

According to the internal model principle, when a replicated internal model of the exogenous input is connected in the feedback path, the closed-loop system transfer function, between the input and the tracking error, has a set of transmission zeros that includes all the eigenvalues of the autonomous dynamical system which generates all such input signal. Thus the exogenous input is asymptotically blocked in its transit through the closed-loop system as a result of pole-zero cancellation. Specifically for a sinusoidal signal with frequency ω_c, it has a pair of critically stable poles at $\pm j\omega_c$ on the imaginary axis in the frequency domain. If the frequency ω_c is known, an accurate internal model with fixed parameters of the sinusoid can be constructed to achieve zero-error regulation.

However, in many applications, the sinusoid's frequency may vary over time or is completely unknown. An IMP controller with fixed parameters will cause unacceptable tracking error. This is the main limitation of the IMP approach which requires the knowledge of the reference or disturbance signals *a priori*, so that corresponding internal model can be suitably produced. The accuracy of regulation depends critically on the fidelity of the internal model. Even errors of less than one percent in model parameters can lead to unacceptable residue errors. Therefore, accurately estimating the periodic signal's frequency becomes the most crucial task in regulation problems.

1.2.1   Frequency estimation

Fourier transform (FT) is a standard tool for spectral analysis in signal processing area. Although the FT is valid under extremely general conditions, there are some crucial restrictions of Fourier analysis: the system must be linear and the data must be strictly periodic or stationary. Natural phenomena measurements are essentially non-linear and non-stationary. Alternatives to the FT for non-stationary signals include the Hilbert transform and wavelet transforms. The Hilbert transform of a signal $X(t)$ is defined as $Y(t) = \frac{P}{\pi} \int_{-\infty}^{\infty} \frac{X(\tau)}{t-\tau} \, d\tau$, where P indicates the Cauchy principal value. The instantaneous frequency (IF) is then defined as $\omega(t) = \frac{d}{dt} \angle (X(t) + jY(t))$ [4]. For narrowband signals, this definition matches our common sense idea of frequency, however, it is not physically meaningful for non narrowband signals.

1.2.1.1   Time-frequency representation based methods

One type of the IF estimation techniques is based on the time-frequency representation. A time-frequency representation (TFR) is a signal representation in which time and frequency information are displayed jointly on a 2-D plane. This representation is useful for analyzing signals with both time and frequency variations. The short-time Fourier transform (STFT) and the Wigner distribution (WD) [5] are two popular choices for TFR-based IF estimation. The STFT guarantees positivity and is computationally efficient and very robust against noise. However, it suffers poor time-frequency resolution. Although the WD has many desirable properties such as high signal concentration in time-frequency, it suffers large cross terms between multiple signal components in time-frequency, which makes it difficult to interpret the WD in many practical applications. In [6], a hidden Markov models (HMMs) based algorithm is used to track the peak of the STFT. The outputs of the HMM tracker provides an estimate of the mean signal frequency as a function of time. In this method, the states of the HMM are chosen to lie in some finite scalar set and transition probabilities between elements of this set are known. White [7] generalized the HMM formalism to include the case when the state set may be regarded as the Cartesian product of a finite number of elementary state sets. This so-called Cartesian HMM (CHMM) based method can track the IF and phase simultaneously. However, the CHMM introduces a large number of states, which makes the computational cost very expensive.

Kwok and Jones [8] proposed an adaptive short-time Fourier transform (ASTFT) based instantaneous frequency estimation that inherits the advantages of the STFT without most of its drawbacks. This is done by using different windows at each time instance to achieve a good TFR. The adaptation rule is a generalized likelihood ratio test based on the STFT. In addition, a post-ASTFT peak tracking algorithm further improves the performance by following the continuous ridge in the time-frequency plane and removing the spurious deviations. The algorithm is constructed under a statistical detection and estimation framework and is an approximate maximum-likelihood sequence estimator (MLSE) of IF tracks.

1.2.1.2 Filter based methods

Another type of IF estimation techniques are filter based, which includes extended Kalman filter (EKF) frequency estimation, adaptive notch filter, and adaptive feed-forward control. The EKF frequency estimator design proceeds from a state space signal model of the process to be estimated. The signal model dynamics describe a mechanism for how the process may be evolving. The initial stage in the filter design process is to perform system identification. Once the system has been identified, Kalman filter theory endeavours to construct an optimal estimator for the state, given the noise covariances Q and R, where optimality is measured in terms of covariance. The EKF is derived by linearizing the signal model about the current predicted state estimate and then using the Kalman filter on this linearized system to calculate a

gain matrix. This gain matrix, along with the nonlinear signal model and new signal measurement, is used to produce the filtered state estimate and then an estimate of the state at the next time instant. In developing extended Kalman filter based on signal models, the design compromises are to balance filter divergence and sensitivity to noise [9]. However, the approach developed in [9] is characterized by a vector of three design parameters. The tuning of these three parameters still remains a difficult task due to the unclear cross-relationships between such parameters. Bittanti and Savaresi [10] proposed a parametrization of the extended Kalman filter frequency tracker that is characterized by just one parameter. This simplification allows an easier and more transparent tuning of its tracking behaviour.

Adaptive notch filter (ANF) is a well-studied technique for removing or retrieving sinusoids of unknown frequency from additive noise. Classically, the adaptive notch filter is parametrized with the polynomial coefficients of its transfer function. These coefficients are a function of the notching frequencies for which the notch filter has or nearly has a zero gain. The frequencies are then computed from the estimated transfer function coefficients. These techniques require stability monitoring, that is, the model stability has to be checked after each adaptation, which leads to a lot of additional computation [11]. In [12], the lattice structure was used to overcome the stability monitoring problem for the general adaptive IIR filtering problem. This lattice-based adaptive IIR notch filter features independent tuning of the notch frequency and attenuation bandwidth. As opposed to minimizing an output error cost

function, this algorithm is designed instead to achieve a stable associated differential equation. This results in a globally convergent unbiased frequency estimator in the single sinusoidal case, independent of the notch filter bandwidth. Using a second-order structure in the multiple sinusoids case, unbiased estimation of one of the input frequencies is achieved by thinning the notch bandwidth. Dragosevic and Stankovic [13] derived an expression for the notch filter output power to serve as a prerequisite for finding the asymptotically optimal values of both pole contraction and forgetting factors. The derived optimality conditions depend on *a priori* knowledge of the signal and noise parameters.

Adaptive feedforward control (AFC) is an approach based on the phase-locked loop technique commonly used in frequency-modulation communication systems. Bodson and Douglas [14] presented two algorithms for the rejection of sinusoidal disturbances with unknown frequency. The first is an indirect adaptive algorithm where the frequency of the disturbance is estimated independently of the cancellation scheme by an adaptive notch filter. The estimate is then used in another adaptive algorithm that adjusts the magnitude and phase of the input needed to cancel the effect of the disturbance. The second is a direct adaptive algorithm in which a single error signal is used to update the frequency and the magnitude estimates simultaneously. This algorithm consists in extending the AFC scheme by integrating a phase-locked loop so that disturbances with unknown frequencies can be directly cancelled. However, the gain of the transfer function of the plant at the identified frequency is explicitly required in

order to implement this direct adaptive algorithm. Thus this algorithm could be very complicated to implement in practice where the plants are often complicated. In [15], a frequency estimator based on a magnitude/phase-locked loop approach is presented. The estimator has the following features: simultaneous estimation of the frequencies, magnitudes, and phases of the components of a periodic signal, simplicity in design and implementation, and fast estimation/tracking of time-varying parameters. This algorithm is derived from the direct adaptive algorithm presented in [14], with an adjustment by adding a proportional term K_f in phase estimation to improve frequency tracking.

1.2.1.3   Signal subspace based methods

Estimating a set of parameters from measurements of the received signals is a problem of significance in many signal processing applications, such as direction-of-arrival (DOA) estimation, system identification, and time series analysis. High-resolution frequency estimation is important in numerous applications, which include the design and control of robots and large flexible space structures. There have been several approaches to such problems including maximum likelihood (ML) method and maximum entropy (ME) method. Although often successful and widely used, these methods have certain fundamental limitations due to the use of an incorrect model of the measurements [16]. The MUSIC (MUltiple SIgnal Classification) algorithm was developed in the late 1970's by Schmidt and Bienvenu independently [16]. This algorithm

first estimates the signal subspace from the array measurements. The parameters of interest are then estimated from the intersections between the array manifold and this estimated subspace. However, although the performance advantages of MUSIC are substantial, they are achieved at a considerable cost in computation and storage. Roy and Kailath [16] proposed a so-called estimation of signal parameters via rotational invariance techniques (ESPRIT) approach that can be applied to a wide variety of problems including accurate detection and estimation of sinusoids in noise. It exploits an underlying rotational invariance among signal subspaces induced by an array of sensors with a translational invariance structure, and generates estimates that are asymptotically unbiased and efficient. This approach produces signal parameter estimates based only on eigen-decompositions. It has important implementational advantages over MUSIC in direction finding applications, as a result of reduction of computation and storage costs. ESPRIT is also manifestly more robust with respect to array imperfection than previous techniques including MUSIC [17].

1.2.1.4 Internal model principle based methods

In order to remove the main limitation of the IMP approach, which requires the knowledge of the exogenous signals *a priori*, many approaches have been developed. One of these developments is the repetitive control scheme presented by Tsao *et al.* in [18]. Their period identification algorithm is based on the gradient minimization of a quadratic energy function. They adopted a sampled data recursive scheme for

identifying the period of a periodic signal with a resolution finer than the sampling interval. The fine adaptation of the controller sampling interval makes the identified signal period an exact integer multiple of the controller sampling interval and renders a superior tracking performance than that of the conventional fixed sampling interval repetitive controllers. But their algorithm is often unstable at the starting phase of identification, a low-pass filter is needed to stabilize their algorithm. Another disadvantage of their algorithm is that the speed of the convergence is slow. If the initial condition and the basic period are not close enough, the adaptation may converge to a local minimum at an integer multiple of the basic period.

Serrani *et al.* [19] employed a canonical parametrization of the internal model to solve the problem of output regulation for nonlinear minimum phase systems driven by an exosystem with unknown frequencies within known bounds. By adaptively tuning the internal model, robust regulation with a semi-global domain of convergence can be obtained. This approach adopts the conventional parallel connection of a robust stabilizer and an internal model. Ding [20] introduced a parameter-dependent state observer without following the parallel structure. In the state observer, a new formulation of internal model is used to generate the contribution of the desired input compensation to a state variable, which is then used in the control design. As a result, the state estimates are involved with unknown parameters which appeared in the internal model. The unknown parameters are dealt with in the control design by adaptive backstepping technique. With this control design, the stabilisation and

compensation control efforts are combined together to achieve global stabilisation and disturbance suppression with respect to state variables. Marino and Tomei [21] designed an output feedback regulator which tunes its own internal model of a linear stable exosystem with unknown frequencies and known order. For a stabilizable and detectable linear system, this output regulator guarantees exponential convergence of regulation error for any initial condition. In [22], the use of IMP is explored for the rejection of time-varying of narrowband disturbances. In this control scheme, the Youla-Kucera parametrization (Q-parametrization) is applied to the controller, which makes it possible to insert and adjust the internal model in the controller by adjusting the parameters of the Q polynomial.

1.2.2 Exponentially damped sinusoidal signals

The sinusoidal signal has proven its efficiency in modelling harmonic or quasi-harmonic signals that present slow time variations. However, such modelling provides poor performance when representing transient signals, typically signal onsets or fadings, which are, by nature, localized both in time and frequency. It can be beneficial to produce a signal representation based on waveforms allowing a better modelling of fast time-varying signals [23]. Exponentially damped sinusoidal (EDS) signal is a more powerful representation of an audio signal such as speech or music than the basic sinusoidal signal.

Traditionally, the EDS signal is associated with a high resolution (HR) parame-

ter estimation method, such as matrix pencil, ESPRIT or Kung's algorithm [24]. Hua and Sarkar [25] presented an approach to exploit the structure of a matrix pencil of the EDS signal for estimating the signal parameters. The SINTRACK method [26] uses a matrix pencil algorithm for the detection and initial estimation of EDS signal parameters. An adaptive Least Mean Square (LMS) algorithm is then used to track the minor fluctuations in parameter values. The use of these two algorithms offers a good compromise between accuracy and computation cost.

In [27], a subspace-based high resolution method is presented for the estimation and tracking of the EDS signal parameters, the damping factor and frequency. The estimation of the signal parameters is achieved in two steps: first the damping factor and frequency are computed using a high resolution method, then they are used to re-synthesis the signal. A simple re-synthesis method is able to realize the adaptive tracking of the slow variation of the signal parameters. Gunnarsson and Gu [28] proposed an analysis and synthesis system for music signals consist of multiple EDS components. The music signal is first divided into overlapped blocks with fixed size which are approximately stationary. A least-squares ESPRIT method is then applied to each data block for estimating associated signal parameters, including frequency, damping factor, amplitude and initial phase of each EDS component. The estimated EDS components are then tracked along the time direction under a continuity constraint to the components in the music signal.

These subspace decomposition based HR methods are very efficient in the con-

text of audio modelling. One of their advantages is that they are not bounded by the Fourier resolution limitation. This advantage turns out to be particularly consistent whenever two spectral components of a complex sound are separated by a distance smaller than the frequency resolution. Also, when there is frequency sliding, these methods can be efficient. Another advantage of HR methods is their ability to provide a good estimation of the parameters over a low number of samples. The use of very short-time analysis windows is then possible without any important loss of estimation performance which allows a good time resolution [23]. However, other than their high computational complexity, these methods do not exploit the harmonic relations between the frequencies and have a high complexity orders. Consequently, these methods become ineffective when the length of the analysis segment is large [24].

Other techniques for EDS parameter estimation include maximum likelihood (ML) [29], polynomial or linear prediction methods, and higher order statistics based approach [30]. Kumaresan and Tufts (KT) [31] presented a linear prediction method by using the principal eigenvectors of the data matrix to separate signal subspace from noise subspace in the form of singular value decomposition (SVD) and the backward linear prediction equations of the noisy observations of the EDS signal. When the analyzed signal is contaminated with a high level noise, this method exhibits a superior performance. Based on the knowledge of the third or fourth order statistics of the observed EDS signal, Papadopoulos and Nikias [30] extended this minimum

norm principal eigenvectors method (KT method) to higher order statistics domains. The signal parameters are calculated by polynomial rooting of a vector of coefficients, which is a solution of a linear system of equations involving third or fourth order statistics.

All methods mentioned above have been proven to be conditionally efficient in estimating parameters of EDS signals form a batch of measurement data. But they all suffer from a common disadvantage, *i.e.*, these techniques are all processed off-line and therefore are not suitable for detecting and tracking the time-varying parameters such as damping factors and frequencies. Zhang *et al.* [32] proposed a novel method of estimating parameters of EDS signals by combining Hankel singular value decomposition (HSVD) with extended complex Kalman filter (ECKF). The HSVD algorithm is essentially used to obtain accurate initial state estimates from a small number of samples. These estimates are subsequently being used by ECKF which is capable of estimating EDS parameters and effectively tracking parameter variations.

The EDS signal described in (1.1) is real. It can also be described in terms of complex exponential signals. Let $\alpha = \frac{1}{2}ae^{j\phi}$, and $z = e^{\sigma + j\omega}$, we have

$$s(k) = \alpha z^k - \alpha^*(z^*)^k \tag{1.2}$$

where the asterisk $(*)$ denotes complex conjugate. Among the methods discussed above, except the iterative method presented in [24], all other methods use the com-

plex exponential description (1.2) to estimate the signal parameters. Since the frequency can be identified by taking derivative of the phase of the complex exponentials, it is easier to deal with complex signals than real signals.

1.2.3 Switched control systems

Many dynamical systems from various areas involve the interactions of discrete events and continuous dynamics. These dynamical systems are usually called hybrid systems. The area of hybrid systems is a fascinating discipline bridging control engineering, computer science, and applied mathematics. A switched system is defined as a dynamical system with a finite number of continuous time subsystems and a logical rule that orchestrates switching between them [33]. The need for switching usually arises from the fact that no single candidate controller would be capable, by itself, of guaranteeing stability and good performance when connected with a poorly modelled process [34]. Switched system have numerous applications in control of mechanical systems, process control, the automotive industry, switching power converters, aircraft and traffic control, and many other fields [35].

Mathematically, a switched system can be described by a differential equation of the form

$$\dot{x}(t) = f_{\sigma(t)}(x(t)) \tag{1.3}$$

where $x(t) \in \mathbb{R}^n$ is the state. $\{f_{\sigma(t)} : \sigma(t) \in \mathcal{P}\}$ is a family of sufficiently regular (at

least locally Lipschitz) functions from $\mathbb{R}^n$ to $\mathbb{R}^n$. $\sigma(t)$ is a piecewise constant function of time: $[0, \infty) \rightarrow \mathcal{P}$, called a switching signal, with $\mathcal{P} = \{1, 2, \cdots, m\}$ being a finite index set. The function $\sigma(t)$ has a finite discontinuities (switching times/instances) on every bounded time interval and takes a constant value on every interval between two consecutive switching times. Normally $\sigma(t)$ is assumed to be continuous from the right everywhere: $\sigma(t) = \lim_{\tau \rightarrow t+} \sigma(\tau)$ for each $\tau \geq 0$. Functions $f_1(\cdot)$, $f_2(\cdot), \cdots, f_m(\cdot)$ are assumed to satisfy

$$f_1(0) = f_2(0) = \cdots = f_m(0) = 0 \tag{1.4}$$

A switched system described by (1.3) and (1.4) imply that all its subsystems have the same state and the same equilibrium point at the origin. If all the individual subsystems are linear time-invariant, a switched linear system can be obtained,

$$\dot{x}(t) = A_{\sigma(t)} x(t) \tag{1.5}$$

A main concern in the switched systems design is the stability issue. There are examples in [36] showing that unconstrained switching may destabilize a switched system even if all individual subsystems are stable. It also may be possible to stabilize a switched system by means of suitably constrained switching even if all individual subsystems are unstable. Liberzon and Morse [37] formulated three basic problems in stability and design of switched systems.

A. Find conditions that guarantee asymptotic stability of the switched system (1.3) for arbitrary switching signals.

B. Identify those classes of switching signals for which the switched system (1.3) is asymptotically stable.

C. Construct a switching signal that makes the switched system (1.3) asymptotically stable.

Instead of just asymptotic stability for each particular switching signal, a stronger property is desirable, namely, asymptotic or exponential stability that is *uniform* over the set of all switching signals. The switched system (1.3) is *uniformly asymptotically stable* if there exist a positive constant δ and a class $\mathcal{KL}$ function β such that for all switching signals $\sigma(t)$ the solutions of (1.3) with $\|x(0)\| \le \delta$ satisfy the inequality

$$\|x(t)\| \le \beta(\|x(0)\|, t), \quad \forall t \ge 0 \tag{1.6}$$

where $\|x\|$ is referred to the Euclidean norm of vector x. If the function β takes the form $\beta(r, s) = cre^{-\lambda s}$ for some $c,\ \lambda > 0$, so that

$$\|x(t)\| \le ce^{-\lambda t}\|x(0)\|, \quad \forall t \ge 0 \tag{1.7}$$

then the system (1.3) is called *uniformly exponentially stable*. The switched system has stability margin λ.

Much of the work on Problem A has been focused on the existence of a common Lyapunov function (CLF). It is well known that the switched system (1.3) is uniformly asymptotically stable for arbitrary switching signals if all of its subsystems share a radially unbounded common Lyapunov function. Particularly for the switched linear system (1.5), its uniform exponential stability under arbitrary switching is equivalent to the existence of a continuously differentiable common Lyapunov function $V(x)$ for its constituent systems [38].

Most of the available results for the arbitrary switching problem are related to the existence of common quadratic Lyapunov functions (CQLF). The function $V(x) = x^T P x$ is a CQLF for the switched linear system (1.5) if (i) P is a positive definite symmetric matrix, and (ii) $A_p^T P + P A_p < 0, \ (p \in \mathcal{P})$. These two conditions are equivalent to a system of linear matrix inequalities (LMIs) in P. Thus, determining whether or not the system (1.5) possess a CQLF amounts to checking the feasibility of a system of LMIs. Solvers for LMIs are built on convex optimization algorithms that quickly converge [39]. However, LMI-based methods are not effective when the number of constituent systems is very large and they cannot be directly applied to check the existence of a CQLF for an infinite family of systems. An alternative numerical technique based on iterative gradient descent methods is presented in [40], which can be combined with randomization algorithms and applied to compact, possibly infinite, family of system matrices A_p. In this case, it has been shown that the algorithm will converge to a CQLF with probability one, provided such a CQLF

exists. For some families of linear systems, certain algebraic properties have proven to be sufficient for the existence of CQLFs. In [37], it is shown that if all matrices in the set $\{A_p : p \in \mathcal{P}\}$ commute or have a solvable Lie algebra, a CQLF exists and the switched linear system is uniformly exponentially stable under arbitrary switching. A brief survey on various attempts to derive the algebraic conditions for the existence of a CQLF is given in [41].

In general, CQLF existence is only a sufficient condition for the exponential stability of a switched linear system under arbitrary switching. And the common Lyapunov function may not necessary be quadratic. Some of the research [42, 43, 44, 45] has focused on the existence conditions and construction of common piecewise linear Lyapunov functions (PLLFs) (also known as polyhedral Lyapunov functions). A PLLF is of the form

$$V(x) = \max_{p \in \mathcal{P}}(w_p^T x) \tag{1.8}$$

where $w_p \in \mathbb{R}^n$, $p \in \mathcal{P}$ and the linear functions $w_p^T x$ are called generators of the PLLF. However, the computational requirements to establish the common PLLF existence is a serious bottleneck in practice. The main reason is that a complex representation (with a large number of parameters) is usually required for a solution to be found rendering the techniques applicable to low-dimensional problems only [38].

One necessary condition for the switched system (1.3) being uniformly asymp-

totically stable under arbitrary switching is that all constituent systems are asymptotically stable. There are some switched systems that become unstable under certain switching signals, even if all their constituent systems are asymptotically stable. In order to achieve stability, one often needs to restrict the class of admissible switching signals. This leads us to Problem B.

It is well known that a switched system is stable if all individual subsystems are stable and the switching is sufficiently slow, so as to allow the transient effects to dissipate after each switch. A notable approach to formulate this idea is the dwell time approach. The concept of dwell time is introduced to specify slow switching. Let $\mathcal{S}[\tau_d]$ denote the set of all admissible switching signals with interval between consecutive switching instances no smaller than a positive constant τ_d. This constant τ_d is called the dwell time. Morse [46] showed that if the switching signal $\sigma(t)$ of switched linear system (1.5) "dwells" at each of its values in $\mathcal{P}$ long enough for the norm of the state transition matrix of A_p, $p \in \mathcal{P}$ to drop to one in value (i.e., at least τ_d time units), then A_σ will be exponentially stable with a decay rate no longer than the smallest of the decay rates of A_p, $p \in \mathcal{P}$. If for each $p \in \mathcal{P}$, A_p is stable, and

$$\|e^{A_p t}\| \leq e^{(a_p - \lambda_p t)}, \quad t \geq 0, \tag{1.9}$$

where $a_p \geq 0$ and $\lambda_p > 0$ are two finite numbers, a lower bound on τ_d is given by

$$\tau_d > \sup_{p \in \mathcal{P}} \left(\frac{a_p}{\lambda_p} \right) \tag{1.10}$$

Dwell time switching requires each constituent system to be active for, at least, τ_d units of time. Specifying a dwell time may be too restrictive for some systems. It is possible that some subsystems may lead to bad transient responses or unacceptable performances during such time interval. An even worse scenario is finite escape may occur for some nonlinear subsystems before the next switching is permitted. Thus it is of interest to relax the concept of dwell time, allowing the possibility of switching fast when necessary and then compensating for it by switching sufficiently slowly later. The concept of average dwell time from [34] serves this purpose. The switching signal set is enlarged by including signals with switching intervals occasionally smaller than a positive constant $\bar{\tau}_d$. But the average of all intervals is no less than $\bar{\tau}_d$. For each switching signal σ and each $t \geq \tau \geq 0$, let $N_\sigma(t, \tau)$ denote the number of discontinuities of σ in the open interval (τ, t). For two given positive numbers $\bar{\tau}_d$ and N_0, denote $\mathcal{S}[\bar{\tau}_d, N_0]$ to be the set of all switching signals for which

$$N_\sigma(t, \tau) \leq N_0 + \frac{t - \tau}{\bar{\tau}_d} \tag{1.11}$$

The constant $\bar{\tau}_d$ is called the average dwell time and N_0 the chatter bound.

Consider the switched linear system (1.5), given a positive constant λ_0 such that

$(A_p + \lambda_0 I)$ is asymptotically stable for each $p \in \mathcal{P}$, Hespanha and Morse [34] proved

that for any $\lambda \in [0, \lambda_0)$, there is a finite constant $\bar{\tau}_d^*$ such that system (1.5) is uniformly

exponentially stable over $\mathcal{S}[\bar{\tau}_d, N_0]$ with stability margin λ, for any average dwell time

$\bar{\tau}_d \geq \bar{\tau}_d^*$ and any chatter bound $N_0 > 0$. Since each $(A_p + \lambda_0 I)$ is asymptotically stable,

there exists a set of symmetric, positive definite matrices $\{Q_p : p \in \mathcal{P}\}$, such that

$$Q_p(A_p + \lambda_0 I) + (A_p + \lambda_0 I)^T Q_p = -I, \quad p \in \mathcal{P} \tag{1.12}$$

Let

$$\mu = \sup_{i,j \in \mathcal{P}} \frac{\sigma_{max}[Q_i]}{\sigma_{min}[Q_j]} \tag{1.13}$$

where $\sigma_{max}[Q]$ and $\sigma_{min}[Q]$ denote the largest and smallest singular values of Q

respectively. After choosing a stability margin λ, one will obtain a lower bound of

the average dwell time as

$$\bar{\tau}_d^* = \frac{\ln \mu}{2(\lambda_0 - \lambda)} \tag{1.14}$$

Similar results for certain classes of switched nonlinear systems were also derived in

[34].

The average dwell time approach discussed above mainly focuses on switched

linear systems consisting of only Hurwitz stable subsystems. However, in practice,

there are cases where switching to unstable subsystems becomes unavoidable. Therefore, slow switching is not sufficient for stability. It is also required that the switched system does not spend too much time in the unstable subsystems. In [47], Hu *et al.* showed that if both Hurwitz stable and unstable subsystems exist, the switched system (1.5) is exponentially stable under the assumption that all subsystem matrices are pairwise commutative. Zhai *et al.* [48] presented an average dwell time based method to analyze the stability of switched systems consisting of both Hurwitz stable and unstable subsystems. If the total activation time ratio between Hurwitz stable subsystems and unstable subsystems is no less than a specified constant, then exponential stability of a desired margin is guaranteed. By introducing the concepts of positive stability margin and negative stability margin for Hurwitz stable and unstable subsystems respectively, a lower bound of the activation time ratio can be computed. Then the average dwell time results from [34] can be applied to prove the exponential stability.

We can see that in both [34] and [48], a series of Lyapunov equations are solved for deriving the lower bound of the average dwell time. The solutions of these Lyapunov equations can be used to construct quadratic Lyapunov functions. Such Lyapunov functions are closely related to the stability of the switched systems. This leads us to another approach for stability analysis: multiple Lyapunov functions (MLF) approach. Rather than using a single common Lyapunov function that applies to all subsystems at all time, MLF approach requires that each subsystem has its corre-

sponding Lyapunov or Lyapunov-like function combined with a bounding condition at each switching time. These multiple functions can be pieced together in some way to produce a non-traditional global Lyapunov function whose overall energy decreases to zero along the system state trajectories [49].

Among all the published work about this approach, Branicky presented a very intuitive version in [50]. Branicky's basic idea was to first define a family of Lyapunov-like functions $\{V_p : p \in \mathcal{P}\}$ corresponding to all subsystems of system (1.3). Instead of being defined globally, each $V_p(x)$ is defined over the region where subsystem p is active. Each function $V_p(x)$ also needs to satisfy two conditions: (i) positive definite, i.e., $V_p(x) > 0$, $\forall x \neq 0$, and $V_p(0) = 0$; (ii) non-positive definite time derivative, $\dot{V}_p(x) \leq 0$. If the values of $V_p(x)$ at the entry points (when subsystem p is switched on) are monotonically nonincreasing for all $p \in \mathcal{P}$, the equilibrium point $x = 0$ of system (1.3) is stable in the sense of Lyapunov. Same result can be obtained if $V_p(x)$ is monotonically nonincreasing at the end points. Zhai *et al.* [51] complemented this result by introducing the idea of evaluating "the average value of multiple Lyapunov functions". For subsystem p, during each of its active time interval, an average value of $V_p(x)$ over this active time interval is calculated. A sequence of these average values corresponding to subsystem p is then used to evaluate the system's stability.

The requirements of Lyapunov-like function in Branicky's result is weakened in [52]. Instead of having non-positive definite derivative, $V_p(x)$ only has to be bounded by a continuous function which is zero at the origin. $V_p(x)$ is called a weak Lyapunov-

like function if it is monotonically nonincreasing at the entry points (or end points). The equilibrium point $x = 0$ of system (1.3) is stable in the sense of Lyapunov if such weak Lyapunov-like functions exist for each subsystem.

A more general stability result using MLF approach is proposed in [53]. It is proved that asymptotic stability is guaranteed by requiring the sequence of values of the Lyapunov-like function candidate at consecutive switching times to be decreasing and the Lyapunov-like function between these times is bounded by a continuous function which is zero at the origin.

Using MLFs to form a single non-traditional Lyapunov function offers much greater freedom and infinitely more possibilities for demonstrating stability, for constructing a non-traditional Lyapunov function, and for achieving the stabilisation of the switched system [49]. But a critical challenge of applying MLF theory in practical switched systems is how to construct a proper family of Lyapunov-like functions. Currently, there is no universal constructive procedure for choosing the best Lyapunov-like functions. However, if one focuses on the linear cases, piecewise quadratic Lyapunov-like function could be an attractive candidate, since the stability conditions can be formulated as LMIs. In [54], the search for continuous piecewise quadratic Lyapunov-like functions is formulated as a convex optimization problem in terms of LMIs.

All the above discussed MLF approaches have a common restriction in which all the candidate Lyapunov-like functions must satisfy the same set of conditions.

This will limit the flexibility of choosing proper candidate Lyapunov-like functions for each subsystem accordingly.

The dwell time and MLF techniques not only can be applied for stability analysis, also give the means of constructing stabilizable switching signals, which provide solutions to Problem C given earlier.

1.3 Introduction of Algorithms

The work presented in this thesis is mainly based on two control algorithms which are briefly introduced here.

1.3.1 Adaptive internal model principle control algorithm

Brown and Zhang developed an IMP based adaptive algorithm to identify unknown frequencies of periodic disturbances in [55, 56]. In this algorithm, a standard IMP controller is implemented using a state space representation as follows

$$\begin{bmatrix} \dot{x}_1 \\ \dot{x}_2 \end{bmatrix} = \begin{bmatrix} 0 & \omega \\ -\omega & 0 \end{bmatrix} \begin{bmatrix} x_1 \\ x_2 \end{bmatrix} + \begin{bmatrix} 0 \\ K_f \end{bmatrix} e(t) \tag{1.15}$$

$$u = \begin{bmatrix} 0 & 1 \end{bmatrix} \begin{bmatrix} x_1 \\ x_2 \end{bmatrix} \tag{1.16}$$

where x_1, x_2 are the two state variables of the controller, the tracking error $e(t)$ is the input, and u is the output control signal. K_f is a tuning gain of the controller. Since the signal frequency ω_c is unknown, according to the certainty equivalence principle, its best estimate ω is used in (1.15). A mapping from the controller's state variables to the frequency estimation error ε can be derived as

$$\varepsilon = -\frac{K_f e x_1}{x_1^2 + x_2^2} \tag{1.17}$$

Ideally, this estimation error can be eliminated in one updating step if the exogenous input is noise-free pure sinusoid. However, this is not a realistic situation. An integral controller was used for eliminating the error as follows,

$$\frac{d\omega}{dt} = -K_\omega \frac{K_f e x_1}{x_1^2 + x_2^2} \tag{1.18}$$

where K_ω is the integral gain. Thus the parameter ω in the IMP controller is constantly updated and asymptotically converges to the true frequency ω_c.

As an alternative approach, a least-squares method was also introduced in [55] to estimate the frequency ω_c, which is given by

$$\frac{d\omega}{dt} = -\frac{a_1}{(a_2 t + 1)} \times \frac{K_f e x_1}{x_1^2 + x_2^2} \tag{1.19}$$

where a_1 is chosen as the estimate of the uncertainty in initial knowledge of ω_c, and

$a_2 = a_1\psi$ with ψ being the variance of (ε/K_f). This approach is only appropriate when the disturbance frequency does not drift with time. By using a Kalman filter, the adaptation gain in (1.19) is replaced by $\frac{a_1 + a_3 t}{a_2 t + 1}$, so that the estimated frequency can be time-varying. With the identification of its frequency, the periodic disturbance is perfectly rejected and zero-error regulation is achieved. The asymptotic stability of this adaptive algorithm was proved using singular perturbation theory and averaging theory.

By placing multiple number of this adaptive IMP controllers in parallel in the feedback path, a periodic signal consisting of multiple sinusoids with different unknown frequencies can be identified and cancelled. According to the IMP, each IMP controller corresponds to a sinusoidal component of the signal. One such application is the power system frequency estimation. In [56], five adaptive IMP controllers are constructed to cancel a signal with 1st to 9th odd harmonics. All five controllers share the same estimated fundamental frequency. In [55], two adaptive IMP controllers are implemented to identify the frequencies of a signal with two non-harmonic components. Compared to the results presented in [57], which uses an adaptive observer technique to identify multiple frequencies, this adaptive IMP algorithm has much faster convergence.

1.3.2   Intermittent cancellation control algorithm

When a system is subjected to both a narrowband disturbance and an additive white noise, a traditional IMP controller and a wideband disturbance controller can be used together. Since the IMP controller introduces a phase lag into the system, it will limit the wideband disturbance controller's capability of minimizing white noise. Brown *et al.* proposed an intermittent cancellation control algorithm in [2, 3]. A wideband disturbance controller is always active in this control algorithm. An IMP controller is active for narrowband disturbance rejection only when the tracking error is significant. The input to the IMP controller is disconnected when the tracking error is smaller than a predefined threshold as a result of near perfect rejection of narrowband disturbance. Note that the IMP controller continues to provide an output, which after convergence provides perfect cancellation of the predictable portion of the disturbance or necessary control action to track the reference. Residual errors will cause the switching mechanism to infrequently close the switch improving the performance of the system with each invocation. It can be seen that when the switch is closed, we have a closed-loop IMP control system, and when the switch is open, the IMP controller provides an open loop cancellation of the error. Thus this intermittent cancellation control system can be modelled as a switched system which switches between open loop and closed-loop control. With this switching mechanism, the wideband disturbance controller can be made more aggressive for attenuating white noise while maintaining the stability margins and control actions. When the narrowband

disturbance is constant, an integral controller is the IMP controller. A traditional IMP controller is implemented when the narrowband disturbance is a known sinusoid. If the narrowband disturbance is a sum of known number of sinusoids, multiple IMP controllers can be placed in parallel for the rejection.

1.4   Contributions of the Thesis

Most of the internal model principle based approaches in regulation problems focus on periodic signals. In this thesis, two advanced applications of the internal model principle control theory are developed.

First, the IMP based adaptive algorithm in [55] is extended to identify EDS signals with unknown parameters in discrete time. Since the amplitude of an EDS signal varies exponentially, an additional parameter, damping factor, needs to be estimated as well as the frequency. In this algorithm, a discrete time state space model of an EDS signal is derived based on its continuous time version. Estimated signal parameters are used in this model according to the certainty equivalence principle. After two mappings between the parameter estimation errors and the states of the state space model are derived, two integral controllers are implemented to update the estimated parameters respectively. This control law results in a system output error that decays exponentially fast with a decay rate independent of the signal's damping factor. A discrete time two time scale averaging theory developed in [58] is used to prove the stability and convergence of the adaptive algorithm. Simulation results

show that this algorithm is capable of tracking time-varying parameters or a signal with multiple EDS components. This work is presented in Chapter 2, and has been published in the Proceedings of the 17th IFAC World Congress [59].

The stability analysis of the intermittent control algorithm presented in [2] was left as an open issue, which is addressed in Chapter 3 in this thesis. The intermittent control system is first modelled as a switched system with an open loop control subsystem and a closed-loop control subsystem. In order to carry out the stability analysis of the switched system model, an extended multiple Lyapunov functions approach is developed to relax some constraints imposed by existing results. In this new approach, not all constituent systems are required to have stable equilibria, as long as those subsystems satisfy a bounding condition. This allows the subsystems to not share a common equilibrium point. Thus subsystems will be defined as not stable if they have unstable equilibrium points or lack the necessary equilibrium point. The not stable subsystems are also allowed to be active for arbitrary long periods of time. In addition, this extension allows the system to switch between controllers having different dimensions or states. The extended MLF theorem and stability analysis of the intermittent integral control system are presented in Chapter 3, and have been published in the Proceedings of the 2010 American Control Conference [60, 61]. In addition, some simulation results are also presented in Chapter 3, which are included in a submission to the IEEE Transactions on Automatic Control [62].

The second advanced implementation of the internal model principle is to com-

bine the intermittent control with the adaptive IMP control algorithm introduced in Section 1.3. This extended switching control strategy can be applied to reject a periodic disturbance with unknown frequencies. The periodic disturbance can be cancelled once its frequencies are identified by the adaptive IMP control algorithm. Thus the input to the adaptive IMP controller is disconnected, and may be reconnected intermittently due to the residue error. A switched system model is formulated as well as a stability theorem. This extended intermittent cancellation control is presented in Chapter 4. Part of this chapter is submitted to the 24th Canadian Conference on Electrical and Computer Engineering [63].

1.5 Organization of the Thesis

In Chapter 2, a discrete time version internal model principle based adaptive algorithm is developed for the identification of exponentially damped sinusoids with unknown parameters. This algorithm has two updating laws, one for the estimated frequency, and one for the estimated damping factor. By using a two time scale averaging theory, this adaptive algorithm is proved to be locally exponentially stable. Three MATLAB/Simulink simulation examples are also presented to illustrate the performance of the algorithm.

In Chapter 3, a combination of open and closed-loop control strategy is presented for attenuating disturbances with both constant component and white Gaussian noise. The system switches between a state feedback control and an augmented

state feedback control with integral action. A multiple Lyapunov functions theorem is developed as an extension to existing approaches. This theorem is then used to prove the stability of the introduced system which is modelled as a switched system. A numerical example is presented to demonstrate the performance of this switching control strategy, as well as comparison with two other traditional controllers.

This switching control strategy is extended in Chapter 4, where the closed-loop mode controller includes a state feedback controller and an adaptive IMP controller. Thus this control strategy can be applied to minimize disturbances consist of white noise and a periodic disturbance with unknown frequencies. A switched system model is derived as well as a stability theorem. Simulation results are presented to demonstrate the performance improvement. In Chapter 5, some concluding remarks are drawn.

Bibliography

[1] B. A. Francis and W. M. Wonham, "The Internal Model Principle of Control Theory," *Automatica*, vol. 12, pp. 457–465, 1976.

[2] L. J. Brown, G. E. Gonye, and J. S. Schwaber, "Non-linear PI Control Inspired by Biological Control Systems," in *Proceedings of the 37th IEEE Conference on Decision and Control*, Tampa, FL, Dec. 1998, pp. 1040–1045.

[3] L. J. Brown and J. S. Schwaber, "Intermittent Cancellation Control: A Control Paradigm Inspired by Mammalian Blood Pressure Control," in *Proceedings of the American Control Conference*, San Diego, CA, Jun. 1999, pp. 139–143.

[4] N. E. Huang and Z. Shen, *et al.*, "The Empirical Mode Decomposition and the Hilbert Spectrum for Nonlinear and Non-Stationary Time Series Analysis," in *Procedures of the Royal Society of London*, vol. A454, 1998, pp. 903–995.

[5] L. Cohen, *Time-Frequency Analysis*, 1st ed. Englewood Cliffs, NJ: Prentice Hall, 1995.

[6] R. L. Streit and R. F. Barrett, "Frequency Tracking Using Hidden Markov Models," *IEEE Transactions on Acoustics, Speech and Signal Processing*, vol. 38, pp. 586–598, Apr. 1990.

[7] L. B. White, "Cartesian Hidden Markov Models with Applications," *IEEE Transactions on Signal Processing*, vol. 40, pp. 1601–1604, Jun. 1992.

[8] H. K. Kwok and D. L. Jones, "Improved Instantaneous Frequency Estimation Using an Adaptive Short-Time Fourier Transform," *IEEE Transactions on Signal Processing*, vol. 48, no. 10, pp. 2964–2972, Oct. 2000.

[9] B. F. La Scala and R. R. Bitmead, "Design of an Extended Kalman Filter Frequency Tracker," *IEEE Transactions on Signal Processing*, vol. 44, no. 3, pp. 739–742, Mar. 1996.

[10] S. Bittanti and S. Savaresi, "On the Parameterization and Design of an Extended Kalman Filter Frequency Tracker," *IEEE Transactions on Automatic Control*, vol. 45, no. 9, pp. 1718–1724, Sep. 2000.

[11] G. Li, "A Stable and Efficient Adaptive Notch Filter for Direct Frequency Estimation," *IEEE Transactions on Signal Processing*, vol. 45, no. 8, pp. 2001–2009, Aug. 1997.

[12] P. A. Regalia, "An Improved Lattice-Based Adaptive IIR Notch Filter," *IEEE Transactions on Signal Processing*, vol. 39, no. 9, pp. 2124–2128, Sep. 1991.

[13] M. V. Dragosevic and S. S. Stankovic, "An Adaptive Notch Filter with Improved Tracking Properties," *IEEE Transactions on Signal Processing*, vol. 43, no. 9, pp. 2068–2078, Sep. 1995.

[14] M. Bodson and S. C. Douglas, "Adaptive Algorithms for the Rejection of Sinusoidal Disturbances with Unknown Frequency," *Automatica*, vol. 33, no. 12, pp. 2213–2221, 1997.

[15] B. Wu and M. Bodson, "A Magnitude/Phase-Locked Loop Approach to Parameter Estimation of Periodic Signals," *IEEE Transactions on Automatic Control*, vol. 48, no. 4, pp. 612–618, Apr. 2003.

[16] R. Roy and T. Kailath, "ESPRIT-Estimation of Signal Parameters via Rotational Invariance Techniques," *IEEE Transactions on Acoustics, Speech, and Signal Processing*, vol. 37, no. 7, pp. 984–995, Jul. 1989.

[17] R. Roy, A. Paulraj, and T. Kailath, "Comparative Performance of ESPRIT and MUSIC for Direction-Of-Arrival Estimation," in *IEEE International Conference on Acoustics, Speech and Signal Processing*, Apr. 1987, pp. 2344–2347.

[18] T. C. Tsao, Y. X. Qian, and M. Nemani, "Repetitive Control for Asymptotic Tracking of Periodic Signals with an Unknown Period," *Journal of Dynamic Systems, Measurement, and Control*, vol. 122, pp. 364–369, Jun. 2000.

[19] A. Serrani, A. Isidori, and L. Marconi, "Semiglobal Nonlinear Output Regulation with Adaptive Internal Model," *IEEE Transactions on Automatic Control*, vol. 46, no. 8, pp. 1178–1194, Aug. 2001.

[20] Z. Ding, "Global Stabilization and Disturbance Suppression of a Class of Nonlinear System with Uncertain Internal Model," *Automatica*, vol. 39, pp. 471–479, 2003.

[21] R. Marino and P. Tomei, "Output Regulation for Linear Systems via Adaptive Internal Model," *IEEE Transactions on Automatic Control*, vol. 48, no. 12, pp. 2199–2202, Dec. 2003.

[22] I. D. Landau, A. Constantinescu, and D. Rey, "Adaptive narrow band disturbance rejection applied to an active suspension - an internal model approach," *Automatica*, vol. 41, pp. 563–574, 2005.

[23] R. Boyer, S. Essid, and N. Moreau, "Non-Stationary Signal Parametric Modeling Techniques with an Application to Low Bitrate Audio Coding," in *Proceedings of the 6th International Conference on Signal Processing*, Aug.26-30, 2002, pp. 430–433.

[24] R. Boyer and J. Rosier, "Iterative Method for Harmonic and Exponentially Damped Sinusoidal Models," in *Proceedings of the 5th International Conference on Digital Audio Effects*, Hamburg, Germany, Sep.26-28, 2002, pp. 145–150.

[25] Y. Hua and T. K. Sarkar, "Matrix Pencil Method for Estimating Parameters of Exponentially Damped/Undamped Sinusoids in Noise," *IEEE Transactions on Acoustics, Speech, and Signal Processing*, vol. 38, no. 5, pp. 814–824, May 1990.

[26] M. Jeanneau, P. Mouyon, and C. Pendaries, "Estimating the Parameters of Exponentially Damped Sinusoids in Light and Flexible Structures using the SIN-TRACK Method," in *Proceedings of the 13th Southeastern Symposium on System Theory*, Morgantown, WV, Mar.8-10 1998, pp. 115–119.

[27] R. Badeau, R. Boyer, and B. David, "EDS Parametric Modeling and Tracking of Audio Signals," in *Proceedings of the 5th International Conference on Digital Audio Effects*, Hamburg, Germany, Sep.26-28, 2002, pp. 1–6.

[28] A. Gunnarsson and I. Y. Gu, "Music Signal Synthesis Using Sinusoid Models and Sliding-Window ESPRIT," in *Proceedings of the 2006 IEEE International Conference on Multimedia and Expo*, Toronto, ON, Jul.9-12, 2006, pp. 1389–1392.

[29] Y. Bresler and A. Macovski, "Exact Maximum Likelihood Parameter Estimation of Superimposed Exponential Signals in Noise," *IEEE Transactions on Acoustics, Speech, and Signal Processing*, vol. ASSP-34, no. 5, pp. 1081–1089, Oct. 1986.

[30] C. K. Papadopoulos and C. L. Nikias, "Parameter Estimation of Exponentially Damped Sinusoids Using Higher Order Statistics," *IEEE Transactions on Acoustics, Speech, and Signal Processing*, vol. 38, no. 8, pp. 1424–1436, Aug. 1990.

[31] R. Kumaresan and D. W. Tufts, "Estimating the Parameters of Exponentially Damped Sinusoids and Pole-zero Modeling in Noise," *IEEE Transactions on Acoustics, Speech, and Signal Processing*, vol. ASSP-30, no. 6, pp. 833–840, Dec. 1982.

[32] J. Zhang, A. K. Swain, and S. K. Nguang, "Parameter Estimation of Exponentially Damped Sinusoids using HSVD based Extended Complex Kalman Filter," in *Proceedings of 2008 IEEE Region 10 Conference - TENCON 2008*, Hyderabad, India, Nov.18-21 2008, pp. 1–6.

[33] A. V. Savkin and R. J. Evans, *Hybrid Dynamical Systems: Controller and Sensor Switching Problems.* Boston, MA: Birkhauser, 2002.

[34] J. P. Hespanha and A. S. Morse, "Stability of Switched Systems with Average Dwell-time," in *Proceedings of the 38th IEEE Conference on Decision and Control*, Phoenix, AZ, Dec. 1999, pp. 2655–2660.

[35] A. S. Morse, Ed., *Control Using Logic-Based Switching*, 1st ed. London, UK: Springer-Verlag, 1997.

[36] D. Liberzon, *Switching in Systems and Control.* Boston, MA: Birkhauser, 2003.

[37] D. Liberzon and A. S. Morse, "Basic Problems in Stability and Design of Switched Systems," *IEEE Control Systems Magazine*, vol. 19, pp. 59–70, 1999.

[38] R. Shorten, F. Wirth, O. Mason, and K. Wulff, "Stability Criteria for Switched and Hybrid Systems," *SIAM Review*, vol. 49, no. 4, pp. 545–592, Nov. 2007.

[39] S. Boyd, L. E. Ghaoui, E. Feron, and V. Balakrishnan, *Linear Matrix Inequalities in System and Control Theory.* Philadelphia, PA: SIAM, 1994.

[40] D. Liberzon and R. Tempo, "Common Lyapunov Functions and Gradient Algorithms," *IEEE Transactions on Automatic Control*, vol. 49, no. 6, pp. 990–994, 2004.

[41] H. Lin and P. J. Antsaklis, "Stability and Stabilizability of Switched Linear Systems: A Survey of Recent Results," *IEEE Transactions on Automatic Control*, vol. 54, no. 2, pp. 308–322, Feb. 2009.

[42] R. K. Brayton and C. H. Tong, "Constructive Stability and Asymptotic Stability of Dynamical Systems: A Constructive Approach," *IEEE Transactions on Circuits and Systems*, vol. 27, no. 11, pp. 1121–1130, Nov. 1980.

[43] H. Kiendl, J. Adamy, and P. Stelzner, "Vector Norms as Lyapunov Functions for Linear Systems," *IEEE Transactions on Automatic Control*, vol. 37, no. 6, pp. 839–842, Jun. 1992.

[44] F. Blanchini, "Nonquadratic Lyapunov Functions for Robust Control," *Automatica*, vol. 31, no. 3, pp. 451–461, 1995.

[45] A. Polański, "On Absolute Stability Analysis by Polyhedral Lyapunov Functions," *Automatica*, vol. 36, no. 4, pp. 573–578, Apr. 2000.

[46] A. S. Morse, "Supervisory Control of Families of Linear Set-Point Controllers–Part 1: Exact Matching," *IEEE Transactions on Automatic Control*, vol. 41, no. 10, pp. 1413–1431, Oct. 1996.

[47] B. Hu, X. Xu, A. N. Michel, and P. J. Antsaklis, "Stability Analysis for a Class of Nonlinear Switched Systems," in *Proceedings of the 38th IEEE Conference on Decision and Control*, Phoenix, AZ, Dec. 1999, pp. 4374–4379.

[48] G. Zhai, B. Hu, K. Yasuda, and A. N. Michel, "Stability Analysis of Switched Systems with Stable and Unstable Subsystems: An Average Dwell Time Approach," in *Proceedings of the American Control Conference*, Chicago, IL, Jun. 2000, pp. 200–204.

[49] R. A. DeCarlo, M. S. Branicky, S. Pettersson, and B. Lennartson, "Perspectives and Results on the Stability and Stabilizability of Hybrid Systems," *Proceedings of the IEEE*, vol. 88, no. 7, pp. 1069–1082, Jul. 2000.

[50] M. S. Branicky, "Multiple Lyapunov Functions and Other Analysis Tools for Switched and Hybrid Systems," *IEEE Transactions on Automatic Control*, vol. 43, no. 4, pp. 475–482, Apr. 1998.

[51] G. Zhai, I. Matsune, J. Imae, and T. Kobayashi, "A Note on Multiple Lyapunov Functions and Stability Condition for Switched and Hybrid Systems," in *Proceedings of the 16th IEEE International Conference on Control Applications*, Singapore, Oct.1-3, 2007, pp. 226–231.

[52] H. Ye, A. N. Michel, and L. Hou, "Stability Analysis of Discontinuous Dynamical Systems with Applications," in *Proceedings of the 13th World Congress of the International Federation of Automatic Control*, vol. E, San Francisco, CA, Jun. 1996, pp. 461–466.

[53] ——, "Stability Theory for Hybrid Dynamical Systems," *IEEE Transactions on Automatic Control*, vol. 43, no. 4, pp. 461–474, Apr. 1998.

[54] M. Johansson and A. Rantzer, "Computation of Piecewise Quadratic Lyapunov Functions for Hybrid Systems," *IEEE Transactions on Automatic Control*, vol. 43, no. 4, pp. 555–559, Apr. 1998.

[55] L. J. Brown and Q. Zhang, "Identification of Periodic Signals with Uncertain Frequency," *IEEE Transactions on Signal Processing*, vol. 51, no. 6, pp. 1538–1545, Jun. 2003.

[56] L. J. Brown and Q. Zhang, "Periodic Disturbance Cancellation with Uncertain Frequency," *Automatica*, vol. 40, pp. 631–637, 2004.

[57] R. Marino and P. Tomei, "Global Estimation of n Unknown Frequencies," *IEEE Transactions on Automatic Control*, vol. 47, no. 8, pp. 1324–1328, Aug. 2002.

[58] E. Bai, L. Fu, and S. S. Sastry, "Averaging Analysis for Discrete Time and Sampled Data Adaptive Systems," *IEEE Transactions on Circuits and Systems*, vol. 35, no. 2, pp. 137–148, Feb. 1988.

[59] J. Lu and L. J. Brown, "Identification of Exponentially Damped Sinusoidal Signals," in *Proceedings of the 17th IFAC World Congress*, Seoul, South Korea, Jul.6-11, 2008, pp. 5089–5094.

[60] ——, "A Multiple Lyapunov Functions Approach for Stability of Switched Systems," in *Proceedings of the 2010 American Control Conference*, Baltimore, MD, Jul. 2010, pp. 3253–3256.

[61] ——, "Stability Analysis of a Proportional with Intermittent Integral Control System," in *Proceedings of the 2010 American Control Conference*, Baltimore, MD, Jul. 2010, pp. 3257–3262.

[62] ——, "Combining Open and Closed-Loop Control via Intermittent Integral Control Action," *IEEE Transactions on Automatic Control*, submitted.

[63] ——, "A Combination of Open and Closed-Loop Control for Disturbance Rejection," *The 24th Canadian Conference on Electrical and Computer Engineering*, submitted.

Chapter 2

Identification of Exponentially Damped

Sinusoidal Signals [1]

2.1   Introduction

In this chapter, we consider signals composed of a sum of exponentially damped sinusoids with the following form,

$$s(k) = \sum_{i=1}^{N} s_i(k) = \sum_{i=1}^{N} a_i e^{-\sigma_i k} \sin(\omega_i k + \varphi_i) \tag{2.1}$$

where the uncertain σ_i and ω_i are the damping factor and the frequency, respectively. This form can also represent constant-amplitude sinusoids, and constant signals. The objective is to estimate the parameters σ_i and ω_i. There have been many techniques developed to deal with predictable signals, such as narrowband or sinusoidal signals,

---

since they appear in both signal processing and control applications, including active noise control, radar signals, rotating mechanical systems, computer hard disk drive *etc.* [1]. These techniques include linear quadratic regulator based modern control, higher harmonic control [2], adaptive notch filter [3], adaptive feedforward cancellation (AFC) [4], adaptive observer technique [5].

Another common approach for perfect cancellation of signals is based on a fundamental control principle, the *internal model principle* (IMP) [6]. This principle states that perfect disturbance rejection or reference tracking is achieved when a model of the dynamic structure of the disturbance or reference signal is incorporated in a stable feedback loop. The accuracy of regulation depends critically on the fidelity of the IMP controller. Errors of less than one percent in model coefficients can lead to unacceptable residual errors. Thus, the ability to adaptively tune the model parameters, which can be completely specified as damping factors and frequencies, is of great benefit. Then adaptive IMP controllers can provide exact reproduction of the predictable part of a signal, and when they do, they provide highly accurate estimates of the signal parameters. One application of the IMP to periodic disturbance rejection is repetitive control for time-lag systems and multi-link manipulators [7]. Serrani *et al.* [8] also presented a solution to a nonlinear output regulation problem based on the IMP.

An IMP based adaptive algorithm for canceling quasi-periodic, or narrowband signals with uncertain frequencies is presented in [1]. This approach begins with a

state space implementation of the standard IMP controller with the best estimate of the frequency used. A simple mapping from the states of the controller to the error in the frequency estimate was developed and this "measurement" of the frequency error is used to update the parameters of the IMP controller. When this adaptive IMP controller is placed into a feedback loop, the resulting closed-loop system achieves perfect frequency estimation of the elements of a sum of sinusoidal signals.

In addition to sinusoidal signals, EDS signals are often used to model audio signals, such as speech or music, which contain relatively fast variations in amplitude. The conventional sinusoidal model is thus extended by allowing the amplitude to evolve exponentially as given by (2.1). A well-known approach to EDS signal parameter estimation is the polynomial or linear prediction method as in [9]. Traditionally, EDS signal model is associated with a high resolution parameter estimation method, such as matrix pencil, ESPRIT or Kung's algorithm, [10]. Hua *et al.* [11] presented a matrix pencil method as an alternative approach which exploits the structure of a matrix pencil of the EDS signal $s_i(t)$, instead of the structure of prediction equations satisfied by $s_i(t)$. In [12], the EDS signal parameters, damping factor and frequency, are estimated using a subspace based matrix pencil high resolution method. The tracking of the slow variation of the signal parameters is achieved using an adaptive least mean square algorithm.

Motivated by the IMP based adaptive algorithm in [1], an extended adaptive algorithm for EDS disturbance cancellation was developed in [13]. The control law

results in a system output error that decays exponentially fast with a decay rate independent of σ_i. This is equivalent to what is meant when integral control is said to provide perfect set-point tracking. This work was developed only in continuous time framework and strictly as a control algorithm. Here we develop a discrete time implementation of this algorithm, and convert the control algorithm into a signal processing algorithm.

This chapter is organized as follows: In Section 2.2, the motivation, the continuous time state space representation of the IMP controller, is introduced. Then the derivation of the IMP based adaptive algorithm for EDS signal identification in discrete time is presented. The convergence and stability property of the proposed adaptive algorithm is analyzed based on a discrete time two time scale averaging theory in Section 2.3. Simulation results are demonstrated in Section 2.4, followed by some conclusions in Section 2.5.

2.2 Internal Model Principle Based Adaptive Algorithm

2.2.1 Adaptive algorithm in continuous time

The basic structure of the feedback system is shown in Fig. 2.1, where L is a tuning function that is properly designed to stabilize the system, H represents the IMP controller. d is an EDS signal, which is defined as follows,
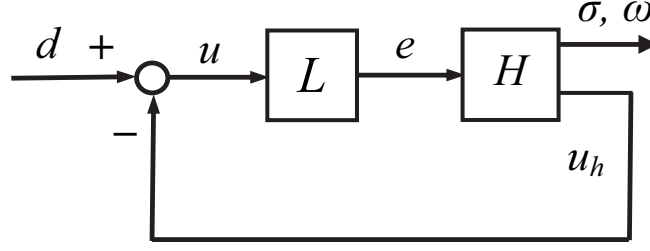
Figure 2.1: Block diagram of an internal model principle control system

$$d(t) = ae^{-\sigma_c t} \sin(\omega_c t + \varphi), \quad \sigma_c > 0, \ \omega_c > 0, \ a > 0 \tag{2.2}$$

where σ_c, ω_c are the damping factor and frequency, respectively. Thus, following IMP

theory, a continuous time state space representation of an IMP controller is

$$\begin{bmatrix} \dot{x}_1 \\ \dot{x}_2 \end{bmatrix} = \begin{bmatrix} -\sigma_c & \omega_c \\ -\omega_c & -\sigma_c \end{bmatrix} \begin{bmatrix} x_1 \\ x_2 \end{bmatrix} + \begin{bmatrix} 0 \\ 1 \end{bmatrix} e \tag{2.3}$$

$$u_h = \begin{bmatrix} K_1 & K_2 \end{bmatrix} \begin{bmatrix} x_1 \\ x_2 \end{bmatrix} \tag{2.4}$$

where K_1, K_2 are tuning gains.

If the initial conditions for x_1 and x_2 are given by $x_1(0) = \dfrac{a \cos \varphi}{\sqrt{K_1^2 + K_2^2}}$, $x_2(0) = \dfrac{a \sin \varphi}{\sqrt{K_1^2 + K_2^2}}$, then for all $t > 0$, $e = 0$ and

$$x_1(t) = \frac{ae^{-\sigma_c t}}{\sqrt{K_1^2 + K_2^2}} \cos(\omega_c t + \varphi) \tag{2.5}$$

$$x_2(t) = \frac{ae^{-\sigma_c t}}{\sqrt{K_1^2 + K_2^2}} \sin(\omega_c t + \varphi) \tag{2.6}$$

By letting $\mathbf{x} = |\mathbf{x}|\angle\theta = x_1(t) + jx_2(t)$, we can get

$$|\mathbf{x}| = \frac{ae^{-\sigma_c t}}{\sqrt{K_1^2 + K_2^2}} \tag{2.7}$$

$$\theta = \tan^{-1}\left(\frac{x_2(t)}{x_1(t)}\right) = \omega_c t + \varphi \tag{2.8}$$

where $\tan^{-1}(\cdot)$ is defined to have a range given by real numbers such that θ is continuous in t. Differentiating both sides of (2.7) and (2.8), we have

$$\sigma_c = -\frac{1}{|\mathbf{x}|}\frac{\mathrm{d}|\mathbf{x}|}{\mathrm{d}t} \tag{2.9}$$

and

$$\omega_c = \frac{\mathrm{d}\theta}{\mathrm{d}t} \tag{2.10}$$

In practice, the model parameters in (2.3) and (2.4) are approximations, giving

$$\hat{\sigma}_c = -\frac{1}{|\mathbf{x}|}\frac{\mathrm{d}|\mathbf{x}|}{\mathrm{d}t} = -\frac{x_1\dot{x}_1 + x_2\dot{x}_2}{x_1^2 + x_2^2} = \sigma - \frac{ex_2}{x_1^2 + x_2^2} \tag{2.11}$$

and

$$\hat{\omega}_c = \frac{\mathrm{d}\theta}{\mathrm{d}t} = \frac{\mathrm{d}}{\mathrm{d}t}\tan^{-1}\left(\frac{x_2(t)}{x_1(t)}\right) = \frac{\dot{x}_1 x_2 - x_1\dot{x}_2}{x_1^2 + x_2^2} = \omega - \frac{ex_1}{x_1^2 + x_2^2} \tag{2.12}$$

Thus the error between $\hat{\sigma}_c$ and σ can be expressed as

$$\tilde{\sigma} = -\frac{ex_2}{x_1^2 + x_2^2} \tag{2.13}$$

Similarly, the error between $\hat{\omega}_c$ and ω is

$$\tilde{\omega} = -\frac{ex_1}{x_1^2 + x_2^2} \tag{2.14}$$

(2.11) and (2.12) can be used to estimate the damping factor and frequency of the EDS signal.

2.2.2 Derivation of the adaptive algorithm in discrete time

The discrete time state space equation of the IMP controller can be converted from its continuous time counterpart (2.3) and (2.4) as

$$\begin{bmatrix} x_1(k+1) \\ x_2(k+1) \end{bmatrix} = e^{-\sigma} \begin{bmatrix} \cos\omega & \sin\omega \\ -\sin\omega & \cos\omega \end{bmatrix} \begin{bmatrix} x_1(k) \\ x_2(k) \end{bmatrix} + \begin{bmatrix} 0 \\ 1 \end{bmatrix} e(k) \tag{2.15}$$

$$u_h(k) = \begin{bmatrix} K_1 & K_2 \end{bmatrix} \begin{bmatrix} x_1(k) \\ x_2(k) \end{bmatrix} \tag{2.16}$$

Therefore at sampling instant $t = kT_s$, continuous time estimation errors (2.13)

and (2.14) are equal to the following discrete time estimation errors

$$\widetilde{\sigma}(k) = -\frac{e(k)x_2(k)}{x_1^2(k) + x_2^2(k)} \tag{2.17}$$

$$\widetilde{\omega}(k) = -\frac{e(k)x_1(k)}{x_1^2(k) + x_2^2(k)} \tag{2.18}$$

and the estimates of the damping factor and frequency can be updated by using two integral controllers

$$\sigma(k+1) = \sigma(k) + \varepsilon\widetilde{\sigma}(k)$$

$$= \sigma(k) - \varepsilon\frac{e(k)x_2(k)}{x_1^2(k) + x_2^2(k)} \tag{2.19}$$

$$\omega(k+1) = \omega(k) + \varepsilon K_b\widetilde{\omega}(k)$$

$$= \omega(k) - \varepsilon K_b\frac{e(k)x_1(k)}{x_1^2(k) + x_2^2(k)} \tag{2.20}$$

where ε is a small adaptation gain, K_b is a constant, and both are positive.

From (2.19) and (2.20), it can be seen that if $x_1(k) = 0$ and $x_2(k) = 0$, the integral update laws are undefined as both the numerators and denominators are 0. This problem can be avoided by adding a small constant C in the denominators of both equations, or setting $\varepsilon = 0$ when $|\mathbf{x}|$ is less than a constant.

Fig. 2.2 and Fig. 2.3 show the structure of the IMP based adaptive feedback system, where AIM means adaptive IMP controller. The function $F_k(\mathbf{x}, e)$ is what have been derived in (2.17) and (2.18). Due to the structure of the IMP controller,
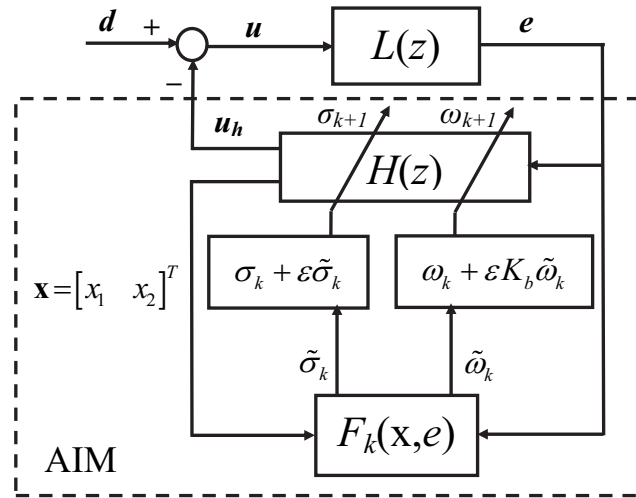
Figure 2.2: Block diagram of the adaptive IMP control system
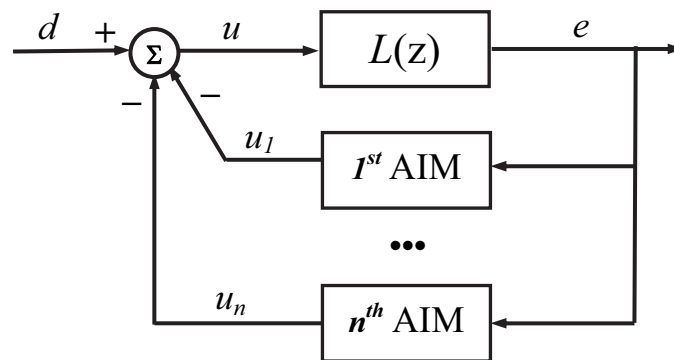
Figure 2.3: Block diagram of an adaptive IMP feedback control system for multi-EDS signals

a controller can only achieve identification of a single EDS mode. If the signal $d(k)$ is composed of multiple EDS modes, multiple adaptive IMP controllers are placed in parallel.

By incorporating the adaptive update laws (2.19)-(2.20), the IMP controller parameters, σ and ω, converge to the true values σ_c and ω_c of the EDS signal. If σ_c or ω_c changes with time, e is not zero and the adaptive algorithm will estimate and track the changing parameters.

Note that for a sampled-data system, some knowledge of the EDS signal frequency is necessary to determine the sampling frequency.

2.3 Convergence and Stability Analysis

The stability analysis of the proposed adaptive algorithm in continuous time is presented in [13]. Singular perturbation theorem [14], and averaging theorem [15], are used for the analysis. Bai *et al.* adapted these two theorems in a combined discrete time version, *Theorem 2.2.4. Exponential Stability Theorem for Two-Time Scale System*, in [16].

The feedback system is now formulated as a two time scale model. Due to the limitation of space, we will address only the case where the signal is composed of a single EDS. The techniques for extending the proof to the multi-EDS case are shown in [1, 17]. The primary change in the proof is that the equilibria x_{10} and x_{20} defined in equations (2.32) and (2.33) will have terms corresponding to each mode, and the calculation of the averaging function will be far more complicated. However, as simple sinusoids, these extra terms will ultimately contribute nothing to the average, beyond possibly requiring longer averaging times. Detailed calculations of the averaged function have also been omitted for space reasons. The state space equations for the adaptive feedback system in Fig. 2.2 are as follows:

$$x_p(k+1) = A_p x_p(k) + B_p u(k) \tag{2.21}$$

$$e(k) = C_p x_p(k) \tag{2.22}$$

$$u(k) = -K_1 x_1(k) - K_2 x_2(k) + d(k) \tag{2.23}$$

$$d(k) = a e^{-\sigma_c k} \sin(\omega_c k) + c_1 \tag{2.24}$$

$$x_1(k+1) = (e^{-\sigma} \cos \omega) x_1(k) + (e^{-\sigma} \sin \omega) x_2(k) \tag{2.25}$$

$$x_2(k+1) = -(e^{-\sigma} \sin \omega) x_1(k) + (e^{-\sigma} \cos \omega) x_2(k) + e(k) \tag{2.26}$$

$$\sigma(k+1) = \sigma(k) - \varepsilon \frac{e(k) x_2(k)}{x_1^2(k) + x_2^2(k)} \tag{2.27}$$

$$\omega(k+1) = \omega(k) - \varepsilon K_b \frac{e(k) x_1(k)}{x_1^2(k) + x_2^2(k)} \tag{2.28}$$

where (2.21) and (2.22) are a state space representation for $L(z)$. The presence of the bias c_1 in the exogenous signal (2.24) does not affect the convergence property of the algorithm if $L(1) = 0$.

Perturbation analysis proceeds by fixing $\sigma(k) = \sigma$, and $\omega(k) = \omega$. Under these conditions, the transfer function of the IMP controller is

$$H(z) = \frac{K_2 z + K_1 e^{-\sigma} \sin \omega - K_2 e^{-\sigma} \cos \omega}{z^2 - 2z e^{-\sigma} \cos \omega + e^{-2\sigma}}$$
$$:= \frac{N(z)}{D(z)}.$$

The tuning function can also be expressed as a rational polynomial form as $L(z) = \frac{B(z)}{A(z)}$. Thus the transfer function from $d(k)$ to $e(k)$ can be given by

$$G_{ed}(z) = \frac{B(z) D(z)}{A(z) D(z) + B(z) N(z)}$$

$$= (z^2 - 2ze^{-\sigma}\cos\omega + e^{-2\sigma})Q(z)$$

where $Q(z) = \frac{B(z)}{A(z)D(z)+B(z)N(z)}$. The transfer functions from $d(k)$ to $x_1(k)$ and $x_2(k)$ can also be derived as

$$G_{x_1 d}(z) = (e^{-\sigma}\sin\omega)Q(z),$$

$$G_{x_2 d}(z) = (z - e^{-\sigma}\cos\omega)Q(z).$$

Now in order to formulate the two time scale model, we introduce new state variables, σ_e, ω_e, x_{pe}, x_{1e}, x_{2e}, as follows:

$$\sigma_e(k) = \sigma(k) - \sigma_c \tag{2.29}$$

$$\omega_e(k) = \omega(k) - \omega_c \tag{2.30}$$

$$x_{pe}(k) = x_p(k) - x_{p0}(k) \tag{2.31}$$

$$x_{1e}(k) = x_1(k) - a|Q|e^{-\sigma_c k - \sigma(k)}\sin\omega(k)\sin(\omega_c k + \angle Q)$$

$$:= x_1(k) - x_{10}(k) \tag{2.32}$$

$$x_{2e}(k) = x_2(k) - a|Q|e^{-\sigma_c k - \sigma(k)}\left[e^{-\sigma_c}\sin\omega_c\cos(\omega_c k + \angle Q)\right.$$

$$\left. + (e^{-\sigma_c}\cos\omega_c - e^{-\sigma(k)}\cos\omega(k))\sin(\omega_c k + \angle Q)\right]$$

$$:= x_2(k) - x_{20}(k) \tag{2.33}$$

where x_{p0}, x_{10}, x_{20} are steady state solutions when the slow states are fixed at σ and

ω. $|Q|$ and $\angle Q$ denote the magnitude and angle of $Q(z)$ evaluated at $z = \mathrm{e}^{-\sigma_c + j\omega_c}$, respectively, and $\sigma = \sigma(k)$, $\omega = \omega(k)$. By letting

$$\mathbf{x}(k) = \begin{bmatrix} \sigma_e(k) \\ \omega_e(k) \end{bmatrix}, \quad \mathbf{y}(k) = \begin{bmatrix} x_{pe}(k) \\ x_{1e}(k) \\ x_{2e}(k) \end{bmatrix},$$

and substituting these new state variables into the system state equations, we can derive a two time scale model form

$$\mathbf{x}(k+1) = \mathbf{x}(k) + \varepsilon \begin{bmatrix} f_1(k, \mathbf{x}, \mathbf{y}) \\ f_2(k, \mathbf{x}, \mathbf{y}) \end{bmatrix} \tag{2.34}$$

$$\mathbf{y}(k+1) = A\big(\mathbf{x}(k)\big)\mathbf{y}(k) \tag{2.35}$$

where

$$f_1 = -\frac{C_p\big(x_{pe}(k) + x_{p0}(k)\big)\big(x_{2e}(k) + x_{20}(k)\big)}{\big(x_{1e}(k) + x_{10}(k)\big)^2 + \big(x_{2e}(k) + x_{20}(k)\big)^2} \tag{2.36}$$

$$f_2 = -\frac{K_b C_p\big(x_{pe}(k) + x_{p0}(k)\big)\big(x_{1e}(k) + x_{10}(k)\big)}{\big(x_{1e}(k) + x_{10}(k)\big)^2 + \big(x_{2e}(k) + x_{20}(k)\big)^2} \tag{2.37}$$

and

$$A = \begin{bmatrix} A_p & -K_1 B_p & -K_2 B_p \\ 0 & \exp(-\sigma_e - \sigma_c)\cos(\omega_e + \omega_c) & \exp(-\sigma_e - \sigma_c)\sin(\omega_e + \omega_c) \\ C_p & -\exp(-\sigma_e - \sigma_c)\sin(\omega_e + \omega_c) & \exp(-\sigma_e - \sigma_c)\cos(\omega_e + \omega_c) \end{bmatrix} \quad (2.38)$$

For the adaptive feedback system (2.34) and (2.35), we have the following stability and convergence theorem.

Theorem 2.1. *Consider the dynamic system* (2.34)-(2.35), *with input signal given by* (2.24), *if the following assumptions are satisfied*

1. *The tuning function* $L(z)$ *is not equal to zero when* $z = e^{-\sigma_c + j\omega_c}$, *and* $a \neq 0$;

2. *For all fixed* σ *and* ω, *matrix A has eigenvalues less than one, i.e., the system of Fig. 2.2 with* $H(z)$ *given by* (2.15), (2.16), *has poles strictly within the unit circle;*

3. $L(1) = 0$,

then there exists ε^*, *such that for all* $0 < \varepsilon < \varepsilon^*$, *the origin of* (2.34) *and* (2.35) *is locally exponentially stable. Note assumption* (3) *is not required if* $d(k)$ *is zero mean, i.e.* $c_1 = 0$.

Proof of this theorem results from direct application of Theorem 2.2.4. in [16]. This has two main requirements. It requires the fast system (2.35) to be stable,

which is satisfied by assumption (2), and the average of the slow system (2.34) is also required to be stable. In [13], it is shown that

$$\frac{\omega_c}{2\pi} \int_0^{2\pi/\omega_c} f_1 \mathrm{d}t = \omega - \omega_c + \frac{\omega_c}{\pi} \times \ln \frac{(\sigma - \sigma_c)^2 + \omega^2}{\omega_c^2}$$

and

$$\frac{\omega_c}{2\pi} \int_0^{2\pi/\omega_c} f_2 \mathrm{d}t = \sigma - \sigma_c + \frac{2\omega_c}{\pi} \tan^{-1} \frac{\sigma - \sigma_c}{\omega}$$

where x_{1e}, x_{2e} and x_{pe} are zero and time index k has been replaced by a continuous time variable. Stability of the resulting average system is easily shown by Lyapunov's first method. The details showing that the average calculated by summation is equivalent is more complicated and has been omitted. Other technical conditions of Theorem 2.2.4 can be easily verified.

The two time scale requirement of the theory leads to the idea that ε^* will be significantly less than the magnitude of the smallest eigenvalue of $(I - A)$. Practically, for exponential stability of $\mathbf{x}(k)$ to require convergence of σ and ω to their true values in the presence of noise, ε must be significantly greater than σ_c. Otherwise, $\mathbf{x}(k)$ will go to zero simply as a result of $d(k)$ going to zero. Thus selection of $L(z)$ and ε must be done to ensure that a three time scale system is generated in order for the algorithm to function.

2.4 Simulations

In this section, the performance of the proposed adaptive algorithm is examined via simulations. All simulations are created in MATLAB and Simulink environment using discrete solver with time units normalized such that $T_s = 1$ unit time. In this case, the frequency unit rad/s means radians per sample. For example, if a signal frequency is $60Hz$, then the Nyquist frequency is $314Hz$, the sampling frequency is $628Hz$, and one sample corresponds to 1.6 milliseconds. Three signals are used to conduct the simulations: (1) A single EDS signal with step changes on both parameters plus a constant offset and Gaussian noise; (2) A single EDS signal with time-varying damping factor plus a constant offset and Gaussian noise; (3) A multi-EDS modes signal plus a constant offset and Gaussian noise. The tuning function is chosen as $L(z) = (z^2 - z)/(z^2 - 0.75z + 0.01)$, so that the closed-loop feedback system is stable. Note that for pure sinusoidal signals, Zhang and Brown [18] presented a performance analysis for the IMP based adaptive algorithm for uncertain frequency identification. In this article, the tuning function $L(z)$ is chosen as a function of ω such that the closed-loop system is a bandpass filter with a notch of width $\mathbf{W}$. By incorporating this bandpass filter in $L(z)$, formulae are derived for calculating the variance for the estimated frequency. With a signal to noise ratio given by SNR, the variance of ω was found to be $\varepsilon^2 * \mathbf{W} * \omega * \mathrm{SNR}$ where ε is the adaptation gain as in this work. This analysis can be extended to EDS signals that we are interested in.

For the first simulation, the EDS signal is given by

$$d(k) = 3\mathrm{e}^{-0.005k} \sin(0.5k) + 1 + n(k), \quad 0 \le k \le 149.$$

At 150 sample point, its damping factor changes from 0.005 to 0.01 and its frequency has a step change from 0.5 rad/s to 0.6 rad/s. In order to avoid the discontinuities in the signal magnitude and phase, the signal is given by

$$d(k) = 3\mathrm{e}^{-0.01k+0.75} \sin(0.6k - 15) + 1 + n(k), \quad 150 \le k \le 300.$$

The additive Gaussian noise $n(k)$ has zero mean and variance 0.0001. The initial conditions are $\sigma(0) = 0.008$, $\omega(0) = 0.2$ rad/s. The tuning parameters are $K_1 = 0.5$, $K_2 = 0.3$, $\varepsilon = 0.05$, $K_b = 2$. The magnitude of the dominant eigenvalue of matrix A is 0.9062. The algorithm presented here, with an integral action contained in the tuning function $L(z)$, is not affected by the presence of constant offsets, unlike other algorithms in the literature. Fig. 2.4 shows the signal and error response plots. The error converges to zero at 40 samples with a decay rate significantly greater than the EDS signal's damping factor. Fig. 2.5 shows that the IMP controller's parameters converge to the true values of the EDS signal at about 40 samples. After the step changes in both parameters, it takes about 50 samples for σ and 25 samples for ω to converge to their new values. In order to evaluate the performance of the algorithm, we measure the variances of estimated parameters in a steady state time
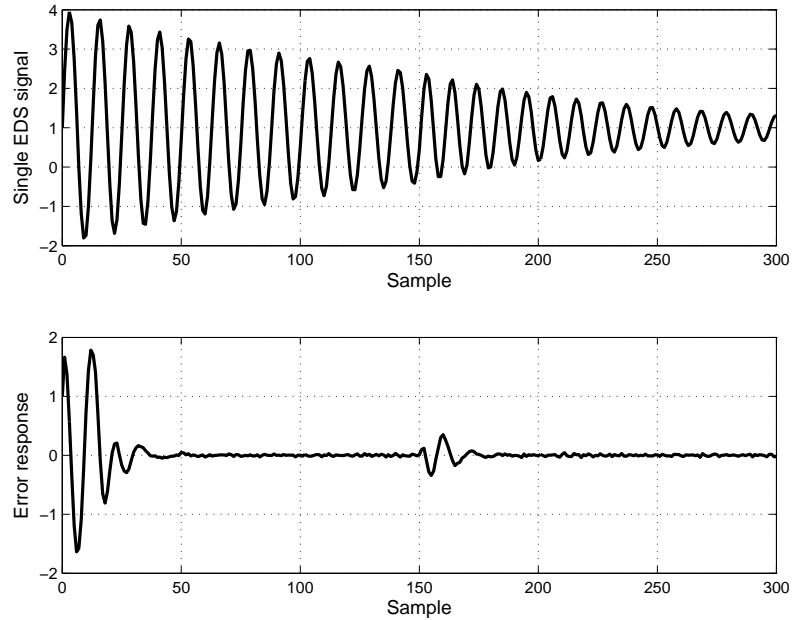
Figure 2.4: Single EDS signal with a parameter step change and error response

period. From sample point 50 to sample point 150, the measurements are $\text{var}(\sigma) = 7.7 \times 10^{-8}$, $\text{var}(\omega) = 1.8 \times 10^{-7}$.

For the second simulation, the EDS signal is

$$d(k) = 3 \exp\left(\sum_{i=0}^{k} 0.02 \sin(0.03i)\right) \sin(0.5k) + 1 + n(k),$$

with its damping factor defined as $\sigma_c(k) = 0.02 \sin(0.03k)$. The additive Gaussian noise has zero mean and variance 0.0001. The initial conditions are $\sigma(0) = 0.05$, $\omega(0) = 0.2 \ rad/s$. The tuning parameters are $K_1 = 0.5$, $K_2 = 0.3$, $\varepsilon = 0.12$, $K_b = 0.83$. Since the damping factor is time-varying, in order to minimize the tracking delay, the integral gain for σ has been increased while keeping the integral gain for ω unchanged. Fig. 2.6 shows the EDS signal with time-varying damping
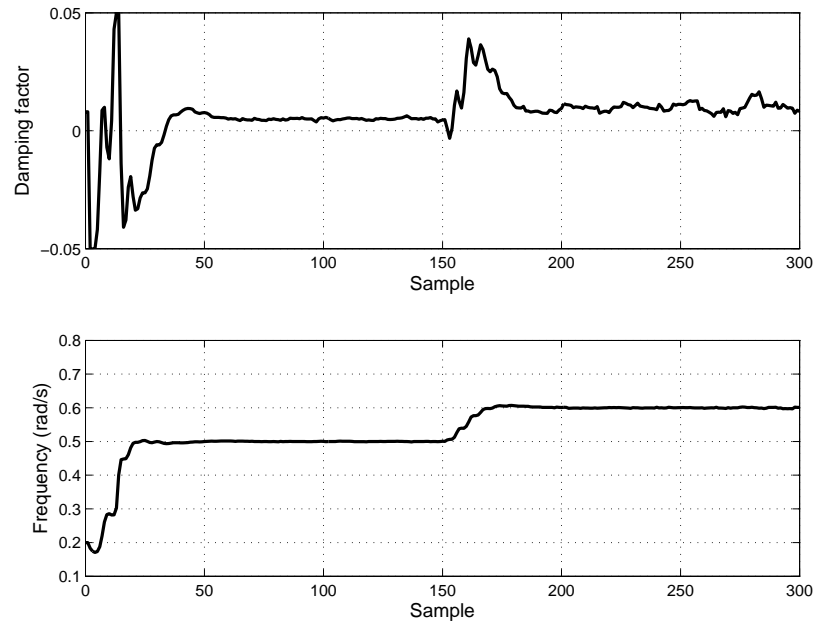
Figure 2.5: Parameter estimation of a single EDS signal with a parameter step change

factor and the error response of the adaptive feedback system. It can be observed that the error decays to zero at a rate independent of the EDS signal's damping factor. The top plot in Fig. 2.7 demonstrates the tracking performance of the adaptive algorithm. The estimated damping factor tracks the true value after 40 samples with 8.5 samples delay. The estimated constant frequency is illustrated in the bottom plot. From sample point 50 to sample point 260, the variances for estimated parameters are calculated as $\text{var}(\omega) = 1.2 \times 10^{-6}$ and the variance of σ defined as $\text{var}(\sigma(i) - 0.02\sin(0.03(i - 8.5)))$ equals 9.3×10^{-7}.

The signal for the third simulation is

$$d(k) = d_1(k) + d_2(k) + 2 + n(k),$$

Figure 2.6: Single EDS signal with time-varying damping factor and error response
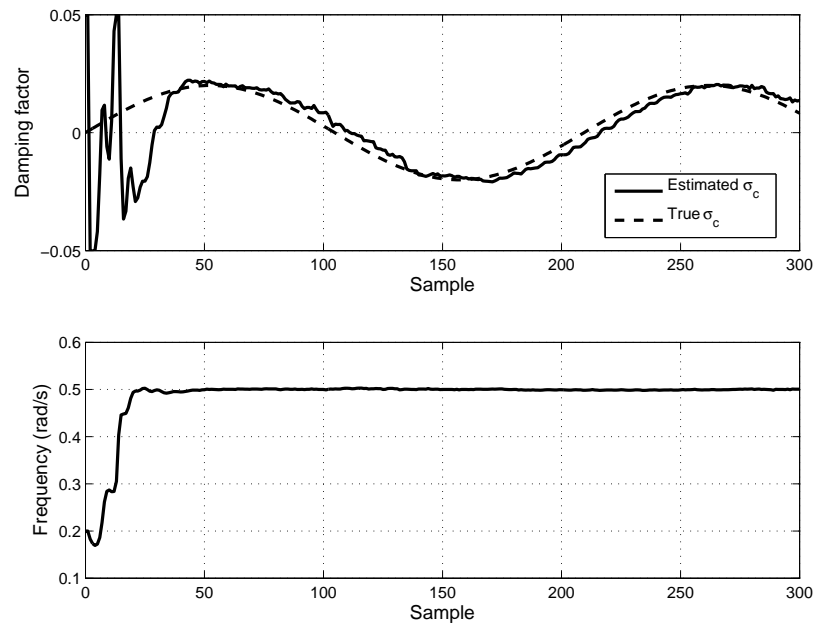
Figure 2.7: Parameter estimation of a single EDS signal with time-varying damping factor

where

$$d_1(k) = 2\mathrm{e}^{-0.007k}\sin(0.3k),$$

$$d_2(k) = 3\mathrm{e}^{-0.012k}\sin(0.5k)$$

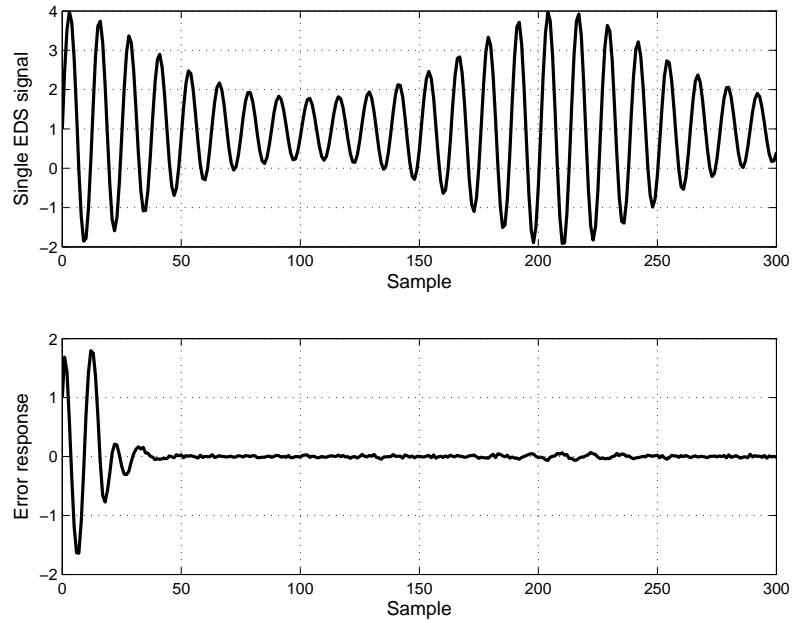with initial conditions

$$\sigma_1(0) = 0.005, \ \omega_1(0) = 0.2 \ rad/s,$$

$$\sigma_2(0) = 0.015, \ \omega_2(0) = 0.65 \ rad/s.$$

The additive Gaussian noise has zero mean and variance 0.0001. The tuning parameters are the same for each IMP controller as $K_1 = 0.1$, $K_2 = 0.1$, $\varepsilon = 0.03$, $K_b = 1$. The magnitude of the dominant eigenvalue of matrix A is 0.9504. Fig. 2.8 shows the multi-EDS signal and the error response of the feedback system. As ε has been reduced, we see slower convergence in Fig. 2.9 and 2.10. This has been seen to be required in practice and can be inferred from the averaging proof as the averaging period is now calculated for a sum of sinusoids. From sample point 200 to sample point 300, the variances for estimated parameters are $\mathrm{var}(\sigma_1) = 3.8 \times 10^{-7}$, $\mathrm{var}(\omega_1) = 1.1 \times 10^{-7}$, $\mathrm{var}(\sigma_2) = 4.6 \times 10^{-7}$, $\mathrm{var}(\omega_2) = 1.5 \times 10^{-7}$.
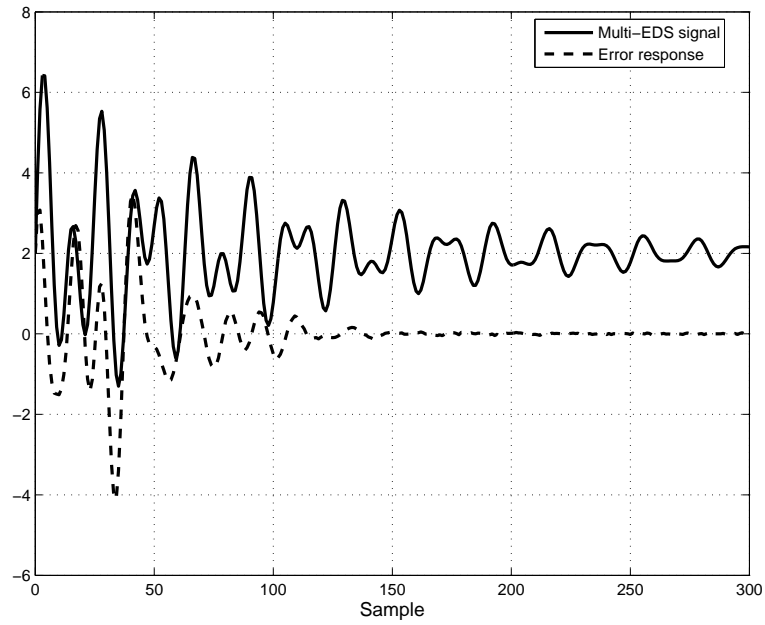
Figure 2.8: Multi-EDS signal and error response
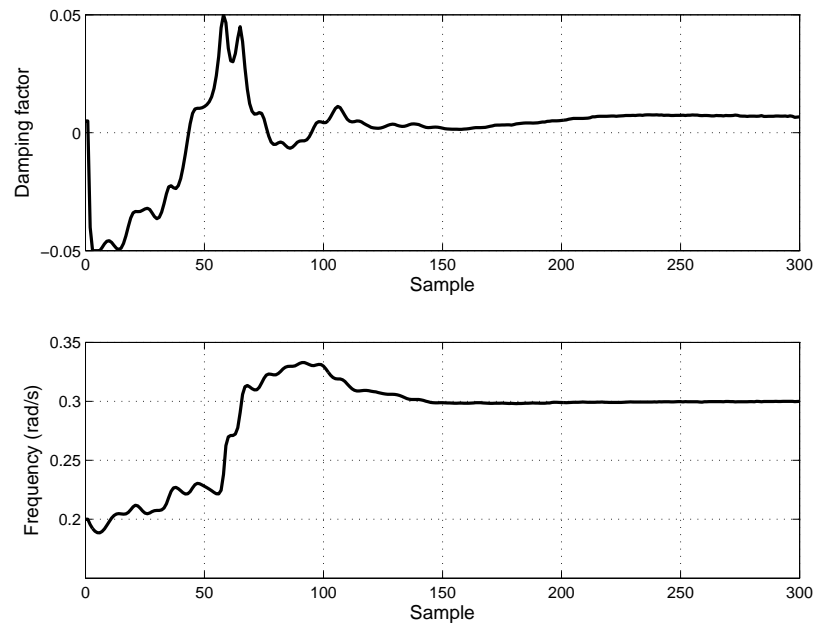
Figure 2.9: Parameter estimation for EDS mode $d_1(k)$
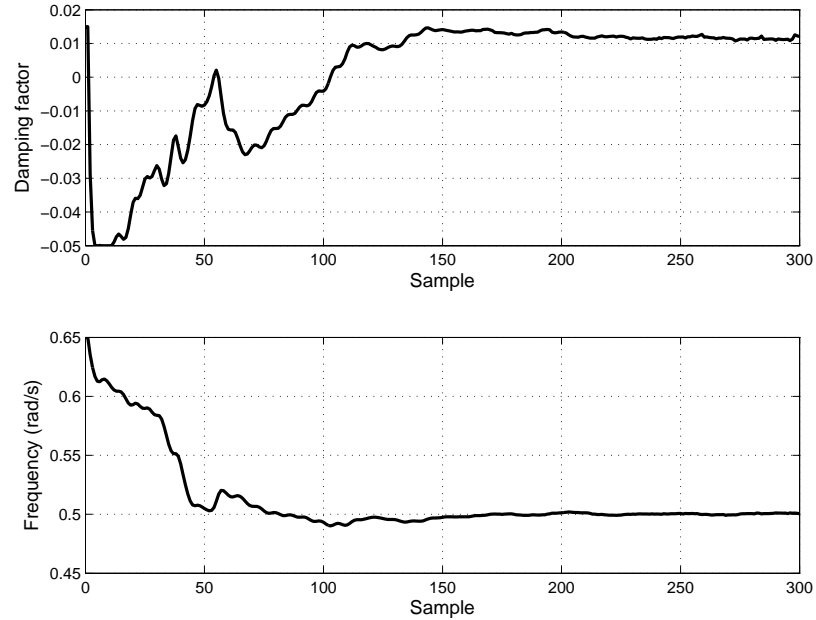
Figure 2.10: Parameter estimation for EDS mode $d_2(k)$

2.5 Conclusions

An IMP based adaptive algorithm is developed in discrete time for identifying exponentially damped sinusoidal signals. Both the damping factor and frequency of the signal can be estimated using the time-varying state variables of the IMP controller. This adaptive algorithm can not only identify constant parameters, but also track slowly time-varying parameters. By constructing a series of IMP controllers in parallel, the adaptive feedback system can identify a signal composed of a sum of EDS components, with each IMP controller corresponding to one EDS component.

In the first simulation, the slow system has almost the same speed as the fast system. In the third simulation, the fast system is faster by a factor of 2 than the slow system. From these simulations, our algorithm has shown its functionality despite

the limitation that the slow system shall be slower than the fast system. In order to speed up our algorithm, we can place the closed-loop poles closer to the origin by tuning the function $L(z)$. Also note that the variance measurements are zero for noise free simulation cases.

The proposed algorithm is shown to be locally exponentially stable, with convergence rates given by the design parameters, independent of the signal strength and almost independent of the signal parameters. (By almost we refer to the natural restrictions that convergence cannot be faster than $1/\omega_c$, and must be faster than σ_c.) Because of the local nature of the stability result, initial choice for σ and ω can be critical.

Bibliography

[1] L. J. Brown and Q. Zhang, "Identification of Periodic Signals with Uncertain Frequency," *IEEE Transactions on Signal Processing*, vol. 51, no. 6, pp. 1538–1545, Jun. 2003.

[2] L. A. Sievers and A. H. von Flotow, "Comparison and Extensions of Control Methods for Narrow-band Disturbance Rejection," *IEEE Transactions on Signal Processing*, vol. 40, no. 10, pp. 2377–2391, Oct. 1992.

[3] P. A. Regalia, "An Improved Lattice-Based Adaptive IIR Notch Filter," *IEEE Transactions on Signal Processing*, vol. 39, no. 9, pp. 2124–2128, Sep. 1991.

[4] M. Bodson and S. C. Douglas, "Adaptive Algorithms for the Rejection of Sinusoidal Disturbances with Unknown Frequency," *Automatica*, vol. 33, no. 12, pp. 2213–2221, 1997.

[5] R. Marino and P. Tomei, "Global Estimation of n Unknown Frequencies," *IEEE Transactions on Automatic Control*, vol. 47, no. 8, pp. 1324–1328, Aug. 2002.

[6] B. A. Francis and W. M. Wonham, "The Internal Model Principle of Control Theory," *Automatica*, vol. 12, pp. 457–465, 1976.

[7] T. C. Tsao, Y. X. Qian, and M. Nemani, "Repetitive Control for Asymptotic Tracking of Periodic Signals with an Unknown Period," *Journal of Dynamic Systems, Measurement, and Control*, vol. 122, pp. 364–369, Jun. 2000.

[8] A. Serrani, A. Isidori, and L. Marconi, "Semiglobal Nonlinear Output Regulation with Adaptive Internal Model," *IEEE Transactions on Automatic Control*, vol. 46, no. 8, pp. 1178–1194, Aug. 2001.

[9] R. Kumaresan and D. W. Tufts, "Estimating the Parameters of Exponentially Damped Sinusoids and Pole-zero Modeling in Noise," *IEEE Transactions on Acoustics, Speech, and Signal Processing*, vol. ASSP-30, no. 6, pp. 833–840, Dec. 1982.

[10] R. Boyer and J. Rosier, "Iterative Method for Harmonic and Exponentially Damped Sinusoidal Models," in *Proceedings of the 5th International Conference on Digital Audio Effects*, Hamburg, Germany, Sep.26-28, 2002, pp. 145–150.

[11] Y. Hua and T. K. Sarkar, "Matrix Pencil Method for Estimating Parameters of Exponentially Damped/Undamped Sinusoids in Noise," *IEEE Transactions on Acoustics, Speech, and Signal Processing*, vol. 38, no. 5, pp. 814–824, May 1990.

[12] R. Badeau, R. Boyer, and B. David, "EDS Parametric Modeling and Tracking of Audio Signals," in *Proceedings of the 5th International Conference on Digital Audio Effects*, Hamburg, Germany, Sep.26-28, 2002, pp. 1–6.

[13] J. Lu and L. J. Brown, "Control of Exponentially Damped Sinusoidal Signals," in *Proceedings of the 2007 American Control Conference*, New York City, NY, Jul.11-13, 2007, pp. 1937–1942.

[14] H. K. Khalil, *Nonlinear Systems*, 3rd ed. Upper Saddle River, NJ: Prentice-Hall, 2002.

[15] S. Sastry and M. Bodson, *Adaptive Control: Stability, Convergence, and Robustness*. Englewood Cliffs, NJ: Prentice-Hall, 1989.

[16] E. Bai, L. Fu, and S. S. Sastry, "Averaging Analysis for Discrete Time and Sampled Data Adaptive Systems," *IEEE Transactions on Circuits and Systems*, vol. 35, no. 2, pp. 137–148, Feb. 1988.

[17] L. J. Brown and Q. Zhang, "Periodic Disturbance Cancellation with Uncertain Frequency," *Automatica*, vol. 40, pp. 631–637, 2004.

[18] Q. Zhang and L. J. Brown, "Noise Analysis of an ALgorithm for Uncertain Frequency Identification," *IEEE Transactions on Automatic Control*, vol. 51, no. 1, pp. 103–110, Jan. 2006.

Chapter 3

Combining Open and Closed-Loop Control Via Intermittent Integral Control Action [2]

3.1 Introduction

Disturbance attenuation is an important issue in many applications. If the disturbance has a predictable component, it can be identified or estimated, and can be compensated using open loop control. However, it is undesirable to use a purely open loop controller for compensation of predictable disturbances, since slow changes, such as drifts could eliminate the compensatory effect. In order to compensate these variations, conventional internal model principle controllers, such as integral control, are used. But conventional internal model principle controllers limit the capabilities for

---

2. A version of this chapter has been submitted for publication.
J. Lu and L. J. Brown, " Combining Open and Closed-Loop Control Via Intermittent Integral Control Action", *IEEE Transactions on Automatic Control*, September, 2010

compensating unpredictable disturbances as a result of the phase lag they introduce at relevant frequencies.

We propose to use internal model principle controllers whose inputs are only connected intermittently, *i.e.*, they switch between learned open loop and closed-loop control. The simplest implementation of the intermittent control is the intermittent integral control [1]. When a constant error is detected, the output error signal is fed to the integral controller, which then learns the necessary offset to apply to the control action. When the integral control loop is opened, the learned control action is maintained. A standard wideband disturbance controller is used in parallel with this switched controller to achieve desirable performance for unpredictable or non-constant disturbances. Since the integral controller is not normally present, this wideband controller can be made more aggressive while maintaining stability margins and/or control actions at similar levels. Some of the work in this chapter was presented in [1, 2], where significant performance improvements of this controller versus traditional PI control were demonstrated.

Due to its control fashion, an intermittent integral control system can be modelled as a switched system, which is defined as a hybrid dynamical system that consists of a finite number of subsystems and a logical rule that orchestrates switching between these subsystems [3]. Therefore, stability analysis approaches for switched systems apply to the intermittent integral control system.

When one designs a switching scheme between multiple subsystems, a main

concern is that switching between these subsystems does not cause instability. There are examples [4] demonstrating that the stability of a switched system depends not only on the dynamics of each subsystem but also on the properties of switching signals. It is well known that a switched system is stable if all individual subsystems are stable and the switching is sufficiently slow, so as to allow the transient effects to dissipate after each switch. A notable approach to formulate this idea is the dwell time approach. This approach has been studied in [4, 5]. For switched linear systems of which all subsystems are Hurwitz stable, Morse [6] established the fact that the switched system is asymptotically stable provided the dwell time is chosen to be larger than a minimum dwell time τ_m. This result was also extended in [7] and [8] to relax some restrictions on each subsystem.

Another well studied approach for stability analysis with constrained switching is based on multiple Lyapunov functions (MLF) theory. Instead of finding a common Lyapunov function that applies for all subsystems at all time, MLF approach requires that each subsystem has its corresponding Lyapunov function combined with a bounding condition at each switching interval. These functions only require non-positive time derivatives along the state trajectories when corresponding subsystems are active. There are several versions of MLF results in the literature. Branicky presented a very intuitive MLF result in [9]. He showed that when all candidate Lyapunov-like functions for each of the individual subsystems satisfy the following conditions, a) each function does not increase when its corresponding subsystem is active, b) each

function does not increase its value at each entering instant, the switched system is stable in the sense of Lyapunov. Some other MLF approaches are discussed in [10, 11, 12].

The intermittent integral control system belongs to a class of switched systems that switch between controllers in the presence of constant disturbances or reference signals or other predictable disturbances. Unless all the controllers have the same gain at zero frequency, they will not share the same equilibrium point preventing direct application of existing results. We extend the results in [9] by replacing the constraint that all Lyapunov functions have negative derivatives when their corresponding subsystems are active with a bounding constraint on those that do not satisfy this stability condition. This allows some of the subsystems to not share a common equilibrium point or even be unstable. Although the phrase "system stability" is used sometimes, strictly speaking, it refers to the stability of a system's equilibrium point. The origin is defined as a not stable equilibrium point if it is either unstable or not an equilibrium point. So by expanding the classes of systems from stable and unstable as in [8] to stable and not stable, we can allow our not stable systems to be active for arbitrarily long. Further, all the aforementioned MLF approaches deal with switched systems that have been defined such that all subsystems have the same states. This unnecessary condition is also dropped to include systems that switch between controllers having different dimensions or state vectors.

This chapter is organized as follows: First, the intermittent integral control

system is introduced in Section 3.2. A stability theorem for switched systems based on MLF is developed in Section 3.3. In Section 3.4, a switched system model of the intermittent integral control system is established, followed by a stability theorem. A numerical example of the intermittent integral control and its performance evaluation is presented in Section 3.5, followed by the conclusion and future work in Section 3.6. The proofs of the stability theorems are given in the appendices. The work in this paper is based on preliminary work previously presented at several American Control Conferences [1, 2, 13, 14].

3.2 Intermittent Integral Control System

The overall intermittent integral control system is shown in Fig. 3.1, where the plant $L(s)$ generally includes a standard wideband controller, such as a proportional controller. The integral controller has a time-varying integral gain with $\dot{K}_i(t) = -K_d K_i(t)$, with K_d and the opening and closing of switch S defined in Table 3.1. (Note $K_i(t) = 0$ is equivalent to switch being open, and $K_i(t) \neq 0$ implies switch is closed.)

The switching mechanisms of this intermittent integral controller are as follows. Initially, the controller begins as open loop control (S open, $i.e.$, $K_i(t) = 0$), and the integral controller is initialized with a nominal offset $x_o(t_0)$. The integrated error x_e is monitored. When x_e exceeds a threshold x_u at time t, the integral controller is turned on by setting $K_i(t) = K_i^*$, and x_o is simultaneously augmented by x_e scaled
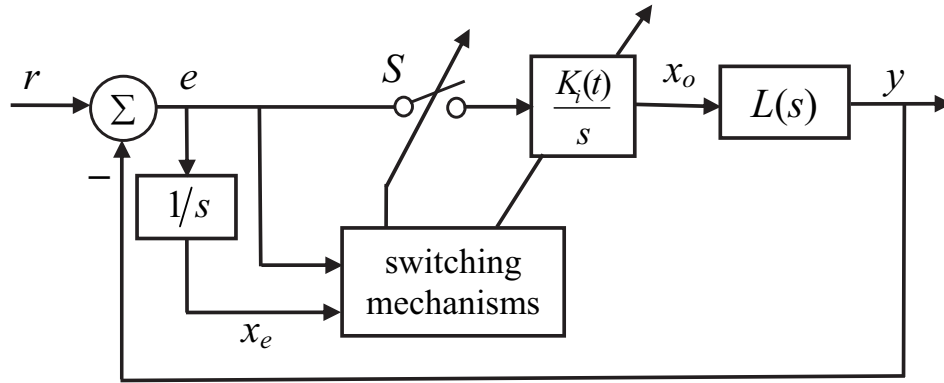
Figure 3.1: Block diagram of an intermittent integral control system

Table 3.1: Definition of parameters for intermittent integral control

If	Then
$K_i(t) = 0$ and $\|x_e(t)\| > x_u$	$K_i(t^+) = K_i^*$, $x_o(t^+) = x_o(t) + \dfrac{K_i^* x_e(t)}{\max(1, K_s(t - t_l))}$
$0 < K_i(t) \leq K_i^l$	$K_i(t^+) = 0, x_e(t) = 0, t_l = t$
$\|e(t)\| \geq e_u$	$K_d = 0$
$\|e(t)\| < e_u$	$K_d = K_{decay}$

by the time spent reaching the threshold as given by

$$K_i(t^+) = K_i^* \tag{3.1}$$

$$x_o(t^+) = x_o(t) + \frac{K_i^* x_e(t)}{\max(1, K_s(t - t_l))} \tag{3.2}$$

where K_s is a scaling factor and the max operation guarantees no division by zero issues. t_l is the last time the integral controller is turned off or the initial time t_0. The integral controller remains active as long as the error $e(t)$ is excessive. Once the error is not significant, i.e., $|e(t)| < e_u$, the integral control action is removed in a

smooth manner. This is achieved by setting $K_d = K_{decay}$, the value of the integral gain $K_i(t)$ decays exponentially. This smooth removal of the integral action prevents the phenomenon called chattering. When the integral gain becomes insignificant, $i.e.$, $K_i(t) = K_i^l$, then $K_i(t)$ is set to zero. Integral action is thus completely turned off (S open). x_e is reset to 0, and t_l is set to t. Table 3.2 gives reasonable methods of choosing those additional parameters listed in Table 3.1 when the design goals are fast response and maximum disturbance attenuation.

Table 3.2: Guidelines for parameter selections

K_i^*	Can be chosen slightly larger than that for traditional PI control.
e_u	Closed-loop level of noise and disturbance gives a reasonable value for e_u.
x_u	e_u value multiplied by the desired response time.
K_i^l	Between $0.1K_i^*$ and $0.25K_i^*$.
K_{decay}	Can be chosen to satisfy requirements of Theorem 3.2, or 0.5 to 5 times the reciprocal of the closed-loop rise time.
K_s	Can be chosen slightly smaller than the product of K_i^* and the plant DC gain

In [1], this intermittent integral control strategy has been shown a 10% reduction in the disturbance response than traditional PI control on plants with infrequent step changes in set-point or load. It also remains well behaved at those operating points where PI control system went unstable. By observing its switching mechanisms, this control system can be modelled as a switched system. Therefore, stability analysis approaches for switched systems can be applied to this system. However, unlike most switched systems, the equilibrium points of this switched system cannot be guaranteed

to be identical or even bounded prior to establishing stability of the system.

3.3 Multiple Lyapunov Functions Based Stability Theory

For a switched system, its switching signal $\sigma(t)$ is defined as a piecewise right continuous constant function of time with $\sigma(t) \in \{1, 2, \cdots, M\}$, where M is the number of subsystems. It is assumed that there are finite number of switches in any finite time interval. Let set $\{t_j\}$ represent the switching times with j being positive integer numbers and $t_j \leq t_{j+1}$. We also define pairs of subsets of $\{t_j\}$ for any $q \in \{1, 2, \cdots, M\}$ as follows,

$$\{\bar{t}_{q,k}\} = \{t_j | \text{when subsystem } q \text{ is switched on}\};$$

$$\{\underline{t}_{q,k}\} = \{t_j | \text{when subsystem } q \text{ is switched off}\}$$

with $\bar{t}_{q,k} < \underline{t}_{q,k}$. Let S be a switching sequence associated with the switched system. The interval completion $\mathcal{I}(S|q)$ is defined as the completion of the set of time intervals during which subsystem q is active, *i.e.*, $\mathcal{I}(S|q) = \bigcup_k \left[\bar{t}_{q,k}, \underline{t}_{q,k} \right]$.

For a switched system that has different state vectors for each of the individual subsystems, its dynamics can be described as

$$\dot{x}_q = f_q\big(x_q(t)\big), \qquad t \in \mathcal{I}(S|q) \tag{3.3}$$

$$x_q(t_j) = H_{q,p}\big(x_p(t_j)\big) \tag{3.4}$$

where $x_q \in \mathbb{R}^{n_q}$, and $q, p \in \{1, 2, \cdots, M\}, (q \neq p)$, and $\sigma(t_j) = p$, $\sigma(t_{j+1}) = q$. Functions $H_{q,p}$ are mappings from $\mathbb{R}^{n_p}$ to $\mathbb{R}^{n_q}$, and satisfy $\|H_{q,p}\big(x_p(t_j)\big)\| \leq C_1\|x_p(t_j)\|$, with C_1 being a constant. From (3.3), it can be seen that each state vector is only required to be defined on its corresponding interval completion. Also note that switching instant t_j in (3.4) is both the switch-off time of subsystem p and switch-on time of subsystem q. In this chapter, the norm of a vector x is referring to the Euclidean norm, $\|x\| = \sqrt{x^T x}$, and the norm of a matrix A is referring to the induced norm, $\|A\| = \max_{\|x\|=1} \|Ax\|$. It is not required that each subsystem in (3.3) has the same equilibrium point and each state vector needs only to be defined over its corresponding interval completion.

Since each subsystem has its own state vector, the traditional definition of Lyapunov stability needs to be modified. For dynamical system (3.3) and (3.4), when $f_q(0) = 0$, we say the origin of subsystem q is stable in the sense of Lyapunov if for each $\varepsilon > 0$, there exist C_2, $\delta(\varepsilon) > 0$, such that if $\|x_q(t_0)\| < \delta$, $\|x_{\sigma(t)}(t)\| < C_2\varepsilon$ for all $t > t_0$, and $\|x_q(t)\| < \varepsilon$ for all $t \in \mathcal{I}(S|q)$, and $t > t_0$. In addition, we can say the origin is an asymptotically stable equilibrium point for the switched system if $\|x_{\sigma(t)}(t)\| \to 0$ as $t \to \infty$, and the origin is stable in the sense of Lyapunov for one subsystem q.

Since we do not require $f_q(0) = 0$ for all q, it will not be possible to find

Lyapunov functions for all of the subsystems. But it is still possible to construct energy-like functions for those not stable subsystems in a similar way as to Lyapunov functions. These energy-like functions preserve the positive definite and continuously differentiable properties of Lyapunov functions. But their derivatives along the solutions of the system can be positive. Despite the signs of their derivatives, together with Lyapunov functions, these energy-like functions are called *candidate Lyapunov-like functions* in this paper. Note that the definition of Lyapunov function requires the origin to be an equilibrium point, but this is not required for candidate Lyapunov-like functions.

An MLF based theorem for the stability of switched systems:

Theorem 3.1. *For a switched system described by (3.3) and (3.4), suppose we have candidate Lyapunov-like functions V_q for each of the individual subsystems. Let Π be the set of all switching sequences associated with the system, and Ξ be a subset of Π. If for each $S \in \Xi$, the following conditions are satisfied,*

1. *There exists at least one V_i, $i \in \{1, 2, \cdots, M\}$, such that*

   (a) *$\dot{V}_i(x_i(t)) \leq 0$, for all $t \in \mathcal{I}(S|i)$;*

   (b) *$V_i(x_i(\bar{t}_{i,k+1})) \leq V_i(x_i(\bar{t}_{i,k}))$, $\forall k$, where $\bar{t}_{i,k}$, $\bar{t}_{i,k+1}$ are two consecutive switch-on instants of subsystem i;*

2. *For all other V_q's, $(q \neq i)$,*

(a) x_q does not have finite escape time, and is guaranteed to enter subsystem i; or the system can be guaranteed to enter subsystem i prior to entering subsystem q;

(b) there exists a positive constant m, such that $|V_q(x_q(t))| \leq m|V_i(x_i(\bar{t}_i^*))|$, for $\bar{t}_{q,j} \leq t \leq \underline{t}_{q,j}$, where interval $[\bar{t}_{q,j}, \ \underline{t}_{q,j}]$ is a subset of $\mathcal{I}(S|q)$ for all j, and $\bar{t}_i^* = \max_k\{\bar{t}_{i,k}|\bar{t}_{i,k} < \bar{t}_{q,j}\}$,

the switched system (3.3), (3.4) is stable in the sense of Lyapunov for all switches in Ξ. Furthermore, if $\dot{V}_i(x_i(t)) < 0$, and one of the following two conditions is satisfied,

- the sequence $\{V_i(x_i(\bar{t}_{i,k}))\}$ converges to zero as $k \to +\infty$;

- $\{\bar{t}_{i,k}\}$ is a finite sequence and the system stays in subsystem i after the last switching,

the switched system is asymptotically stable.

Proof of this theorem is given in Appendix A.

3.4 Switched System Model and Stability Theorem

Let

$$\dot{x} = Ax + Bx_o$$

$$y = Cx \tag{3.5}$$

be a state space representation of $L(s)$ shown in Fig. 3.1 , where $x \in \mathbb{R}^n$. From Fig. 3.1, we have

$$e = r - y = r - Cx \tag{3.6}$$

$$\dot{x}_o = K_i(t)e = -K_i(t)Cx + K_i(t)r \tag{3.7}$$

By letting $z = [x_o \ x^T]^T$, $z \in \mathbb{R}^{n+1}$, the intermittent integral control system can be expressed as

$$\dot{z} = \begin{bmatrix} \dot{x}_o \\ \dot{x} \end{bmatrix} = \begin{bmatrix} 0 & -K_i(t) \ C \\ B & A \end{bmatrix} \begin{bmatrix} x_o \\ x \end{bmatrix} + \begin{bmatrix} K_i(t) \\ 0 \end{bmatrix} r$$

$$:= A_\sigma(t)z + B_\sigma(t)r \tag{3.8}$$

$$y = \begin{bmatrix} 0 & C \end{bmatrix} \begin{bmatrix} x_o \\ x \end{bmatrix} \tag{3.9}$$

where $A_\sigma(t) \in \mathbb{R}^{(n+1) \times (n+1)}$, $B_\sigma(t) \in \mathbb{R}^{(n+1) \times 1}$. The initial condition is given as $z(t_0) = z_0$. As described in (3.2), x_o is augmented when the integral controller is turned on.

By observing the switching mechanisms, this intermittent integral control system can be modelled as a switched linear system consisting of two subsystems. The

switching signal $\sigma(t)$ is defined as

$$\sigma(t) = \begin{cases} 1, & \text{if } K_i(t) \in (K_i^l, K_i^*] \\[2mm] 2, & \text{if } K_i(t) \in [0, K_i^l] \end{cases} \tag{3.10}$$

Matrices $A_\sigma(t),\ B_\sigma(t)$ can be written as follows,

$$A_1(t) = \begin{bmatrix} 0 & -K_i^* \exp(\int_{\bar{t}_{1,k}}^t -K_d \mathrm{d}\tau)C \\ B & A \end{bmatrix}, \quad B_1(t) = \begin{bmatrix} K_i^* \exp(\int_{\bar{t}_{1,k}}^t -K_d \mathrm{d}\tau) \\ 0 \end{bmatrix} \tag{3.11}$$

$$A_2(t) = \begin{bmatrix} 0 & 0 \\ B & A \end{bmatrix}, \qquad\qquad B_2(t) = \begin{bmatrix} 0 \\ 0 \end{bmatrix} \tag{3.12}$$

with $t \geq \bar{t}_{1,k}$ in (3.11). Pair $\big(A_1(t), B_1(t)\big)$ describes the closed-loop control subsystem with integral action, and $\big(A_2(t), B_2(t)\big)$ describes the open loop control subsystem without integral action. For the switched linear system (3.8), (3.9), we have the following lemma from [15],

Lemma: If the time-varying system $\dot{z}(t) = A_1(t)z(t)$ satisfies the following:

1. The function $t \to A_1(t)$ is a matrix-valued piecewise continuous function bounded on $\mathbf{R}_+$, *i.e.*, $\sup_{t\geq 0} \|A_1(t)\| := \alpha_1 < \infty$;

2. There exists a positive constant μ_1 such that every point-wise eigenvalue of $A_1(t)$ satisfies $\mathrm{Re}\big[\mathrm{eig}_i[A_1(t)]\big] \leq -2\mu_1,\ \forall i,\ \forall t \geq 0$;

3. $\sup_{t \geq 0} \|\dot{A}_1(t)\| := \beta$ satisfies $\beta \leq \mu_1^2/m_1^4$, where $m_1 = R_d(\frac{R_d}{2} + \alpha_1)^2/\mu_1^3$, and

$R_d \geq 2|\text{eig}_i[A_1(t)]|, \; \forall i, \; \forall t \geq 0,$

the equilibrium of the system is uniformly exponentially stable.

To simplify the analysis, the modification of x_o when subsystem 2 is switched on is ignored by letting K_s be infinity. We then have the following theorem,

Theorem 3.2. *If K_i^*, K_i^l, and K_{decay} are chosen such that the following assumptions are satisfied,*

1. *The equilibrium of subsystem 1 is uniformly exponentially stable, i.e., there exist finite positive constants γ_1, λ_1, such that $\|\Phi_1(t,\tau)\| \leq \gamma_1 e^{-\lambda_1(t-\tau)}$, where $\Phi_1(t,\tau)$ is the transition matrix of subsystem 1;*

2. *There exists a constant $\mu_2 > 0$, such that each eigenvalue of A satisfies $\text{Re}[\text{eig}_i(A)] \leq -\mu_2$;*

3. *The minimum active time of subsystem 1, τ_{1m}, given by $\tau_{1m} = \ln(K_i^*/K_i^l)/K_{decay}$, satisfies $\tau_{1m} \geq \ln\left(\gamma_1^2\gamma_3\sqrt{\alpha_1/\lambda_1}\right)/\lambda_1$, where γ_3 is a positive constant defined in proof,*

the intermittent integral control system (3.8), (3.9) is stable in the sense of Lyapunov.

Note that assumption 1 is true if all conditions of either the Lemma or Theorem 7.4 in [16] are satisfied. The latter requires the existence of a symmetric matrix $Q_1(t)$ with bounding conditions.

The proof of Theorem 3.2 is given in Appendix B.

In Fig. 3.1, the constant reference/disturbance signal $r(t)$ is assumed to have infrequent step changes. Let the amplitude of the first step be 1, and the second step be R_s. The first step occurs at $t_0 = 0$, and the second step occurs at t_s. From assumption 1 of Theorem 3.2, we have $\|z(t)\| \leq \gamma_1 \mathrm{e}^{-\lambda_1 t}$, for all $t \in \mathcal{I}(S|1)$ and $t \in [0, t_s]$. After the second step, this inequality becomes $\|z(t)\| \leq R_s \gamma_1 \mathrm{e}^{\lambda_1(t-t_s)}$, for all $t \in \mathcal{I}(S|1)$ and $t \geq t_s$. Let $\bar{t}_{1,k}$ be the first switch-on time of subsystem 1 after the second step change of $r(t)$. In order to maintain stability, condition (1.b) of Theorem 3.1 needs to be modified as: t_s is lower bounded such that $V_1\big(z(\bar{t}_{1,k+1})\big) \leq V_1\big(z(\bar{t}_{1,k-1})\big)$. The lower bound of t_s is a function of R_s.

3.5   A Numerical Example

In order to demonstrate the performance of the intermittent integral control system, a numerical example is given below that shows the benefits achieved relative to simple feedback control and a state feedback control with an augmented integrator which is presented in [17]. We consider a simple second order plant given by

$$\dot{x}_p = \begin{bmatrix} -0.8 & -1 \\ 1 & 0 \end{bmatrix} x_p + \begin{bmatrix} 1 \\ 0 \end{bmatrix} u \tag{3.13}$$

$$y = \begin{bmatrix} \frac{1}{3} & 1 \end{bmatrix} x_p \tag{3.14}$$

Step responses of systems with state feedback control, state feedback control with augmented integrator, and the intermittent integral control are simulated. In order to understand both steady state behaviour and transient behaviour, the reference signal $r(t)$ is chosen to have a step change from 0 to 1 at $t = 50$, which is the midpoint of the simulation. A white Gaussian noise $n(t)$ with zero mean and standard deviation $\sigma = 0.2$ is added as the wideband disturbance to the system.

To evaluate the benefits of intermittent integral control, the controller design is formulated as stochastic optimal linear regulator problems with the presence of wideband disturbances. The optimization criterion is defined as follows,

$$J = E\left\{ \lim_{t_f \to \infty} \int_{t_0}^{t_f} [y^2(t) + u^T(t)Ru(t)]\mathrm{d}t \right\} \tag{3.15}$$

where R is a weighting matrix.

3.5.1   Controller 1

By implementing linear quadratic regulator (LQR) design method, the optimal state feedback controller gain is [18]

$$K = -R^{-1}B_p^T P, \tag{3.16}$$

where P is the solution to the algebraic Riccati equation (ARE),

$$A_p^T P + P A_p - P(B_p R^{-1} B_p^T) P + C_p^T C_p = 0 \qquad (3.17)$$

and (A_p, B_p, C_p) is a state representation of the plant. A smaller weighting of R results in larger absolute values of K, which gives faster response and smaller overshoot. But the trade-off is a greater variance in the steady state error. With the choice of $R = 0.5$, the optimal state feedback gain for controller 1 is $K = [-0.7252, \; -0.7321]$.

3.5.2 Controller 2

An augmentation method is implemented for the design of an optimal state feedback controller with integral action. An additional state x_o, given as the integral of the difference between the output and reference signal, is added to the plant. The LQR design is then applied to the augmented system to obtain an optimal state feedback gain K_e. Note the third value of this vector is the integral gain K_i^*. For design purposes only, the optimization criterion is $J = E\{\int_{t_0}^{\infty} (y^2 + \rho x_o^2 + Ru^2) dt\}$, where ρ is the weighting on the state x_o. When the value of ρ is zero, the augmented system is not observable. As ρ approaches zero, the controller converges to the proportional controller and step response becomes unacceptably slow. With the choice of $\rho = 0.4$, which is explained in next subsection, the optimal state feedback gain for controller 2 is $K_e = [-1.2079, \; -1.2866, \; 0.8944]$, and $K_i^* = 0.8944$.

3.5.3 Intermittent integral controller

In this example, $L(s)$ in Fig. 3.1 is designed as the combination of the plant and controller 1 obtained earlier. K_i^* is the gain for the augmented state x_o obtained from controller 2 above. Since the response with controller 1 has standard deviation $\sigma_1 = 0.005$ and rise time $t_r = 1.24$, according to the guidelines in Table 3.2, we choose the parameters of the intermittent integral controller as follows, $e_u = 4\sigma_1 = 0.02$, $x_u = e_u t_r = 0.025$, $K_s = 0.8$, $K_i^l = 0.1 * K_i^*$, and $K_{decay} = 0.25$. From hereinafter, intermittent integral controller is also referred to as controller 3.

In order to verify the assumptions of Theorem 3.2, two positive definite symmetric matrices Q_1 and Q_2, corresponding to the two subsystems, are calculated by solving corresponding Lyapunov equations. According to Theorem 7.4 in [16], the existence of these two matrices can guarantee assumptions 1 and 2. For subsystem 1, we obtain Q_1 by solving the Lyapunov equation $A_1^T(t)Q_1 + Q_1 A_1(t) = -I$ at $t = 0$, i.e., $K_i(t) = K_i^*$. For all $K_i(t) \in [K_i^l, K_i^*]$, we verified that Q_1 satisfies $A_1^T(t)Q_1 + Q_1 A_1(t) \leq -\nu I$, where ν is a positive constant. Since matrix A is time invariant, Q_2 can be simply obtained by solving equation $A^T Q_2 + Q_2 A = -I$.

$$Q_1 = \begin{bmatrix} 1.9784 & -0.5 & -1.1907 \\ -0.5 & 1.018 & 0.9035 \\ -1.1907 & 0.9035 & 2.3391 \end{bmatrix}, \quad Q_2 = \begin{bmatrix} 0.5171 & 0.2887 \\ 0.2887 & 1.3359 \end{bmatrix}$$

The existence of these two matrices justifies the first two assumptions of Theorem

3.2. Consequently, following parameter values from Appendix B can be calculated,

$\lambda_1 = 0.5$, $\gamma_1 = 2$, $\alpha_1 = 2.7115$, $\mu_2 = 0.7626$, $\gamma_2 = 1.4755$, $\alpha_2 = 2.4104$, and

$\gamma_3 = 2.9133$. Thus the lower bound of the minimum active time of subsystem 1 is

$\ln(\gamma_1^2 \gamma_3 \sqrt{\alpha_1/\lambda_1})/\lambda_1 = 6.6018$. The minimum active time is $\tau_{1m} = \ln(K_i^*/K_i^l)/K_{decay} =$

$9.2103 > 6.6018$. Assumption 3 of Theorem 3.2 is satisfied.

Cost functions are calculated using the following formula for different values of

ρ and shown in Table 3.3,

$$J = \int_0^{t_f} (e^2(t) + u^2(t)R)\mathrm{d}t \tag{3.18}$$

where $t_f = 100$. To distinguish between the transient performance and noise rejection

capability of the approach, the cost is broken into two time periods, $0 \le t \le 50$ where

the cost J_s is driven by the additive noise, and $50 < t \le 100$ where the cost J_t

is primarily a function of the step response. It can be seen that as ρ increases,

for controller 2, J_s increases and J_t decreases. To achieve better constant reference

tracking, the integral controller must trade off its wideband disturbance attenuation

performance. For controller 3, since the optimal state feedback gain K, which is

independent of ρ, does not change, J_s remains unchanged. However, as ρ increases,

J_t decreases first and increases after reaching its minimum value at $\rho = 0.4$.

To illustrate the step response performances of the controllers, we choose $\rho = 0.4$

for the following results. Thus the state feedback gain and integral gain for controller

Table 3.3: Cost function values of controller 2 & controller 3's step responses

ρ	K_i^*	controller 2		controller 3	
		J_s	J_t	J_s	J_t
0.2	0.6325	0.00222	0.9738	0.00186	0.7495
0.3	0.7746	0.00230	0.9072	0.00186	0.7055
0.4	0.8944	0.00238	0.8668	0.00186	0.6912
0.6	1.0954	0.00250	0.8177	0.00186	0.6991
0.7	1.1832	0.00256	0.8010	0.00186	0.7121
1.0	1.4142	0.00271	0.7659	0.00186	0.7711

3 are $K = [-0.7252, \; -0.7321]$, and $K_i^* = 0.8944$. Fig. 3.2 shows the intermittently invoked integral control action of controller 3. After the first switch-on, the integral control is at its full strength with maximum integral gain K_i^* because the tracking error is excessive. When the tracking error decreases below the threshold e_u, the integral gain starts to decay exponentially. When $K_i(t)$ decays to about 0.86 at $t = 52$, the effects of the noise cause $|e(t)|$ to be greater than e_u again. According to the switching mechanisms defined in Table 3.1, $K_d = 0$ when $|e(t)| > e_u$, which means $K_i(t)$ stops decaying and keeps its value as it is. At about $t = 54$, the condition $|e(t)| < e_u$ is satisfied again, $K_i(t)$ continues its decaying and stops decreasing again between $t = 54.4$ and $t = 56.9$. It is then set to zero when the lower bound K_i^l is reached. This process is also shown in the inset plot. Note there remains a small residual error in the system that results in the integrator again being invoked at about $t = 67$. The integral gain immediately starts to decrease because the tracking error has already decreased below the threshold. There remains an exponentially decreasing residual error between the set point and the system output that continues

to cause the integral action to be invoked. However, the time between invocations increases exponentially.
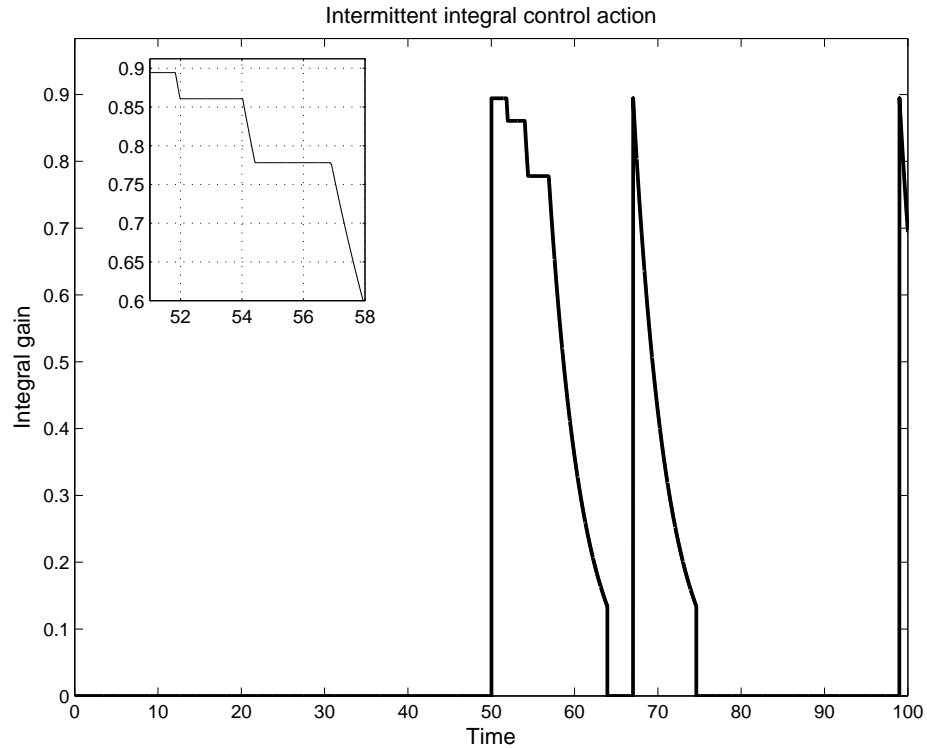

Figure 3.2: Integral gain of the intermittent integral control system

The top plot in Fig. 3.3 shows the tracking errors of the three controllers' step responses. The bottom plot shows the control signals during the transient period. The steady state control signals of controller 2 and controller 3 are plotted in Fig. 3.4. The variance of controller 3's control signal is 1.32×10^{-5}, which is a significant improvement than that of controller 2 (3.46×10^{-5}).

Compared with the costs of controller 2 and 3 for $\rho = 0.4$, the costs of controller 1 is $J_s = 0.00186$, and $J_t = 9.3588$. As we can see, in steady state, when
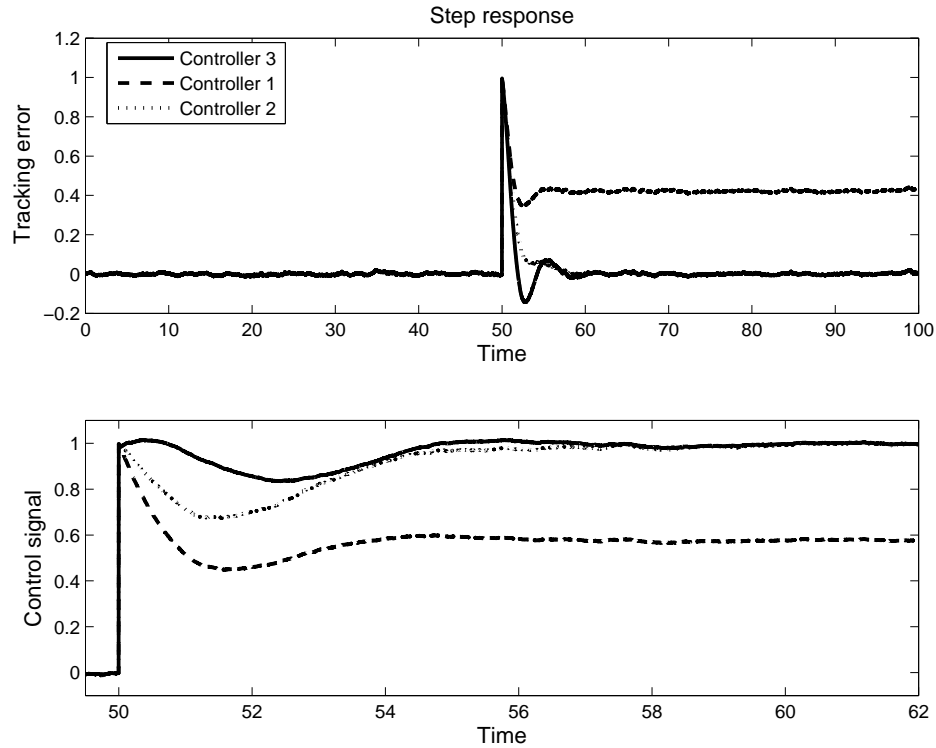
Figure 3.3: Tracking errors and control signals of the three control systems

the parameter e_u is larger than the steady state noise, performance equivalent to optimal control without integral action is achieved. Further the switching mechanism successfully allows the system to perfectly reject constant disturbances and perfectly follow infrequent step changes in set points with minimal increase in costs during the transient.

3.6 Conclusions

A new control strategy that combines the benefits of closed-loop control with open loop control of predictable disturbances is presented. A tool that can be used to test
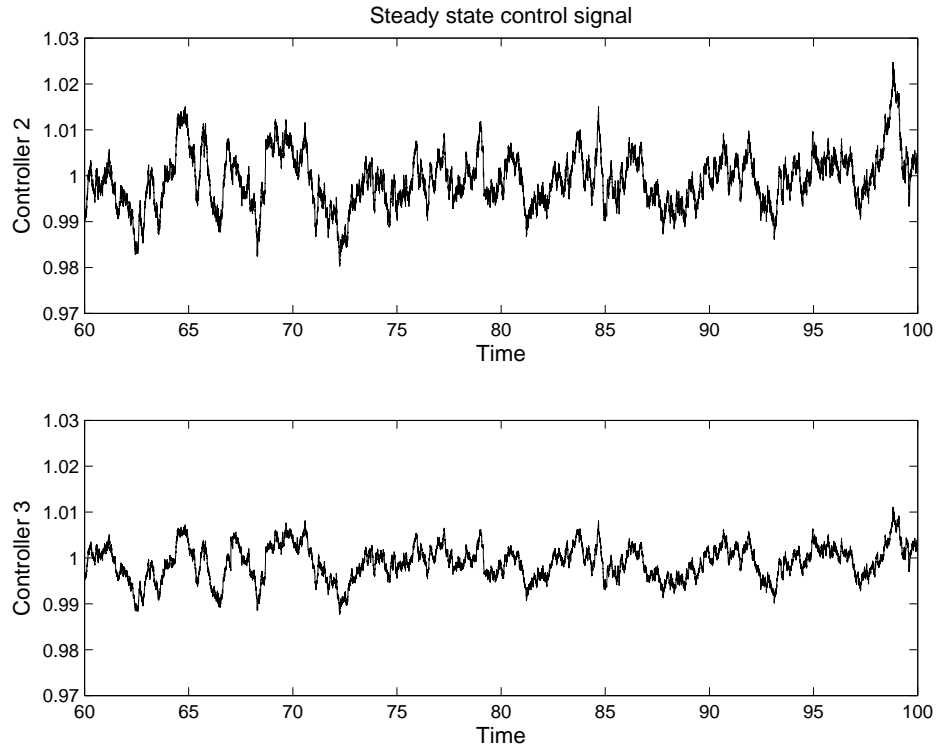
Figure 3.4: Comparison of steady state control signals of controller 2 & controller 3

for stability of the resulting system is also presented. This tool can then be used to assist in selecting the switching parameters. Due to the intermittent control fashion of the integral action, a feedback system with the intermittent integral controller can be modelled as a switched system with two constituent systems. Since the two subsystems do not share common equilibrium point, and have different state variables, existing approaches can not be applied to the intermittent integral control system directly. By extending the MLF result in [9], a new MLF theorem is developed with relaxations on the constraints on constituent systems. The intermittent integral control system is proved to be stable in the sense of Lyapunov by applying this new

MLF theorem. A numerical example shows that the intermittent integral control system improves the reference tracking and disturbance rejection performance than traditional state feedback control systems with or without integral control.

This intermittent integral control approach is capable of cancelling constant disturbances and attenuating unpredictable disturbances. But for systems subject to narrowband disturbances and unpredictable disturbances, this approach has its limitations. In [2], the concept of integral control was extended to deal with any predictable disturbances using Internal Model Principle (IMP) controller. This control strategy is known as Intermittent Cancellation Control (ICC). However, ICC is restricted to plants that have infrequent changes in set point or disturbance characteristics, and the period of the predictable disturbance is required *a priori*. As of our future work, we will extend the IMP controller in the ICC approach to an adaptive IMP control algorithm, developed by Brown and Zhang [19]. The adaptive IMP feedback loop is invoked to identify and cancel the predictable disturbances. Once the predictable disturbances are cancelled, the feedback loop is opened creating an open loop controller. The main challenge will be finding a switching sequence to stabilize the switched system.

Appendix A Proof of Theorem 3.1

Proof: The proof follows directly the proof of Theorem 2.3 in [9]. We do the proof for the case of $M = 2$. It can be easily extended to the case of $M > 2$.

Assume $V_1(x_1(t))$, $V_2(x_2(t))$ are two candidate Lyapunov-like functions cor-responding to subsystem 1 and 2 respectively. x_1 and x_2 are corresponding state vectors. $V_1(x_1(t))$ satisfies condition 1 of the theorem, and $V_2(x_2(t))$ satisfies condition 2. There is no requirement on the sign of time derivative of $V_2(x_2(t))$. As shown in Fig. 3.5, $V_2(x_2(t))$ may increase or decrease its value during active time intervals. In this figure, t_i's are switching instants. If $\dot{V}_2(x_2(t)) \leq 0$, this theorem is equivalent to Theorem 2.3 in [9]. We consider the worst case of $\dot{V}_2(x_2(t)) > 0$ in the proof. At initial time, either subsystem could be active. If subsystem 2 is active initially, $V_2(x_2(t))$ can only reach a finite value when subsystem 1 is switched on in finite time because of condition (2.b).
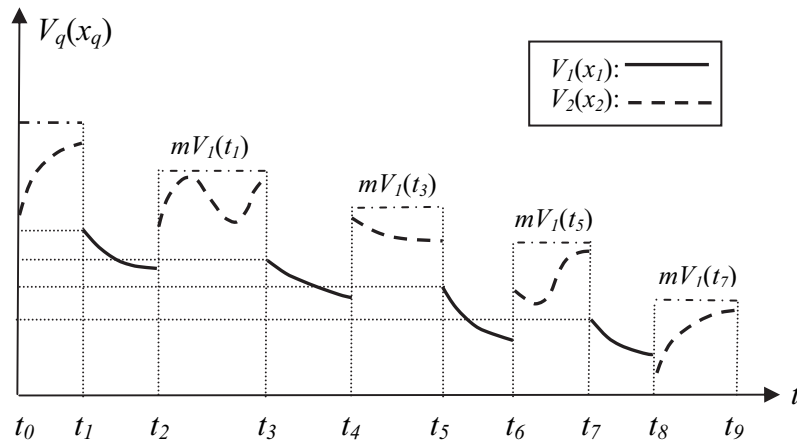

Figure 3.5: Multiple Lyapunov functions stability

Let $S_p(r)$, $B(r)$ represent the sphere, and ball of Euclidean radius r about the origin respectively. Let $\min_i(r)$ denote the minimum value of $V_i(x_i(t))$ on $S_p(r)$. During time interval $[t_1, t_2]$, subsystem 1 is active. For any given R_1, we can pick a

$r_1 \in (0, R_1)$, such that in $B(r_1)$, we have $V_1(x_1(t)) < \min_1(R_1)$. This is achievable via the continuity of $V_1(x_1(t))$. Then if $x_1(t_1)$ starts in $B(r_1)$, $x_1(t)$ will stay in $B(R_1)$ during this interval.

At t_2, subsystem 2 is switched on. Since $V_2(x_2(t))$ is upper bounded by $mV_1(x_1(t_1))$ from condition (2.a), we let this bound be the minimum value of $V_2(x_2(t))$ on a sphere of radius R_{21}, *i.e.*, $\min_2(R_{21}) = mV_1(x_1(t_1))$. Then during time interval $[t_2, t_3]$, $x_2(t)$ will move away from the origin, but is confined within $B(R_{21})$.

From condition (1.b), we know that $V_1(x_1(t_3)) \leq V_1(x_1(t_1))$, which means if $x_1(t_1)$ starts in $B(r_1)$, $x_1(t_3)$ starts in $B(r_1)$. Then $x_1(t)$ stays in $B(R_1)$ during interval $[t_3, t_4]$. Therefore, if $x_1(t_1)$ starts in $B(r_1)$, $x_1(t)$ will stay in $B(R_1)$ during every time interval when subsystem 1 is active.

Because $V_1(x_1(t_3)) \leq V_1(x_1(t_1))$, the upper bounds on $V_2(x_2(t))$ also have the relationship $mV_1(x_1(t_3)) \leq mV_1(x_1(t_1))$. If we let $\min_2(R_{22}) = mV_1(x_1(t_3))$, the radius R_{22} of $B(R_{22})$ is no larger than R_{21}. Then during time intervals when subsystem 2 is active, $x_2(t)$ is always confined within $B(R_{21})$.

As depicted in Fig. 3.6, for any given R_1, we can always find a r_1 and a R_{21}, such that if $x_1(t)$ starts in $B(r_1)$, $x_1(t)$ stays in $B(R_1)$ when subsystem 1 is active, and $x_2(t)$ stays in $B(R_{21})$ when subsystem 2 is active. This proves that the switched system is *stable in the sense of Lyapunov*.

If $\dot{V}_1(x_1(t)) < 0$, when subsystem 1 is active, $x_1(t)$ will approach its equilibrium point at the origin as time elapses. First, if the switching sequence $\{t_j\}$ is infinite,
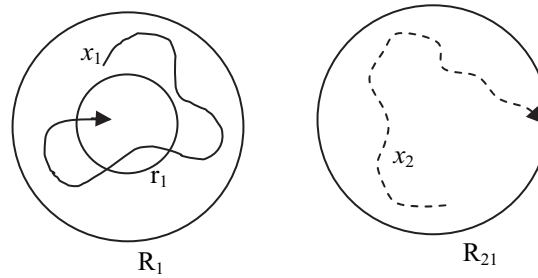
Figure 3.6: Switched system with different equilibria

and the sequence $\{V_1(x_1(t_1)), V_1(x_1(t_3)), \cdots, V_1(x_1(\bar{t}_{1,k})), \cdots\}$ converges to zero as $k \to \infty$, $x_1(t)$ approaches the origin. The upper bounds on $V_2(x_2(t))$ also converges to zero under this condition. Thus $x_2(t)$ is confined within a ball that is getting smaller and smaller every time subsystem 2 is active, and eventually, this ball will shrink to the origin as $k \to \infty$. Therefore, state trajectory $x_1(t)$ approaches its equilibrium points at the origin, and $x_2(t)$ approaches the origin as well. Second, if the sequence $\{t_1, t_3, t_5, \cdots, \bar{t}_{1,k}, \cdots\}$ is finite and after the last switching, the system stays in subsystem 1, which is asymptotically stable, $x_1(t)$, which is now the state of the switched system, will approach its equilibrium point at the origin. In both circumstances, the switched system's state trajectories approach the origin. This proves the *asymptotic stability* of the switched system.

Appendix B Proof of Theorem 3.2

Proof: By studying the structure of the system matrices (3.11) and (3.12), Theorem 3.1 developed in Section 3.3 can be applied for the stability analysis of system (3.8),

(3.9). In order to apply Theorem 3.1, each subsystem is analysed so that correspond-

ing candidate Lyapunov-like functions can be constructed.

Analysis of Subsystem 1

It can be seen from (3.11) to (3.12) that subsystem 1 is linear time-varying (LTV),

while subsystem 2 is linear time invariant (LTI). The equilibrium of subsystem 1 is

at the origin.

Since all entries in $A_1(t)$ are bounded for all $t > 0$, there exists $\alpha_1 > 0$ such

that $\|A_1(t)\| \leq \alpha_1$. From Theorem 7.8 in [16], matrix

$$Q_1(t) = \int_t^\infty \Phi_1^T(\sigma, t)\Phi_1(\sigma, t)\mathrm{d}\sigma \tag{3.19}$$

satisfies

$$\frac{1}{2\alpha_1} \leq \|Q_1(t)\| \leq \frac{\gamma_1^2}{2\lambda_1} \tag{3.20}$$

We can pick a candidate Lyapunov-like function for subsystem 1 as $V_1\big(z(t)\big) = z^T Q_1(t)z$. Then we have

$$\frac{1}{2\alpha_1}\|z\|^2 \leq V_1(z(t)) \leq \frac{\gamma_1^2}{2\lambda_1}\|z\|^2 \tag{3.21}$$

and

$$\dot{V}_1 = z^T[A_1^T(t)Q_1(t) + Q_1(t)A_1(t)]z + z^T\dot{Q}_1(t)z = -\|z\|^2 \tag{3.22}$$

Analysis of Subsystem 2

The state-space equations of subsystem 2 are

$$\dot{x}_o = 0 \tag{3.23}$$

$$\dot{x} = Ax + Bx_o \tag{3.24}$$

Since x_o remains constant when subsystem 2 is active, subsystem 2 can be considered as a forced linear system with reduced number of states. As expressed in (3.24), the state x_o in subsystem 1 can be seen as a constant input to (3.24). The number of states for (3.24) is n, while subsystem 1 has $(n+1)$ states.

Since $\text{Re}[\text{eig}_i(A)] \leq -\mu_2$ from assumption 2, the state transition matrix of A satisfies

$$\|e^{A(t-\tau)}\| \leq \gamma_2 e^{-\mu_2(t-\tau)} \tag{3.25}$$

where constant γ_2 can be derived following the Lemma in [20]. For $n \times 1$ matrix

$$Q_2 = \int_0^\infty e^{A^T \tau} e^{A\tau} d\tau, \tag{3.26}$$

it satisfies

$$\frac{1}{2\alpha_2} \leq \|Q_2\| \leq \frac{\gamma_2^2}{2\mu_2} \tag{3.27}$$

where α_2 is an upper bound of $\|A\|$. We can pick a candidate Lyapunov-like function

for subsystem 2, $V_2(x(t)) = x^T Q_2 x$. Then we have

$$\frac{1}{2\alpha_2} \|x(t)\|^2 \leq V_2(x(t)) \leq \frac{\gamma_2^2}{2\mu_2} \|x(t)\|^2 \tag{3.28}$$

The complete solution of (3.24) is

$$x(t) = e^{A(t - \bar{t}_{2,k})} x(\bar{t}_{2,k}) + \int_{\bar{t}_{2,k}}^t e^{A(t - \sigma)} B x_o d\sigma \tag{3.29}$$

with switch-on time at $\bar{t}_{2,k}$. Therefore, for all t, τ, such that $\bar{t}_{2,k} \leq \tau < t \leq \underline{t}_{2,k}$,

$$\begin{bmatrix} x_o(t) \\ x(t) \end{bmatrix} = \begin{bmatrix} 1 & 0 \\ \int_\tau^t e^{A(t-\sigma)} B d\sigma & e^{A(t-\tau)} \end{bmatrix} \begin{bmatrix} x_o(\tau) \\ x(\tau) \end{bmatrix} := e^{A_2(t-\tau)} \begin{bmatrix} x_o(\tau) \\ x(\tau) \end{bmatrix} \tag{3.30}$$

Let w be partitioned as $[w_s, w_v^T]^T$, where w_s is a scalar, and w_v is an $n \times 1$ vector.

We have

$$e^{A_2(t-\tau)}w = \begin{bmatrix} w_s \\ \int_\tau^t e^{A(t-\sigma)}Bd\sigma w_s + e^{A(t-\tau)}w_v \end{bmatrix} \tag{3.31}$$

Thus

$$\|e^{A_2(t-\tau)}w\| = \sqrt{w_s^2 + \|\int_\tau^t e^{A(t-\sigma)}Bd\sigma w_s + e^{A(t-\tau)}w_v\|^2}$$

$$\leq \sqrt{w_s^2 + 2\|\int_\tau^t e^{A(t-\sigma)}Bd\sigma\|^2 w_s^2 + 2\|e^{A(t-\tau)}w_v\|^2} \tag{3.32}$$

Let w_{vm} be the vector that maximizes $\|e^{A(t-\tau)}w_v\|$, *i.e.*,

$$\|e^{A(t-\tau)}\| = \max_{\|w_v\|=1} \|e^{A(t-\tau)}w_v\| = \|e^{A(t-\tau)}w_{vm}\| \tag{3.33}$$

Clearly, vector w that maximizes (3.32) is of the form

$$w = \begin{bmatrix} \alpha \\ \sqrt{1-\alpha^2}w_{vm} \end{bmatrix}, \qquad (0 \leq \alpha \leq 1) \tag{3.34}$$

Since B is known, and from (3.25), we have

$$\|\int_\tau^t e^{A(t-\sigma)}Bd\sigma\| \leq \int_\tau^t \|e^{A(t-\sigma)}\|d\sigma\|B\|$$

$$\leq \int_{\tau}^{t} \gamma_2 e^{-\mu_2(t-\sigma)} d\sigma \|B\|$$

$$= \frac{\gamma_2}{\mu_2}(1 - e^{-\mu_2(t-\tau)})\|B\|$$

$$\leq \frac{\gamma_2}{\mu_2}\|B\| \tag{3.35}$$

Inequality (3.32) can be further simplified as

$$\|e^{A_2(t-\tau)}w\| \leq \sqrt{\left(1 + \frac{2\gamma_2^2}{\mu_2^2}\|B\|^2\right)\alpha^2 + 2(1-\alpha^2)\gamma_2^2} \tag{3.36}$$

$\|e^{A_2(t-\tau)}w\|$ takes maximum value when $\alpha = 0$ or 1. Thus

$$\|e^{A_2(t-\tau)}\| \leq \max\left\{\sqrt{1 + \frac{2\gamma_2^2}{\mu_2^2}\|B\|^2}, \ \sqrt{2}\gamma_2\right\} := \gamma_3 \tag{3.37}$$

Analysis of the Overall Control System

For switched system (3.8), its switching signal $\sigma(t) \in \{1,2\}$. $\{A_1, A_2\}$ in (3.11)-(3.12) constitute a family of matrices describing the subsystems. As stated in Section 3.2, initially, the switched system begins with open loop control, *i.e.*, subsystem 2 is active initially. Let N be the number of switches over the interval (t_0, t) with set $\{t_1, t_2, \cdots, t_N\}$ representing the switching times. The switching on and off time sets for the two subsystems are

$$\{\bar{t}_{1,k}\} = \{t_1, t_3, \cdots, t_N\}; \quad \{\underline{t}_{1,k}\} = \{t_2, t_4, \cdots, t_{N-1}\}; \tag{3.38}$$

$$\{\bar{t}_{2,k}\} = \{t_2, t_4, \cdots, t_{N-1}\}; \quad \{\underline{t}_{2,k}\} = \{t_3, t_5, \cdots, t_N\}. \tag{3.39}$$

The interval completions for the two subsystems are

$$\mathscr{I}(S|1) = [t_1, t_2] \bigcup [t_3, t_4] \bigcup \cdots \bigcup [t_N, t] \tag{3.40}$$

$$\mathscr{I}(S|2) = [t_0, t_1] \bigcup [t_2, t_3] \bigcup \cdots \bigcup [t_{N-1}, t_N] \tag{3.41}$$

Note that the initial time t_0 and final time t are not considered as switching times, but they are included in the interval completions.

In Subsection 3.6, candidate Lyapunov-like function $V_1(z(t))$ has been shown to satisfy condition (1.a) of Theorem 3.1 in (3.22). Since there are only two subsystems and the switching sequence is minimal, for any four consecutive switching times, t_{k-1}, t_k, t_{k+1}, t_{k+2},

$$z(t_{k+2}) = e^{A_2(t_{k+2}-t_{k+1})} z(t_{k+1}) = e^{A_2(t_{k+2}-t_{k+1})} \Phi_1(t_{k+1}, t_k) z(t_k) \tag{3.42}$$

where it is assumed that subsystem 1 is switched on at t_k and t_{k+2}, and subsystem 2 is switched on at t_{k-1} and t_{k+1}.

From assumption 1 of Theorem 3.2 and (3.37), we have

$$\|z(t_{k+2})\| \le \|e^{A_2(t_{k+2}-t_{k+1})}\| \cdot \|\Phi_1(t_{k+1}, t_k)\| \cdot \|z(t_k)\| \le \gamma_1 \gamma_3 e^{-\lambda_1 \tau_k} \|z(t_k)\|$$

$$\tag{3.43}$$

where $\tau_k = t_{k+1} - t_k$ is the active time of subsystem 1 between the two consecutive switches.

Since subsystem 1 switches to subsystem 2 when $K_i(t)$ decays to its lower bound K_i^l, the minimum active time for subsystem 1 can be obtained as,

$$\tau_{1m} = \frac{1}{K_d} \ln \frac{K_i^*}{K_i^l} \tag{3.44}$$

Considering assumption 3 of Theorem 3.2, which can also be written as

$$\frac{\gamma_1^2 \gamma_3}{\sqrt{2\lambda_1}} \mathrm{e}^{-\lambda_1 \tau_{1m}} \leq \frac{1}{\sqrt{2\alpha_1}} \tag{3.45}$$

Inequality (3.43) is then equivalent to

$$\frac{\gamma_1}{\sqrt{2\lambda_1}} \|z(t_{k+2})\| \leq \frac{\gamma_1^2 \gamma_3}{\sqrt{2\lambda_1}} \mathrm{e}^{-\lambda_1 \tau_{1m}} \|z(t_k)\| \leq \frac{1}{\sqrt{2\alpha_1}} \|z(t_k)\| \tag{3.46}$$

or

$$\frac{\gamma_1^2}{2\lambda_1} \|z(t_{k+2})\|^2 \leq \frac{1}{2\alpha_1} \|z(t_k)\|^2 \tag{3.47}$$

Considering the upper and lower bounds on $V_1(z(t))$ in (3.21), we have

$$V_1\big(z(t_{k+2})\big) \leq \frac{\gamma_1^2}{2\lambda_1} \|z(t_{k+2})\|^2 \leq \frac{1}{2\alpha_1} \|z(t_k)\|^2 \leq V_1\big(z(t_k)\big) \tag{3.48}$$

which means that at t_{k+2}, V_1 is no greater than its value last time when subsystem 1 is switched on at t_k. Thus condition (1.b) of Theorem 3.1 is verified.

At t_{k+1},

$$\|z(t_{k+1})\|^2 = \|x_o(t_{k+1})\|^2 + \|x(t_{k+1})\|^2 \geq \|x(t_{k+1})\|^2 \qquad (3.49)$$

During interval $[t_{k+1}, t_{k+2}]$, subsystem 2 is active, so for all $t \in [t_{k+1}, t_{k+2}]$

$$\|x_o(t)\| = \|x_o(t_{k+1})\|$$

$$\|x(t)\| \leq \gamma_2 e^{-\mu_2(t-t_{k+1})}\|x(t_{k+1})\|$$

and from (3.28),

$$V_2(x(t)) \leq \frac{\gamma_2^2}{2\mu_2}\|x(t)\|^2 \leq \frac{\gamma_2^4}{2\mu_2}\exp(-2\mu_2(t-t_{k+1}))\|x(t_{k+1})\|^2 \leq \frac{\gamma_2^4}{2\mu_2}\|x(t_{k+1})\|^2$$

$$(3.50)$$

From (3.49) and (3.50), we have

$$V_1(z(t_{k+1})) \geq \frac{1}{2\alpha_1}\|z(t_{k+1})\|^2 \geq \frac{1}{2\alpha_1}\|x(t_{k+1})\|^2 \geq \frac{\mu_2}{\alpha_1\gamma_2^4}V_2(x(t)) \qquad (3.51)$$

Since during $[t_k, t_{k+1}]$, $\dot{V}_1 < 0$, we have $V_1(z(t_k)) \geq V_1(z(t_{k+1}))$, which gives

$$V_2(x(t)) \leq \frac{\alpha_1\gamma_2^4}{\mu_2} V_1(z(t_k)) \qquad (3.52)$$

for all $t \in [t_{k+1}, t_{k+2}]$.

All conditions of Theorem 3.1 are thus satisfied. Therefore, the switched system

(3.8) is stable in the sense of Lyapunov, which proves Theorem 3.2.

Bibliography

[1] L. J. Brown, G. E. Gonye, and J. S. Schwaber, "Non-linear PI Control Inspired by Biological Control Systems," in *Proceedings of the 37th IEEE Conference on Decision and Control*, Tampa, FL, Dec. 1998, pp. 1040–1045.

[2] L. J. Brown and J. S. Schwaber, "Intermittent Cancellation Control: A Control Paradigm Inspired by Mammalian Blood Pressure Control," in *Proceedings of the American Control Conference*, San Diego, CA, Jun. 1999, pp. 139–143.

[3] A. V. Savkin and R. J. Evans, *Hybrid Dynamical Systems: Controller and Sensor Switching Problems.* Boston, MA: Birkhauser, 2002.

[4] R. A. DeCarlo, M. S. Branicky, S. Pettersson, and B. Lennartson, "Perspectives and Results on the Stability and Stabilizability of Hybrid Systems," *Proceedings of the IEEE*, vol. 88, no. 7, pp. 1069–1082, Jul. 2000.

[5] H. Ye, A. N. Michel, and L. Hou, "Stability Theory for Hybrid Dynamical Systems," *IEEE Transactions on Automatic Control*, vol. 43, no. 4, pp. 461–474, Apr. 1998.

[6] A. S. Morse, "Supervisory Control of Families of Linear Set-Point Controllers–Part 1: Exact Matching," *IEEE Transactions on Automatic Control*, vol. 41, no. 10, pp. 1413–1431, Oct. 1996.

[7] J. P. Hespanha and A. S. Morse, "Stability of Switched Systems with Average Dwell-time," in *Proceedings of the 38th IEEE Conference on Decision and Control*, Phoenix, AZ, Dec. 1999, pp. 2655–2660.

[8] G. Zhai, B. Hu, K. Yasuda, and A. N. Michel, "Stability Analysis of Switched Systems with Stable and Unstable Subsystems: An Average Dwell Time Approach," in *Proceedings of the American Control Conference*, Chicago, IL, Jun. 2000, pp. 200–204.

[9] M. S. Branicky, "Multiple Lyapunov Functions and Other Analysis Tools for Switched and Hybrid Systems," *IEEE Transactions on Automatic Control*, vol. 43, no. 4, pp. 475–482, Apr. 1998.

[10] D. Liberzon, *Switching in Systems and Control*. Boston, MA: Birkhauser, 2003.

[11] G. Zhai, I. Matsune, J. Imae, and T. Kobayashi, "A Note on Multiple Lyapunov Functions and Stability Condition for Switched and Hybrid Systems," in *Proceedings of the 16th IEEE International Conference on Control Applications*, Singapore, Oct.1-3, 2007, pp. 226–231.

[12] H. Ye, A. N. Michel, and L. Hou, "Stability Analysis of Discontinuous Dynamical Systems with Applications," in *Proceedings of the 13th World Congress of the International Federation of Automatic Control*, vol. E, San Francisco, CA, Jun. 1996, pp. 461–466.

[13] J. Lu and L. J. Brown, "A Multiple Lyapunov Functions Approach for Stability of Switched Systems," in *Proceedings of the 2010 American Control Conference*, Baltimore, MD, Jul. 2010, pp. 3253–3256.

[14] ——, "Stability Analysis of a Proportional with Intermittent Integral Control System," in *Proceedings of the 2010 American Control Conference*, Baltimore, MD, Jul. 2010, pp. 3257–3262.

[15] C. A. Desoer, "Slowly Varying System $\dot{x} = A(t)x$," *IEEE Transactions on Automatic Control*, pp. 780–781, Dec. 1969.

[16] W. J. Rugh, *Linear System Theory*, 2nd ed. Upper Saddle River, NJ: Prentice-Hall, 1996.

[17] C.-T. Chen, *Linear System Theory And Design*, 3rd ed. New York, NY: Oxford University Press, 1999.

[18] H. Kwakernaak and R. Sivan, *Linear Optimal Control Systems*. John Wiley and Sons, Inc., 1972.

[19] L. J. Brown and Q. Zhang, "Periodic Disturbance Cancellation with Uncertain Frequency," *Automatica*, vol. 40, pp. 631–637, 2004.

[20] B. Barkat, "Stability of linear time-varying systems," in *Proceedings of International Symposium on Signal Processing and its Applications*, Gold Coast, Australia, Aug.25-30, 1996, pp. 246–249.

Chapter 4

A Combination of Open and Closed-loop Control for Disturbance Rejection [3]

4.1   Introduction

Disturbance rejection is a major control issue in control systems which has been studied for several decades. In general, disturbances can be categorized into two types: predictable and unpredictable. Predictable disturbances are also referred to as narrowband disturbances, which include sinusoidal or sum of sinusoidal signals. Unpredictable disturbances include white or colored noises which have wide bandwidth in frequency domain. For these two types of disturbances, two different controllers can be designed with their own attempts to achieve best performance.

A popular technique for predictable disturbance rejection is based on the *Internal Model Principle* (IMP) proposed by Francis and Wonham in 1976. The main

---

3. A version of this chapter has been submitted for publication.
J. Lu and L. J. Brown, " A Combination of Open and Closed-loop Control for Disturbance Rejection", *24th Canadian Conference on Electrical and Computer Engineering*, December, 2010

idea of IMP is that a suitably reduplicated model of the dynamic structure of the disturbance or reference should be incorporated in a stable feedback loop for perfect disturbance cancellation or reference tracking. The purpose of the IMP controller is to supply right-half plane closed-loop transmission zeros to cancel the unstable poles of exogenous signals [1]. The IMP approach requires the knowledge of the disturbance *a priori*. The accuracy of regulation depends on the fidelity of the IMP controller.

If the frequencies of the predictable signals drift over time or are unknown, the traditional IMP approach cannot achieve perfect or possibly acceptable rejection. There are many algorithms that can identify or estimate unknown parameters of predictable disturbances to achieve perfect rejection. These algorithms include higher harmonic control [2], LMS adaptive feedforward filtering [3], adaptive feedforward cancellation (AFC) [4], and adaptive IIR notch filter [5].

In [6, 7], an IMP based adaptive algorithm was developed to identify and cancel quasi-periodic or narrowband disturbances with uncertain frequencies. According to the IMP, for a sinusoidal disturbance with frequency ω_c, the IMP controller must have a pair of marginally stable poles at $s = \pm j\omega_c$. Since ω_c is unknown, a standard IMP controller is implemented through a block diagonal state space model, in which the best estimate of the frequency is used. A simple mapping from the states of the IMP controller to the errors in the frequency estimates was developed. This "measurement" of the frequency error is then used in the adaptation of the IMP controller parameters, so that these parameters converge to their true values. When

this adaptive IMP controller is placed into a feedback loop, the resulting closed-loop system produces zero steady state error for sinusoidal disturbances with unknown frequencies. Periodic or quasi-periodic disturbances that consist of multiple sinusoidal components, can also be perfectly cancelled by placing a number of these adaptive modules in parallel. Since adaptation is always present, this method is able to track slow variations in frequency, causing it to have almost perfect rejection for narrowband and sums of narrowband signals.

However, when a system is subject to both predictable and unpredictable disturbances, the presence of an IMP controller introduces a phase lag at relevant frequencies which will limit the wideband disturbance controller's capabilities for compensating unpredictable disturbance. This limitation can be resolved by using the intermittent cancellation control technique introduced by Brown *et al.* in [8, 9]. A simple implementation of this techniques is introduced in [10], where the predictable disturbance is constant. The constant disturbance is rejected using an integral controller, which is one of the simplest IMP controllers. When the error between output and disturbance signal is excessive, the integral control action is fully engaged with the maximum gain by design. When the error is not significant, the input to the integral controller is removed and the control action is maintained. A standard wideband disturbance controller is used to achieve desirable performance for unpredictable disturbances. Since the integral controller is not always present, this wideband disturbance controller can be made more aggressive while maintaining stability margins

and/or control actions at similar levels.

As an extension to the intermittent integral control, this chapter considers periodic signals with unknown frequencies as predictable disturbance. An adaptive IMP controller will be used to identify the unknown frequency and cancel the sinusoid. The input to the IMP controller is connected intermittently as to allow a wideband disturbance controller to minimize the unpredictable disturbance more efficiently. This chapter is organized as follows. The intermittent cancellation control strategy is discussed in Section 4.2. A switched system model of the intermittent control is derived followed by a stability theorem in Section 4.3. Numerical examples are presented in Section 4.4, followed by some concluding remarks in Section 4.5.

4.2 Open and Closed-Loop Control Strategy

The block diagram of the proposed control system is shown in Fig. 4.1. The block $L(s)$ generally includes both the process to be controlled with a standard wideband disturbance controller. The sinusoidal disturbance is $r(t) = a \sin(\omega_c t + \phi)$, where its parameters a, ω_c, ϕ are all unknown. The unpredictable disturbance $n(t)$ is an additive white Gaussian noise.

According to [6], a state space representation of the adaptive IMP controller
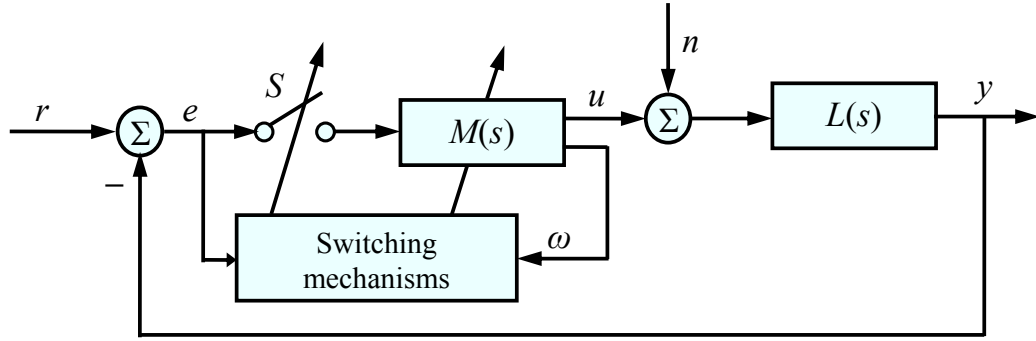
Figure 4.1: Block diagram of open and closed-loop control system

$M(s)$ is given by,

$$\begin{bmatrix} \dot{x}_1 \\ \dot{x}_2 \end{bmatrix} = \begin{bmatrix} 0 & \omega \\ -\omega & 0 \end{bmatrix} \begin{bmatrix} x_1 \\ x_2 \end{bmatrix} + \begin{bmatrix} 0 \\ f(t) \end{bmatrix} e \tag{4.1}$$

$$u = \begin{bmatrix} K_1 & K_2 \end{bmatrix} \begin{bmatrix} x_1 \\ x_2 \end{bmatrix} \tag{4.2}$$

$$\dot{\omega} = \begin{cases} K_\omega \frac{ex_1}{x_1^2 + x_2^2}, & \text{if } (x_1^2 + x_2^2) \geq \bar{x}_u \\ 0, & \text{if } (x_1^2 + x_2^2) < \bar{x}_u \end{cases} \tag{4.3}$$

where K_1, K_2 are two tuning gains of the IMP controller. Normally, the scalar function $f(t)$ takes its value at 0 or 1, where the 0 state represents the switch S in Fig. 4.1 being open. Although the true frequency of the sinusoid ω_c is unknown, according to the certainty equivalence principle, it can be replaced by its best estimate ω as shown in (4.1). This estimated frequency ω is then updated in (4.3) with an

adaptation gain K_ω, and is proved to converge to the true frequency in [6]. In order to avoid noise issues related to dividing a small number by another small number, the frequency adaptation is stopped when the squared norm of the two states is less than a threshold $\bar{x}_u$.

The tracking error $e(t)$ is the input to the IMP controller, and is connected intermittently with the opening and closing of the switch S. The switching control of S is based on two monitored signals: $e(t)$ and $x_m(t)$, where $x_m = \sqrt{x_{m1}^2 + x_{m2}^2}$, and x_{m1}, x_{m2} are the states of a monitored internal model given by

$$\begin{bmatrix} \dot{x}_{m1} \\ \dot{x}_{m2} \end{bmatrix} = \begin{bmatrix} 0 & \omega \\ -\omega & 0 \end{bmatrix} \begin{bmatrix} x_{m1} \\ x_{m2} \end{bmatrix} + \begin{bmatrix} 0 \\ 1 \end{bmatrix} e \qquad (4.4)$$

Correspondingly, there are two predefined thresholds e_u and x_u for the switching control.

The system begins as open loop control (S open, *i.e.*, $f(t) = 0$) with the adaptive IMP controller being initialized. When the monitored signal x_m exceeds the threshold x_u at time t, the closed-loop control is switched on by setting $f(t)$ to its maximum value 1. The states of the IMP controller are also modified,

$$f(t^+) = 1 \qquad (4.5)$$

$$x_j(t^+) = x_j(t) + \frac{x_{m,j}(t)}{K_s(t - t_l)}, \quad j \in \{1, 2\} \qquad (4.6)$$

where K_s is a scaling factor, and t_l is the last time the IMP controller is turned off or the initial time t_0. In (4.6), the IMP controller's states are augmented by the states of monitored internal model which are scaled by the time spent reaching the threshold x_u. With this modification to the states, the transient period can be reduced once the IMP controller is switched on for fast convergence.

The adaptive IMP controller remains active as long as the error $e(t)$ is excessive. Once the error is insignificant, the value of $f(t)$ starts to decrease as described by

$$\dot{f}(t) = -K_d(t)f(t) \tag{4.7}$$

$$K_d(t) = \begin{cases} K_{decay}, & |e(t)| < e_u \text{ \& } \left|e(t - \frac{T}{4})\right| < e_u \\ \\ 0, & \text{otherwise} \end{cases}$$

Since with a sinusoidal disturbance, the absolute error goes through zero every half cycle, the insignificance of $e(t)$ cannot be determined by condition $|e(t)| < e_u$ alone. In addition, the error value at $(t - \frac{T}{4})$ should also be compared with e_u, where $T = \frac{2\pi}{\omega}$ is the estimated period of the sinusoid. If the error is less than the threshold at both time instants, $f(t)$ is then reduced exponentially at a rate of K_{decay}. This smooth removal of $f(t)$ is adopted to avoid the phenomenon called chattering. Once $f(t)$ is reduced to insignificance, as measured by f^l, it is set to zero. The IMP controller stops the adaptation of the estimated frequency. With no input, a fixed sinusoid is cancelled via an open loop mechanism. If perfect cancellation is not achieved, the

states of the monitored marginally stable internal model will grow linearly and will eventually cause the switch S to close again. t_l is set to current time t.

Table 4.1 lists reasonable methods of choosing related parameters for fast response and maximum disturbance attenuation.

Table 4.1: Guidelines for parameter selections

K_1, K_2	Must be chosen such that the phase of the IMP controller plus the phase of $L(s)$ at ω is between $-45°$ and $-135°$.
e_u	Closed-loop level of noise and disturbance gives a reasonable value for e_u.
x_u	e_u value multiplied by the desired response time.
f^l	Between 0.05 and 0.2.
K_{decay}	Can be chosen up to 5 times the reciprocal of the closed-loop rise time.
K_ω	Can be chosen that the dominant closed-loop poles are at least twice faster than the frequency adaptation speed.

4.3   Switched System Model and Stability Analysis

Let

$$\dot{x} = Ax + Bu \tag{4.8}$$

$$y = Cx \tag{4.9}$$

be a state space representation of $L(s)$ shown in Fig. 4.1, where $x \in \mathbb{R}^n$. From (4.1)-(4.2) and (4.8)-(4.9), by letting $z = [x^T, x_1, x_2]^T$, $z \in \mathbb{R}^{n+2}$, the overall intermittent control system shown in Fig. 4.1 can be expressed as

$$\dot{z} = \begin{bmatrix} A & BK_1 & BK_2 \\ 0 & 0 & \omega \\ -f(t)C & -\omega & 0 \end{bmatrix} z + \begin{bmatrix} 0 \\ 0 \\ f(t) \end{bmatrix} r(t)$$

$$:= A_\sigma(t)z + B_\sigma(t)r(t) \tag{4.10}$$

$$y = \begin{bmatrix} C & 0 & 0 \end{bmatrix} z \tag{4.11}$$

Based on the switching mechanisms described in Section 4.2, this intermittent control system can be modelled as a switched system with two subsystems. The switching signal $\sigma(t)$ is defined as

$$\sigma(t) = \begin{cases} 1, & \text{if } f(t) \in (f^l, 1] \\ 2, & \text{if } f(t) = 0 \end{cases} \tag{4.12}$$

Let set $\{t_i\}$ represent the switching time instants with i being positive integer numbers and $t_i \leq t_{i+1}$. We also define pairs of subsets of $\{t_i\}$ for any $q \in \{1, 2\}$ as follows

$$\{\bar{t}_{q,k}\} = \{t_i | \text{when subsystem } q \text{ is switched on}\},$$

$$\{\underline{t}_{q,k}\} = \{t_i | \text{when subsystem } q \text{ is switched off}\}$$

with $\bar{t}_{q,k} < \underline{t}_{q,k}$. Let S be a switching sequence associated with the switched system. The interval completion $\mathcal{I}(S|q)$ is defined as the completion of the set of time intervals during which subsystem q is active, *i.e.*, $\mathcal{I}(S|q) = \bigcup_k \left[\bar{t}_{q,k}, \underline{t}_{q,k}\right]$.

Matrices $A_\sigma(t)$, $B_\sigma(t)$ can be written as

$$A_1(t) = \begin{bmatrix} A & BK_1 & BK_2 \\ 0 & 0 & \omega \\ -\exp(\int_{\bar{t}_{1,k}}^t -K_d d\tau)C & -\omega & 0 \end{bmatrix}, \tag{4.13}$$

$$B_1(t) = \begin{bmatrix} \mathbf{0} \\ 0 \\ \exp(\int_{\bar{t}_{1,k}}^t -K_d d\tau) \end{bmatrix}, \tag{4.14}$$

$$A_2 = \begin{bmatrix} A & BK_1 & BK_2 \\ 0 & 0 & \omega \\ 0 & -\omega & 0 \end{bmatrix}, \tag{4.15}$$

$$B_2 = \begin{bmatrix} \mathbf{0} \\ 0 \\ 0 \end{bmatrix}, \tag{4.16}$$

with $\bar{t}_{1,k} \le t \le \underline{t}_{1,k}$. Pair $\left(A_1(t), B_1(t)\right)$ describes the closed-loop control subsystem with adaptive frequency estimation, and $\left(A_2, B_2\right)$ describes the open loop control subsystem without frequency adaptation.

For simplicity, analysis of the algorithm has been performed with K_s set to

infinity. Under this condition, for the switched system described by (4.10) and (4.11), we have

Theorem 4.1. *If K_1, K_2, f^l, and K_{decay} are chosen such that the following assumptions are satisfied,*

1. *The equilibrium of subsystem 1 is uniformly exponentially stable, i.e., there exist finite positive constants γ_1, λ_1, such that $\|\Phi_1(t,\tau)\| \leq \gamma_1 e^{-\lambda_1(t-\tau)}$, where $\Phi_1(t,\tau)$ is the transition matrix of subsystem 1;*

2. *There exists a constant $\mu_2 > 0$, such that each eigenvalue of A satisfies $Re[\mathrm{eig}(A)] \leq -\mu_2$;*

3. *The minimum active time of subsystem 1, τ_{1m}, given by $\tau_{1m} = -\ln(f^l)/K_{decay}$, satisfies $\tau_{1m} \geq \tau_s$, where τ_s is dependent on $A_\sigma(t)$,*

the switched system (4.10), (4.11) is stable in the sense of Lyapunov.

The proof of this theorem is based on a multiple Lyapunov functions approach developed in [11], and is similar to the proof of Theorem 1 in [10], thus is omitted here. Note assumption 1 is guaranteed if the time derivative of matrix $A_1(t)$ is upper bounded by the condition given in [12]. This condition is always satisfiable for sufficiently small K_{decay}.

4.4 Simulation Results

The performance of the intermittent cancellation control strategy is demonstrated via two examples.

4.4.1 Example 1

A simple second order plant given by

$$\dot{x}_p = \begin{bmatrix} -1 & -1 \\ 1 & 0 \end{bmatrix} x_p + \begin{bmatrix} 1 \\ 0 \end{bmatrix} u + \begin{bmatrix} 1 & 0 \\ 0 & 1 \end{bmatrix} n(t) \tag{4.17}$$

$$y = \begin{bmatrix} \frac{1}{3} & 1 \end{bmatrix} x_p \tag{4.18}$$

is considered. As shown in Fig. 4.1, the disturbance consists of a sinusoidal signal, $r(t) = 1.5\sin(0.6t)$, and a vector of Gaussian noise $n(t)$ with zero mean and standard deviation 0.05. With this noise level, the standard deviation of the open loop system output is 0.0037. The goal of this example is to design a wideband disturbance controller and an adaptive internal model principle controller to identify the sinusoidal frequency and minimize both disturbance components. This design is based on two non-intermittent controllers which are introduced first.

4.4.1.1   Controller 1

This controller is a wideband disturbance controller and is designed using linear quadratic regulator (LQR) method. The optimization criterion is defined as

$$J = \int_{t_i}^{t_f} (y^2 + u^T R u) \mathrm{d}t \tag{4.19}$$

where R is a weighting matrix, t_i, $t_f = \infty$ are the initial and final times respectively. The optimal state feedback gain is given by [13]

$$K_m = -R^{-1} B_p^T P, \tag{4.20}$$

where P is the solution to the algebraic Riccati equation (ARE),

$$A_p^T P + P A_p - P(B_p R^{-1} B_p^T)P + C_p^T C_p = 0 \tag{4.21}$$

and (A_p, B_p, C_p) is a state representation of the plant, such as those given in (4.17)-(4.18). By choosing the weighting matrix $R = 0.2$, we obtain $K_m = [-1.1106, \ -1.4495]$.

4.4.1.2   Controller 2

In order to reject the sinusoidal disturbance with unknown frequency, we need to tune the adaptive IMP controller described by (4.1)-(4.3). Using the augmenting method presented in [14], we can treat the two states of the IMP controller as additional

states together with the plant states to implement LQR method. The state equations

of this augmented system are

$$
\begin{bmatrix} \dot{x}_p \\ \dot{x}_1 \\ \dot{x}_2 \end{bmatrix} = A_e \begin{bmatrix} x_p \\ x_1 \\ x_2 \end{bmatrix} + B_e u + W_e n(t) \tag{4.22}
$$

$$
y = C_e \begin{bmatrix} x_p \\ x_1 \\ x_2 \end{bmatrix} \tag{4.23}
$$

where

$$
A_e = \begin{bmatrix} A_p & 0 & 0 \\ 0 & 0 & \omega \\ -C_p & -\omega & 0 \end{bmatrix}, \ B_e = \begin{bmatrix} B_p \\ 0 \\ 0 \end{bmatrix},
$$

$$
C_e = \begin{bmatrix} C_p & 0 & 0 \end{bmatrix}, \ W_e = \begin{bmatrix} 1 & 0 \\ 0 & 1 \\ 0 & 0 \\ 0 & 0 \end{bmatrix}.
$$

The optimization criterion (4.19) is then written as

$$J = \int_{t_i}^{t_f} (y^2 + \rho_1 x_1^2 + \rho_2 x_2^2 + u^T R u) \mathrm{d}t \tag{4.24}$$

for this augmented system. Note that weight must be applied to an augmented state to satisfy the observability requirement of LQR control. The weighting R is the same as in controller 1's design. ρ_1, ρ_2 are two weightings on the IMP controller states. For the choice of $\rho_1 = 0$, $\rho_2 = 0.3$, we obtain the optimal state feedback gain for the augmented system as $K_e = [-1.5708, \ -2.1427, \ -0.4159, \ 1.1520]$. The dominant closed-loop poles are $-0.254 \pm j0.539$. The adaptation gain for the estimated frequency is chosen as $K_\omega = -0.1$, such that the dominant poles are 2.5 times faster than the adaptation speed.

4.4.1.3   Intermittent cancellation controller

In this example, $L(s)$ in Fig. 4.1 is designed as the combination of the plant and controller 1. Thus a state representation of $L(s)$ is given by $(A_p + B_p K_m, B_p, C_p)$, with the same K_m value as for controller 1. We take the same gain for the adaptive IMP controller $M(s)$ as in controller 2, which are $K_1 = -0.4159$, $K_2 = 1.1520$, and $K_\omega = -0.1$. The standard deviation of the tracking error and the rise time of the closed-loop system are measured as $\sigma_1 = 0.004$ and $t_r = 25$. According to the guidelines in Table 4.1, corresponding parameters for the intermittent control are chosen as $f^l = 0.1$, $e_u = 0.01$, $x_u = 0.25$, $K_s = 20$, and $K_{decay} = 0.1$. The initial

value of the estimated frequency is chosen as $0.5 \ rad/s$.

The simulation was run for a total of 800 time units. The sinusoidal component $r(t)$ is only present between 199 and 612 while the Gaussian noise $n(t)$ is always present. To better demonstrate the disturbance rejection performance of the intermittent control, we compare its optimization cost function values with controller 1 and controller 2. The cost functions are calculated using the following criterion

$$J = \int_{0}^{t_f} [y(t) - r(t)]^2 + [u(t) - u_{ss}(t)]^2 R \mathrm{d}t \tag{4.25}$$

where $u_{ss}(t)$ is the steady state control signal, and t_f is the simulation time. Since the frequency response of the plant at $\omega = 0.6 \ rad/s$ is $G(j\omega) = 1.1625\angle - 31.84°$, in steady state, between $t = 199$ and $t = 612$, $u_{ss}(t) = 1.2903\sin(0.6t + 31.84°)$, otherwise it is zero. For controller 1, $u_{ss}(t) = 0.9794\sin(0.6t + 173.47°)$ for $199 < t < 612$ and is zero otherwise. To distinguish between the transient response performance and disturbance rejection capability of the approaches, the costs are broken into five time intervals as follows.

(I) $0 \leq t \leq 199$, only the additive Gaussian noise is present.

(II) $199 < t \leq 250$, transient period after the sinusoidal disturbance is introduced at $t = 199$.

(III) $250 < t \leq 612$, steady state period after the sinusoid is introduced.

(IV) $612 < t \leq 640$, transient period after the sinusoid is removed at $t = 612$.

(V) $640 < t \leq 800$, steady state period after the sinusoid is removed.

The costs of the controllers are listed In Table 4.2 and Table 4.3. The intermittent cancellation controller is referred to as controller 3. The costs of controller 2 and controller 3 in Table 4.2 are calculated with frequency adaptation. In Table 4.3, the costs are calculated when the frequency adaptation was turned off for both controllers. In this case, the sinusoid's frequency is known. Since there is no IMP control in controller 1, the costs for both cases are the same.

Table 4.2: Costs of disturbance rejection performance with frequency adaptation

Interval	Controller 1	Controller 2	Controller 3
I	0.0034	0.0041	0.0034
II	9.9529	13.9305	5.7661
III	71.1713	0.0186	0.0174
IV	0.0160	3.7715	3.7128
V	0.0029	0.0043	0.0036

Table 4.3: Costs of disturbance rejection performance without frequency adaptation

Interval	Controller 2	Controller 3
I	0.0042	0.0034
II	4.1699	3.6713
III	0.0125	0.0115
IV	3.7875	3.7462
V	0.0039	0.0030

Compared to controller 2, controller 3 has 20% improvements during intervals I and V. During transient interval II, controller 3 has a significant 1.4 times improvement. The improvement of controller 3 during interval III is not significant, because

the algorithm has not completely converged. If the simulation time was extended, we could get similar percentage improvements as during intervals I and V. From both tables, we can see controller 3 has less costs than the other two controllers during each time interval. Both controller 2 and controller 3 have less costs when the frequency adaptation is turned off compared to unknown frequency case.
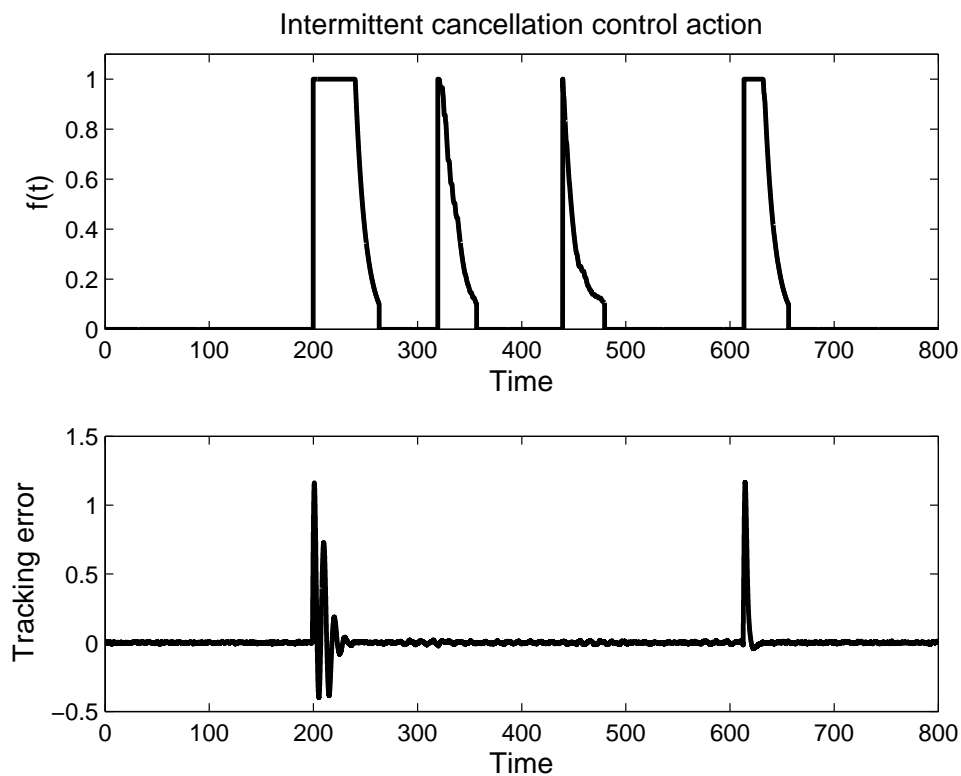

Figure 4.2: Intermittent IMP control and tracking error

The intermittent IMP control action is illustrated in the top plot of Fig. 4.2 by showing the value of $f(t)$ of the adaptive IMP controller. The tracking error $e(t)$ is shown in the bottom plot. The estimated disturbance frequency is shown in the top plot of Fig. 4.3. Before the sinusoidal disturbance is introduced, the frequency stays
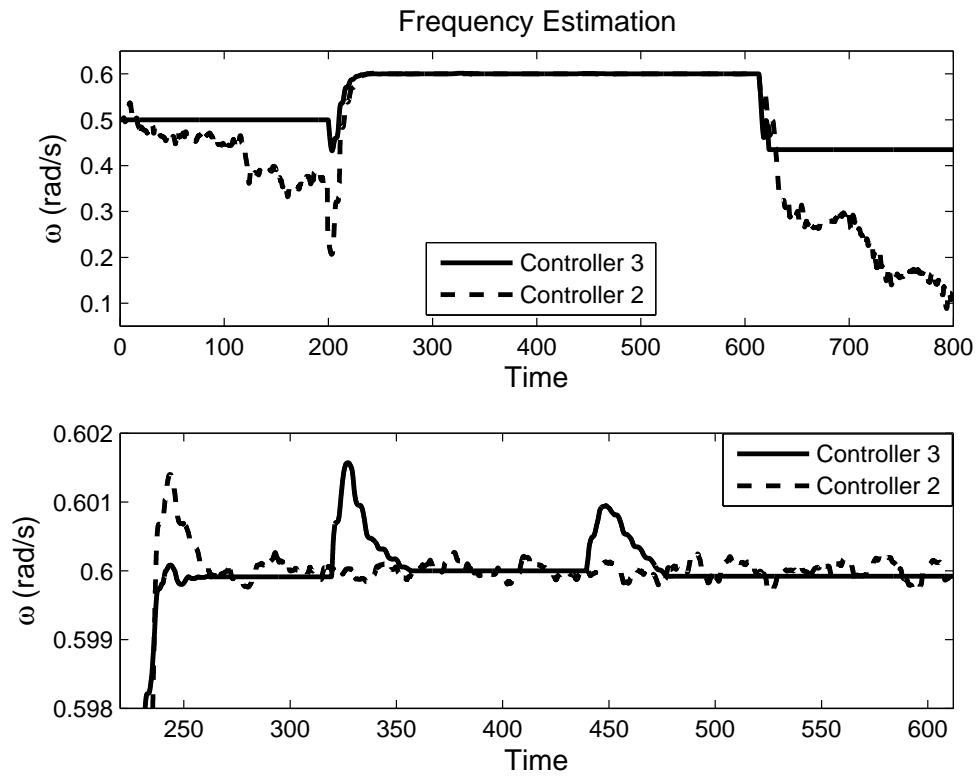
Figure 4.3: Frequency estimation of the intermittent and non-intermittent control

at its initial value 0.5 rad/s. When the monitored signal $x_m(t)$ is greater than the

threshold x_u after the sinusoid is introduced at $t = 199$, the IMP controller is turned

on by setting $f(t) = 1$. The adaptation of the disturbance frequency starts. In the

mean time, the plant output starts to track the sinusoidal disturbance.

When the tracking error $e(t)$ is less than e_u at both the current instant and

one quarter period earlier as defined in section 4.2, $f(t)$ starts to decay exponentially

with a rate of K_{decay}. When $f(t)$ decreases to the lower threshold f^l, the input

to the adaptive IMP controller $e(t)$ is removed by setting $f(t) = 0$. The estimated

frequency stops updating until next switch-on of the controller. This can be seen in
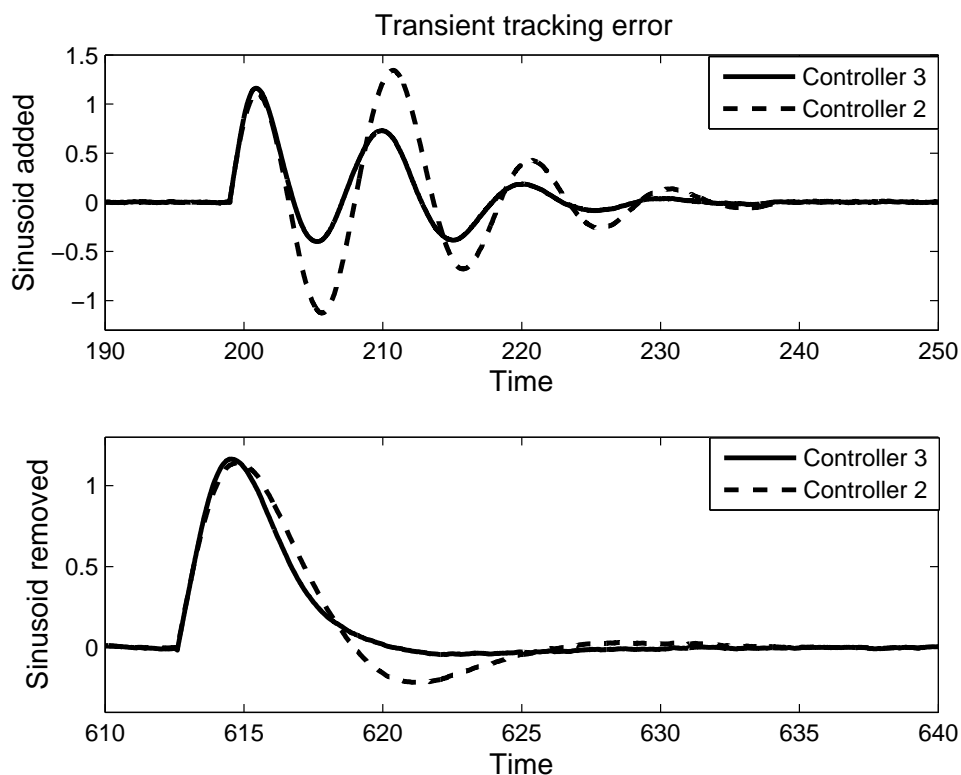
Figure 4.4: Tracking error during transient periods

the bottom plot of Fig. 4.3, where the estimated frequency using controller 2 is also plotted for comparison. In Fig. 4.2, $f(t)$ starts to decrease immediately after the second switch-on of the controller which indicates the insignificance of the tracking error. There remains an exponentially decaying residue error that continues to cause the IMP controller to be invoked.

One of the stability requirements for controller 2 is that a predictable component exists. However, this assumption is violated when $t < 199$ and $t > 612$. As a result, controller 2's frequency estimation changes drastically when $t < 199$ and $t > 612$, which is shown in the top plot of Fig. 4.3. The abrupt removal of the sinusoidal

disturbance introduces a decaying exponential term in the output. Mathematically, this can be modelled as a complex frequency with zero real part. The adaptive IMP control algorithm 'perceives' this and responds by having the identified frequency converge to zero. Controller 3 automatically avoids this by disabling the IMP control when the predictable component is absent. As a result, the frequency stops adaptation and stays as it is, which is shown in the top plot of Fig. 4.3. From this plot, it can also be seen that estimated frequency of controller 2 decays towards zero, *i.e.* the IMP controller becomes an integral controller. If the wideband disturbance controller included in $L(s)$ contains integral action, the two parallel integral controllers can lead to stability problems. Controller 3 provides a major improvement to avoid this issue. The tracking error of controller 3 during transient periods, during which the sinusoid is added and removed, are shown in Fig. 4.4 together with controller 2's performance for comparison.

4.4.2 Example 2

In this example, a periodic disturbance with two sinusoidal components is considered. That is

$$r(t) = 1.5\sin(0.6t) + \sin(t + 0.2)$$

The standard deviation of the zero mean Gaussian noise vector $n(t)$ is 0.1, which results in a standard deviation of 0.0071 for the open loop system output. The

same plant as in Example 1 is considered. The open loop system controller is exactly the same as in previous example, which has the state feedback gain as

$K_m = [-1.1106, -1.4495]$.

4.4.2.1 Controller 2

Since there are two sinusoidal components in the disturbance, two corresponding adaptive IMP controllers need to be designed for estimating both frequencies. Following the same augmentation method used in Example 1, a state representation of the augmented system can be obtained as

$$
\begin{bmatrix} \dot{x}_p \\ \dot{x}_{11} \\ \dot{x}_{12} \\ \dot{x}_{21} \\ \dot{x}_{22} \end{bmatrix} = A_e \begin{bmatrix} x_p \\ x_{11} \\ x_{12} \\ x_{21} \\ x_{22} \end{bmatrix} + B_e u + W_e n(t) \tag{4.26}
$$

$$
y = C_e \begin{bmatrix} x_p \\ x_{11} \\ x_{12} \\ x_{21} \\ x_{22} \end{bmatrix} \tag{4.27}
$$

where x_{11}, x_{12} and x_{21}, x_{22} are the states of the two IMP controllers, ω_1, ω_2 are estimates of the two sinusoids frequencies, and

$$
A_e = \begin{bmatrix} A_p & 0 & 0 & 0 & 0 \\ 0 & 0 & \omega_1 & 0 & 0 \\ -C_p & -\omega_1 & 0 & 0 & 0 \\ 0 & 0 & 0 & 0 & \omega_2 \\ -C_p & 0 & 0 & -\omega & 0 \end{bmatrix}, \quad B_e = \begin{bmatrix} B_p \\ 0 \\ 0 \\ 0 \\ 0 \end{bmatrix},
$$

$$
C_e = \begin{bmatrix} C_p & 0 & 0 & 0 & 0 \end{bmatrix}, \quad W_e = \begin{bmatrix} 1 & 0 \\ 0 & 1 \\ 0 & 0 \\ 0 & 0 \\ 0 & 0 \end{bmatrix}.
$$

The optimization criterion is

$$
J = \int_{t_i}^{t_f} (y^2 + \rho_{11} x_{11}^2 + \rho_{12} x_{12}^2 + \rho_{21} x_{21}^2 + \rho_{22} x_{22}^2 + u^T R u)\mathrm{d}t \qquad (4.28)
$$

for this augmented system with corresponding weightings. By choosing $\rho_{11} = \rho_{21} = 0$, $\rho_{12} = 0.3$, $\rho_{22} = 0.2$, the optimal state feedback gain is

$$K_e = [-1.8657, -2.6591, -0.6941, -1.0091, -0.0527, -0.9986]$$

4.4.2.2   Intermittent cancellation controller

For the two adaptive IMP controllers, their gains are the same as those of controller 2, which are $K_{11} = -0.6941$, $K_{12} = -1.0091$, $K_{21} = -0.0527$, $K_{22} = -0.9986$. The initial estimates of the two frequencies are 1.2 rad/s and 0.8 rad/s respectively. The frequency adaptation gain for both controllers is $K_\omega = 0.05$. The two IMP controllers also share the same set of parameters for intermittent control, which are $f^l = 0.1$, $x_u = 0.25$, $e_u = 0.01$, $K_s = 20$, and $K_{decay} = 0.05$.

The simulation was run for 800 time units for both controller 2 and the intermittent cancellation controller (controller 3). The disturbance $r(t)$ is present from $t = 98.37$, and the Gaussian noise is present for the whole time. Using the same criterion as in (4.25), cost functions are calculated over three time intervals: (I) $0 \leq t \leq 98.37$, (II) $98.37 < t \leq 200$, and (III) $200 < t \leq 800$. The steady state control signal for this example is calculated as

$$u_{ss}(t) = 1.2903\sin(0.6t + 31.84°) + 0.9487\sin(t + 71.57°)$$

for $t > 98.37$, otherwise it is zero. For controller 1, the steady state control signal is

$$u_{ss}(t) = 0.9794 \sin(0.6t + 173.47^\circ) + 0.7132 \sin(t + 161.94^\circ)$$

$t > 98.37$, otherwise it is zero.

Table 4.4 gives the costs of the three controllers' rejection performance during different time intervals. When the periodic disturbance $r(t)$ is not present, controller

Table 4.4: Costs of rejection of multiple sinusoids

Interval	Controller 1	Controller 2	Controller 3
I	0.0053	0.0082	0.0053
II	67.4366	11.7477	6.9143
III	419.7938	2.2155	2.1941

3 has over 54% improvement than controller 2. Controller 3 has almost 70% less cost than controller 2 during the transient after $r(t)$ is introduced. After the transient dies out, controller 3 still has less cost than that of controller 2.

Fig. 4.5 shows the intermittent control actions of the two IMP controllers, where $f_1(t)$, $f_2(t)$ are the same functions as in (4.1) for the two IMP controllers, respectively. The two estimated frequencies are shown in Fig. 4.6 . For comparison, controller 2's frequency estimates are also plotted. It can be seen that controller 2's estimated frequencies decay towards zero when $r(t)$ is absent, while controller 3's estimates stay at their initial values. The tracking errors of the two controllers during the transient period are shown in Fig. 4.7.
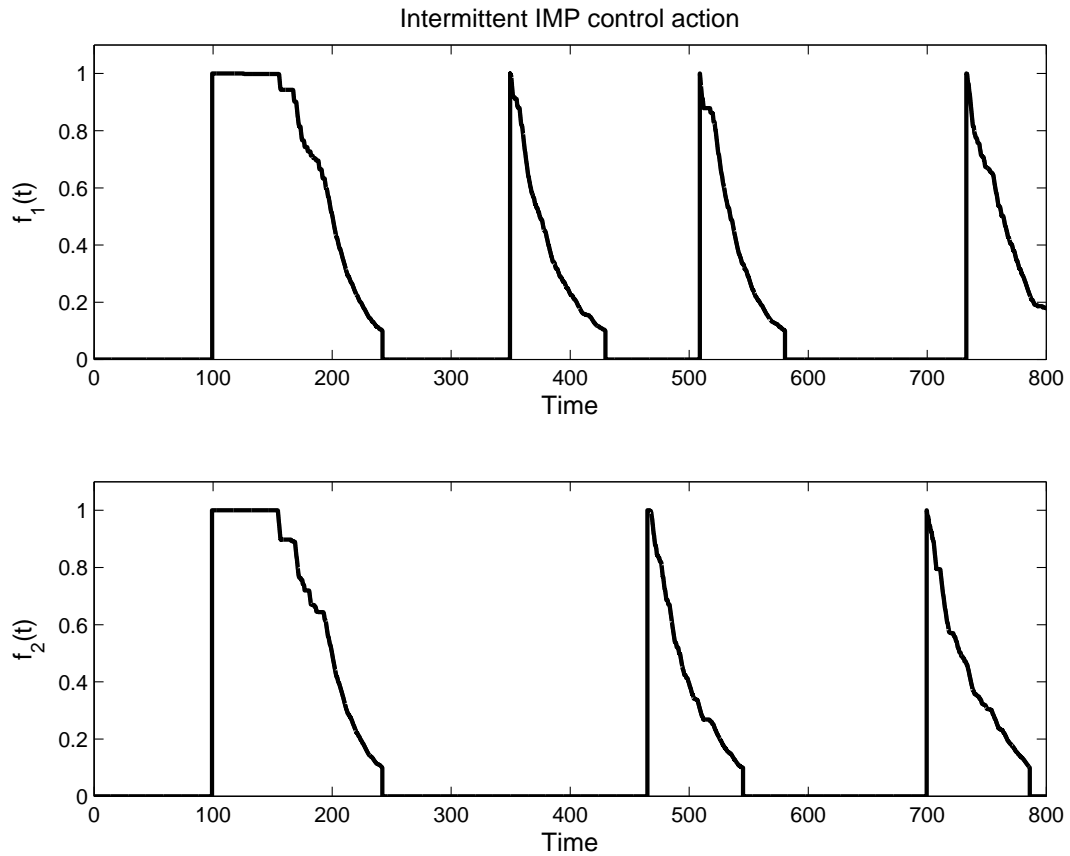
Intermittent IMP control action

Figure 4.5: Intermittent IMP control action

4.5 Conclusions

A control strategy is presented for cancelling disturbances with both predictable and unpredictable components. By intermittently connecting the input to an adaptive IMP controller, which can cancel the predictable component (sinusoidal signal), the control system operates between open and closed-loop control modes. In closed-loop mode, the IMP controller can identify the unknown frequency of the sinusoid using an adaptive algorithm. In open loop mode, a state feedback controller is imple-
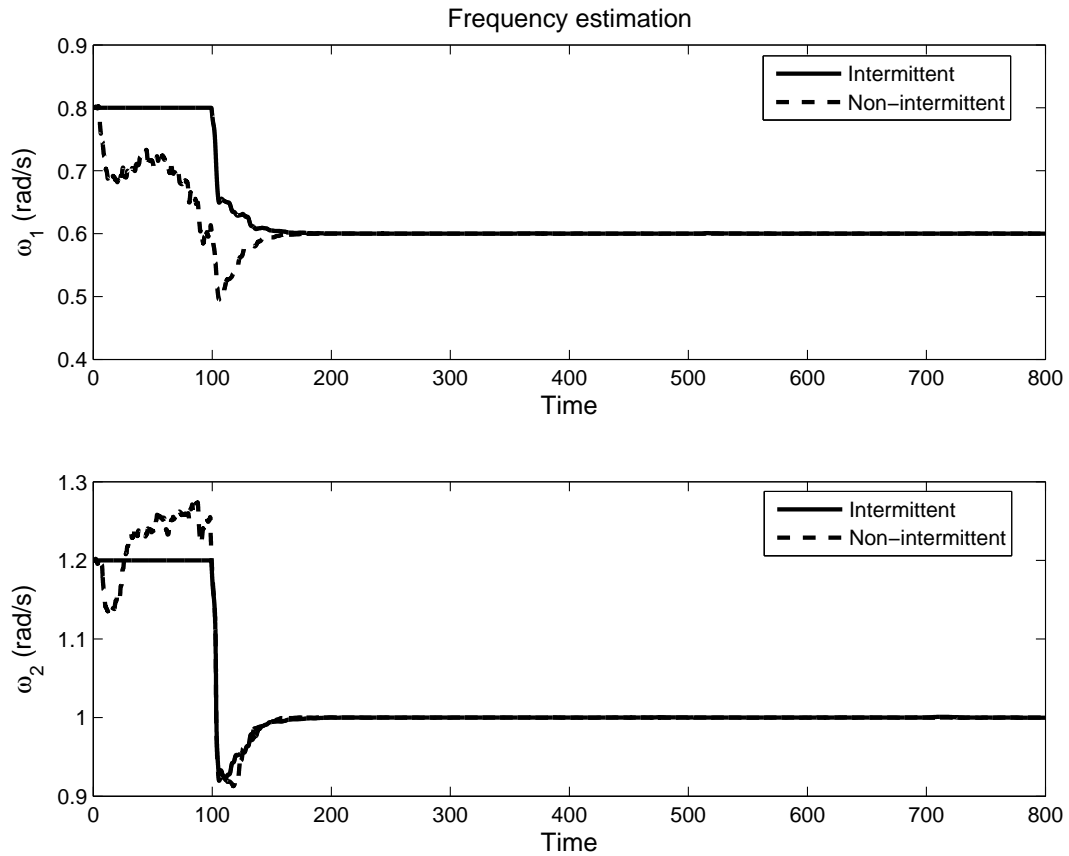
Figure 4.6: Frequency estimation using adaptive IMP algorithm

mented to minimize the unpredictable component (white Gaussian noise). With the IMP controller being turned off, the state feedback controller can be made more aggressive while maintaining stability margin and control actions. The advantage of the intermittent control strategy is demonstrated through numerical examples. This intermittent control system is modelled as a switched system for stability analysis, which is based on an extended multiple Lyapunov functions approach developed in [11]. One of the main difficulties of safely implementing the algorithm in [7] is the requirement of perfect knowledge of the number of sinusoids to be tracked or cancelled.
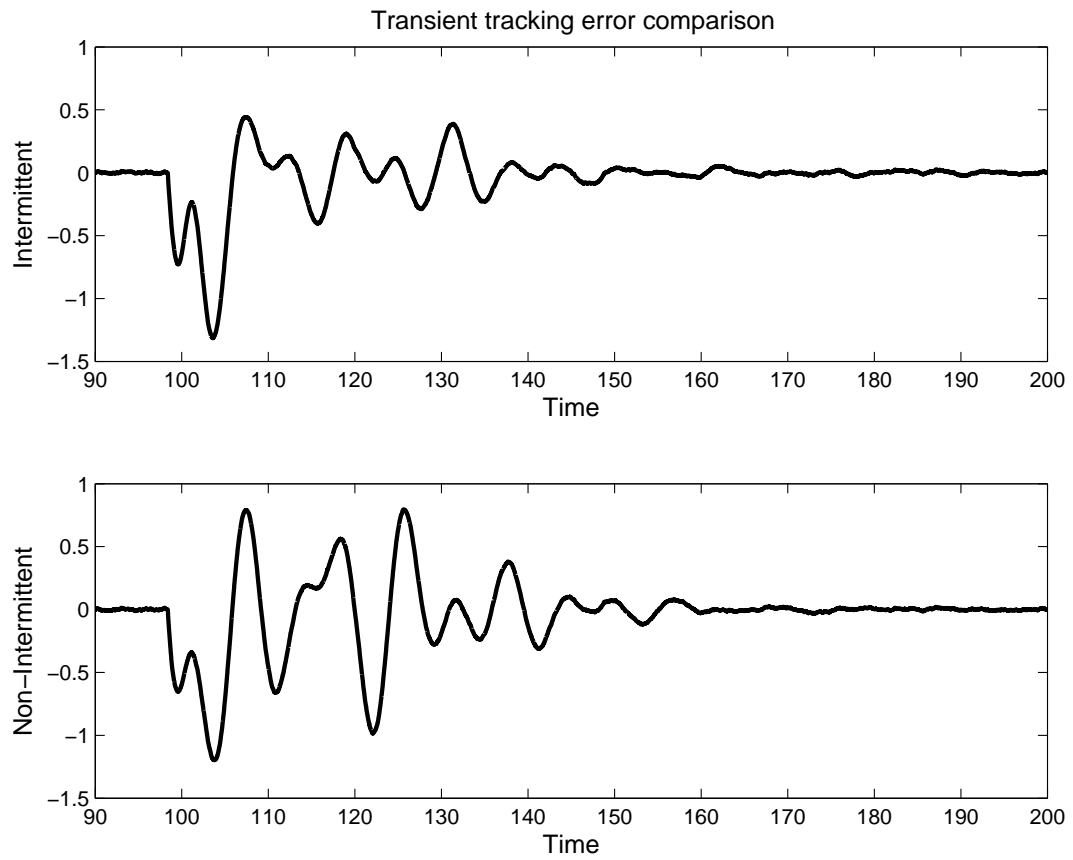
Figure 4.7: Transient tracking error comparison between intermittent and non-intermittent control

This switching algorithm can be used to eliminate that requirement.

Bibliography

[1] B. A. Francis and W. M. Wonham, "The Internal Model Principle of Control Theory," *Automatica*, vol. 12, pp. 457–465, 1976.

[2] L. A. Sievers and A. H. von Flotow, "Comparison and Extensions of Control Methods for Narrow-band Disturbance Rejection," *IEEE Transactions on Signal Processing*, vol. 40, no. 10, pp. 2377–2391, Oct. 1992.

[3] J. R. Glover, "Adaptive Noise Canceling Applied to Sinusoidal Interferences," *IEEE Transactions on Acoustics, Speech, and Signal Processing*, vol. ASSP-25, no. 6, pp. 484–491, Dec. 1977.

[4] M. Bodson, J. S. Jensen, and S. C. Douglas, "Active Noise Control for Periodic Disturbances," *IEEE Transactions on Control Systems Technology*, vol. 9, no. 1, pp. 200–205, Jan. 2001.

[5] P. A. Regalia, "An Improved Lattice-Based Adaptive IIR Notch Filter," *IEEE Transactions on Signal Processing*, vol. 39, no. 9, pp. 2124–2128, Sep. 1991.

[6] L. J. Brown and Q. Zhang, "Identification of Periodic Signals with Uncertain Frequency," *IEEE Transactions on Signal Processing*, vol. 51, no. 6, pp. 1538–1545, Jun. 2003.

[7] L. J. Brown and Q. Zhang, "Periodic Disturbance Cancellation with Uncertain Frequency," *Automatica*, vol. 40, pp. 631–637, 2004.

[8] L. J. Brown, G. E. Gonye, and J. S. Schwaber, "Non-linear PI Control Inspired by Biological Control Systems," in *Proceedings of the 37th IEEE Conference on Decision and Control*, Tampa, FL, Dec. 1998, pp. 1040–1045.

[9] L. J. Brown and J. S. Schwaber, "Intermittent Cancellation Control: A Control Paradigm Inspired by Mammalian Blood Pressure Control," in *Proceedings of the American Control Conference*, San Diego, CA, Jun. 1999, pp. 139–143.

[10] J. Lu and L. J. Brown, "Stability Analysis of a Proportional with Intermittent Integral Control System," in *Proceedings of the 2010 American Control Conference*, Baltimore, MD, Jul. 2010, pp. 3257–3262.

[11] ——, "A Multiple Lyapunov Functions Approach for Stability of Switched Systems," in *Proceedings of the 2010 American Control Conference*, Baltimore, MD, Jul. 2010, pp. 3253–3256.

[12] C. A. Desoer, "Slowly Varying System $\dot{x} = A(t)x$," *IEEE Transactions on Automatic Control*, pp. 780–781, Dec. 1969.

[13] H. Kwakernaak and R. Sivan, *Linear Optimal Control Systems*. John Wiley and Sons, Inc., 1972.

[14] C.-T. Chen, *Linear System Theory And Design*, 3rd ed. New York, NY: Oxford University Press, 1999.

Chapter 5

Conclusions

5.1   Summary

Two advanced applications of the internal model principle control theory are discussed in this thesis.

First, as a signal processing problem, an IMP based adaptive algorithm is developed for the identification of exponentially damped sinusoidal signals with unknown parameters. Estimation of the two key parameter, damping factor and frequency, is the focus of this algorithm. This algorithm is developed in discrete time based on its continuous time version presented in [2]. A state space representation of the signal model in terms of estimated parameters is derived. The differences between the parameter estimations and their true values can be described in terms of the model state variables and the tracking error. By using integral controllers, the two parameter estimation errors can be eliminated asymptotically. Local exponential stability and convergence of this adaptive algorithm is proved using a two time scale averaging theory developed in [3].

Simulation results in the MATLAB/Simulink environment show that this algorithm can not only identify constant parameters, but also track slowly time-varying parameters of the EDS signal. By constructing a series of IMP controllers in parallel, the adaptive feedback system can identify a signal composed of a sum of EDS modes, with each IMP controller corresponding to one EDS mode. From the simulation results, this algorithm has shown its functionality despite the limitation that the slow system shall be slower than the fast system. In order to speed up the algorithm, the closed-loop poles can be placed closer to the origin by tuning the function $L(z)$.

The second advance in IMP control theory is its application in switched systems. For a system subjected to a disturbance with both predictable and unpredictable components, two disturbance controllers need to be designed with their own attempts to achieve best performance. An IMP controller is a perfect candidate for cancelling the narrowband disturbance. A state feedback controller is designed using the LQR method to minimize the white noise. But when both controllers are present in a feedback system, they affect each other's rejection capabilities. Especially, the state feedback controller's capability of minimizing the white noise is limited due to the phase lag introduced by the IMP controller.

In order to achieve an optimal disturbance rejection performance, a combination of open and closed-loop control strategy is presented. When the narrowband disturbance is significant, both controllers are active, in a closed-loop mode, to achieve fast rejection. The system switches to open loop control mode when the narrowband dis-

turbance is cancelled within an acceptable range. In this control mode, the input to the IMP controller, which is the tracking error, is disconnected. The IMP controller's output is maintained. Thus the state feedback controller is made more aggressive in minimizing the white noise while maintaining the stability margins and control actions. Depending on the level of the tracking error, the IMP controller's input may be connected intermittently. Simulation results confirm the performance improvement of this control strategy compared with two other controllers, a state feedback controller and an augmented state feedback controller with IMP control action.

In this thesis, two types of narrowband signals are considered, constant and periodic with unknown frequencies. For a constant disturbance, a simple IMP controller, integrator, is used. For the periodic case, traditional adaptive IMP controllers are used to first identify the unknown frequencies before the periodic disturbance can be cancelled. If the periodic signal contains multiple sinusoidal components with unknown frequencies, the same number of adaptive IMP controllers need to be placed in parallel.

Due to its intermittent control fashion, this control strategy is modelled as a switched system for stability analysis. Since existing stability analysis techniques cannot be applied directly, an extended multiple Lyapunov functions approach is developed to relax some constraints.

5.2 Concluding Remarks

Internal model principle control theory has drawn many researchers' attention in the area of output regulation. The adaptive IMP control algorithm developed in [1] is capable of estimating frequencies of periodic or quasi-periodic signals to achieve zero-error regulation. The advantages of applying this algorithm include its ability of online real time fast estimation and low computational cost.

However, two of the main drawbacks of this approach is the requirement to design stabilizing feedback gains and the need for *a priori* knowledge of the number of signals to be cancelled. Note that the feedback design problem becomes increasingly difficult and even infeasible as the number of frequencies increases.

By integrating the intermittent control to the adaptive IMP control algorithm, the number of sinusoids to be cancelled is not necessarily required. Based on the level of tracking error, the switching control mechanism determines the number of adaptive IMP controllers to be turned on. This switching control thus makes the feedback design feasible even with a large number of sinusoids.

This control strategy can also relax two design constraints in linear control, which are the trade-off between response speed and noise rejection ability, as well as the trade-off between the speed and actuator control effort. This improvement is demonstrated through the simulation results in Chapter 3 and Chapter 4.

5.3 Future Work

Active acoustic noise control is an important area in many applications. The acoustic noise can be cancelled using speakers. Due to the nature of some applications, such as rotating electric fans, we know the noise signals are periodic but their frequencies are uncertain. It will be of our interest to build a model of such application and to implement the adaptive IMP control algorithm for identifying and cancelling the noise.

From the simulation results in Chapter 2, we notice that the estimation performance of the proposed adaptive algorithm degrades as the number of EDS modes increases. It will be worthy investigating the estimation performance by combining the intermittent control with the adaptive IMP control for EDS signals. And apply this approach to real musical signals, which have more complicated spectrum contents. This would be a possible future work in this area.

Bibliography

[1] L. J. Brown and Q. Zhang, "Identification of Periodic Signals with Uncertain Frequency," *IEEE Transactions on Signal Processing*, vol. 51, no. 6, pp. 1538–1545, Jun. 2003.

[2] J. Lu and L. J. Brown, "Internal model principle based control of exponentially damped sinusoids," *International Journal of Adaptive Control and Signal Processing*, vol. 24, no. 3, pp. 219–232, 2010.

[3] E. Bai, L. Fu, and S. S. Sastry, "Averaging Analysis for Discrete Time and Sampled Data Adaptive Systems," *IEEE Transactions on Circuits and Systems*, vol. 35, no. 2, pp. 137–148, Feb. 1988.

Curriculum Vitae

Name:	Jin Lu
Post-secondary Education and Degrees:	2004-2006 M.E.Sc. Electrical Engineering The University of Western Ontario London, Ontario, Canada
	1992-1996 B.Eng. Electrical Engineering Zhejiang University Hangzhou, China
Related Work Experience:	2004-2010 Research/Teaching Assistant The University of Western Ontario London, Ontario, Canada
	2000-2003 Product Engineer ABB Beijing Drive Systems Co., Ltd. Beijing, China
	1996-2000 Control Systems Engineer Beijing Mechanical Equipment Institute Beijing, China

Publications:

[1] J. Lu and L. J. Brown, "Internal Model Principle Based Control of Exponentially Damped Sinusoids", in *International Journal of Adaptive Control and Signal Processing*, 24(2010), no.3, pp.219-232.

[2] J. Lu and L. J. Brown, "A Combination of Open and Closed-loop Control for Disturbance Rejection", Submitted to *24th IEEE Canadian Conference on Electrical and Computer Engineering*, December, 2010.

[3] J. Lu and L. J. Brown, "Combining Open and Closed-Loop Control Via Intermittent Integral Control Action", Submitted to *IEEE Transactions on Automatic Control*, September, 2010.

[4] J. Lu and L. J. Brown, "A Multiple Lyapunov Functions Approach for Stability of Switched Systems" in *Proceedings of the 2010 American Control Conference*, Baltimore, MD, July, 2010, pp. 3253-3256.

[5] J. Lu and L. J. Brown, "Stability Analysis of a Proportional with Intermittent Integral Control System" in *Proceedings of the 2010 American Control Conference*, Baltimore, MD, July, 2010, pp. 3257-3262.

[6] J. Lu and L. J. Brown, "Identification of Exponentially Damped Sinusoidal Signals" in *Proceedings of the 17th IFAC World Congress*, Seoul, South Korea, July, 2008, pp. 5089-5094.

[7] J. Lu and L. J. Brown, "Control of Exponentially Damped Sinusoidal Signals" in *Proceedings of the 2007 American Control Conference*, New York City, NY, July, 2007, pp. 1937-1942.